Syntheses of Azulene Analogues of Triphenylmethyl Cation: Extremely Stable Hydrocarbon Carbocations and the First Example of a One-Ring Flip as the Threshold Rotation Mechanism for Molecular Propellers[1)]

Shunji Ito, Noboru Morita, and Toyonobu Asao*

Department of Chemistry, Faculty of Science, Tohoku University, Kawauchi, Aoba-ku, Sendai 980-77

(Received October 27, 1994)

A series of azulene analogues of triphenylmethyl cation (tri(1-azulenyl)methyl, di(1-azulenyl)phenylmethyl, and (1-azulenyl)diphenylmethyl hexafluorophosphates) were synthesized by hydride abstraction from the corresponding methane derivatives with DDQ. In order to examine the effect of substituents on the cations, and to enhance their stabilities, a series of cations bearing 3-methyl, 3-methoxycarbonyl, 3,6-di-*t*-butyl, 6-*t*-butyl, or 3-*t*-butyl groups on each of the azulene rings were also synthesized. Their pK_{R+} values showed that the stabilities of these cations dramatically increase with the number of azulene rings. Tris(3,6-di-*t*-butyl-1-azulenyl)methyl cation showed the highest pK_{R+} value (14.3) ever observed. The high stabilities of these cations were attributed to a large conjugative effect between the central cation and the azulene ring(s). The dynamic stereochemistry of these cations was also studied based on the temperature-dependent ^{1}H NMR spectra, which were analyzed by a flip mechanism. Low-temperature NMR studies indicated that tri(1-azulenyl)methyl cations exist in two types of propeller conformations (symmetrical and unsymmetrical propellers, which have C_3 ($A\overline{A}$) and C_1 ($B\overline{B}$) symmetries, respectively), and at higher temperature the NMR reflect the rapid isomerization. The lower activation energy of the process $B \rightarrow \overline{A}$(or $\overline{B} \rightarrow A$), compared with that of $B \rightarrow \overline{B}$, indicates that the threshold rotation mechanism for the cation is a one-ring flip. This is the first example of a molecular propeller with a threshold rotation mechanism comprising a one-ring flip.

Hydrocarbon carbocations, which comprise only carbon and hydrogen, are generally reactive species. Recently, some extremely stable hydrocarbon carbocations, which exist even under weak basic conditions, have been reported in the literature.[2—8)] However, most of these examples are cyclic cations, such as cyclopropenylium or tropylium ions. The most stable hydrocarbon carbocation ever reported is the tropylium ion (**1**) annelated with three bicyclo[2.2.2]octenes, whose pK_{R+} value was determined to be 13.0.[2)] The cyclopropenylium ion (**2**) stabilized by three cyclopropyl groups, which has a pK_{R+} value of 10.0, has also been reported (Chart 1).[3—7)] In contrast to the cyclic cation, substituted methyl cations are not expected to show high stabilities, e.g., triphenylmethyl cations (**3**) show a lower pK_{R+} value (−6.4) compared with that of triphenylcyclopropenylium ion (**4**) (pK_{R+} =3.0).[10)]

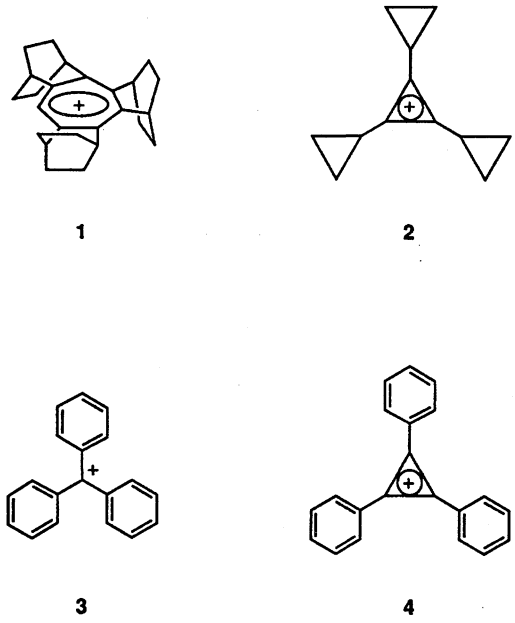

Chart 1.

Theoretical calculations[11)] and its large dipole moment (1.08 D)[12)] have suggested that azulene should stabilize carbocations attached at the 1-position through p–p interactions, e.g., the cyclopropenylium ion (**5**) substituted by three guaiazulene rings, whose pK_{R+} value is over 10.0 (Chart 2).[8)] Therefore, the tri(1-azulenyl)methyl cations (**6**), which are also classified as substituted methyl cations, are expected to show extraordinary stabilities due to the contribution of the

resonance forms, e.g., **6′**.

Here, we report on the syntheses of a series of azulene analogues of triphenylmethyl cation (**3**), i.e., tri(1-azulenyl)methyl (**6a**), di(1-azulenyl)phenylmethyl (**7a**), and (1-azulenyl)diphenylmethyl (**8a**) hexafluorophosphates by hydride abstraction from the corresponding methane derivatives (Chart 3). In order to examine the effect of substituents on the cations and to enhance their stabilities, a series of the cations (**6**, **7**, and **8**) bearing a 3-methyl (**6b**, **7b**, and **8b**), 3-methoxycarbonyl (**6c**, **7c**, and **8c**), 3,6-di-*t*-butyl (**6d**, **7d**, and **8d**), 6-*t*-butyl (**6e**, **7e**, and **8e**), or 3-*t*-butyl (**6f**, **7f**, and **8f**) group on each of the azulene ring(s) were also synthesized. The bulky *t*-butyl groups effectively stabilized **6**, **7**, and **8** by their steric and inductive effects, the latter being induced by the contribution of C–C hyperconjugation.

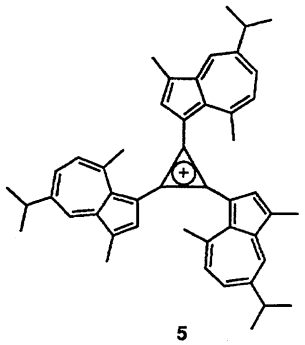

5

Chart 2.

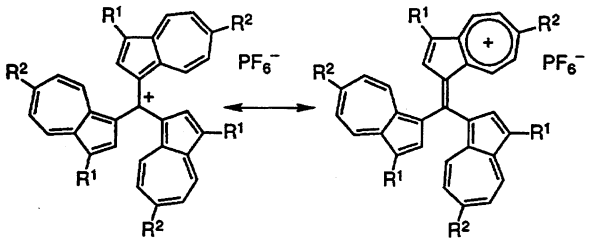

6a: R^1=H, R^2=H
6b: R^1=Me, R^2=H
6c: R^1=COOMe, R^2=H
6d: R^1=*t*-Bu, R^2=*t*-Bu
6e: R^1=H, R^2=*t*-Bu
6f: R^1=*t*-Bu, R^2=H

6′

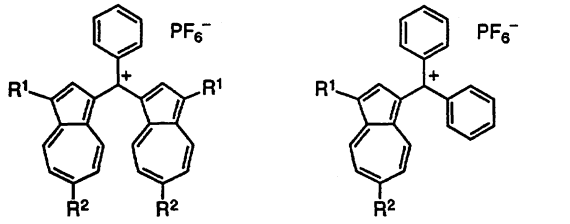

7a: R^1=H, R^2=H
7b: R^1=Me, R^2=H
7c: R^1=COOMe, R^2=H
7d: R^1=*t*-Bu, R^2=*t*-Bu
7e: R^1=H, R^2=*t*-Bu
7f: R^1=*t*-Bu, R^2=H

8a: R^1=H, R^2=H
8b: R^1=Me, R^2=H
8c: R^1=COOMe, R^2=H
8d: R^1=*t*-Bu, R^2=*t*-Bu
8e: R^1=H, R^2=*t*-Bu
8f: R^1=*t*-Bu, R^2=H

Chart 3.

Rotations of the azulene rings of most of these cations (**6**, **7**, and **8**) were observed below ambient temperature via ^{1}H NMR spectroscopy. These cations (**6**, **7**, and **8**) and their corresponding methane derivatives (**9**, **10**, and **11**) have the general structures Ar_3Z and Ar_3ZH (Ar =azulenyl or phenyl group and Z=C^+ or C), which are classified as molecular propellers.[13,14] The correlated rotation of the molecular propellers is commonly analyzed in terms of the flip mechanism postulated by Kurkland et al.[15—18] Conformational analyses of triarylcarbenium ions,[19—21] triarylboranes,[22,23] triarylmethanes,[24—29] triarylsilanes,[30—32] and triarylamines[33,34] were carried out on the basis of this mechanism.

The representative flip mechanism for molecular propellers, such as triphenylmethyl cation (**3**), which exists in two enantiomeric forms (*A* and $\overline{A}$), is illustrated in Fig. 1. These mechanisms are classified into four processes, i.e., from a zero-ring flip to a three-ring flip, depending on the number of flipping rings. The ring flip is defined by the rotation of the rings through the plane which is perpendicular to the reference plane (the plane which is defined by the three arylic ipso carbons), whereas a nonflipping ring rotates concomitantly with the ring flip to the opposite direction, which passes through the reference plane.

The mechanism is independent of conjugative effect between the central atom and the three rings, even in the cases of triarylmethyl cations or triarylboranes, and the lowest energy (threshold) rotation mechanism for these systems is uniformly a two-ring flip.[13] Recently, Rappoport et al. noted that the mechanism for vinyl derivatives (**12**) of molecular propellers is dependent on the steric effects between the substituent (R=H or OH) and the three rings (Chart 4).[35,36] Therefore, the threshold rotation mechanism for the molecular propellers must also be variable. However, the three rings of molecular propellers are in close proximity to each

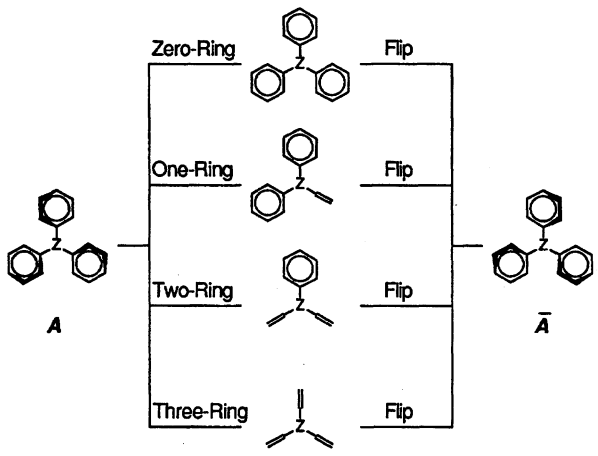

Fig. 1. Representative flip mechanism for the molecular propeller (**3**) such as Ar_3Z.

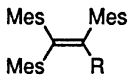

12a: R=H
12b: R=OH

Mes=2,4,6-$Me_3C_6H_2$

Chart 4.

other, compared with those of **12**, so that stronger conjugative interactions are needed to change the threshold rotation mechanism.

The high stabilities of cations **6**, **7**, and **8** may be rationalized as being due to the large conjugative effect between the cationic carbon (C^+) and the azulene ring(s), which would contribute to the transition state of the ring flipping as well as to the ground state. Therefore, in the case of tri(1-azulenyl)methyl cations (**6**) the threshold mechanism is expected to change from a two-ring flip to a one-ring flip. We herein also report on analyses of the dynamic stereochemistry of the cations **6**, **7**, and **8** based on the flip mechanism.

Results and Discussion

Syntheses of Tri(1-azulenyl)methyl Hexafluorophosphates (6a—f). Previously, two groups have already reported the syntheses of **6**. (1) Hafner et al. reported that the reaction of azulene with tetraethyl orthocarbonate in nitromethane in the presence of HCl afforded tri(1-azulenyl)methyl chloride, and that the addition of $NaClO_4$ in formic acid gave its perchlorate.[37] (2) Matsubara et al. reported that tri(1-azulenyl)methyl tetrafluoroborate and its 3,3′,3″-trimethyl derivative were obtained by hydride abstraction from tri(1-azulenyl)methanes **9a** and **9b** with $Ph_3C^+BF_4^-$.[38,39] However, we found that neither method gave the desired **6**.

We also obtained cationic materials from the reaction of azulene with tetraethyl orthocarbonate in the presence of HCl. However, the complexity of the ^1H NMR spectrum of the product and its low solubility led us to suspect that it was polymeric. We also obtained a similar cationic compound in the absence of tetraethyl orthocarbonate. Therefore, Hafner's product must be a polymeric cation, whose structure has not been clarified.

Tri(1-azulenyl)methanes **9a** and **9b** have been obtained by the autooxidation of azulene (**13a**) and 1-methylazulene (**13b**) with O_2 in 3.2 and 4.0% yields, respectively, among many other products.[38,39] However, we found that **9a** was effectively synthesized by the reaction of **13a** with 1-formylazulene (**14a**) under acidic conditions. A mixture of **14a** with two molar equivalents of **13a** in acetic acid was stirred at room temperature for 3 d to yield **9a** in 30% yield, along with 1,3-bis[di(1-azulenyl)methyl]azulene (**15**) in 14% yield. Similarly, 3,3′,3″-trimethyl (**9b**) and 3,3′,3″-trimethoxycarbonyl (**9c**) derivatives were also obtained by the reaction of 1-methyl- (**13b**) and 1-methoxycarbonylazulene (**13c**) with 1-formyl-3-methyl- (**14b**) and 3-formyl-1-methoxycarbonylazulenes (**14c**)[40] in 70 and 94% yields, respectively.

Attempted hydride abstraction from **9a—c** by a reaction with $Ph_3C^+PF_6^-$ afforded the corresponding di(1-azulenyl)methyl hexafluorophosphates (**16a—c**) in 98, 98, and 65% yields, respectively, via the extrusion of one azulene ring each. The azulene rings were recovered as the corresponding 1-triphenylmethylazulenes (**17a**[41,42]—**c**) and 1,3-bis(triphenylmethyl)azulene (**18**)[41,42] from **9a**. Therefore, reports concerning the preparation of **6a** or **6b** from the reaction of **9a** or **9b** with $Ph_3C^+BF_4^-$ by Matsubara et al. are also doubtful.

The synthesis of **6a** was accomplished by hydride abstraction from tri(1-azulenyl)methane (**9a**) using DDQ. The reaction of **9a** with DDQ in dichloromethane, followed by an exchange of the counter anion with PF_6^- by the addition of a 60% aqueous HPF_6 solution was found to yield tri(1-azulenyl)methyl hexafluorophosphate (**6a**) in 86% yield as deep-blue colored crystals. Similarly, 3,3′,3″-trimethyl (**6b**) and 3,3′,3″-trimethoxycarbonyl (**6c**) derivatives were also obtained quantitatively from the reaction of DDQ with **9b** and **9c**, respectively.

The syntheses of *t*-butyl derivatives (**6d—f**) were accomplished as follows. 6-*t*-Butylazulene (**13e**) was prepared in 99% yield starting from 4-*t*-butylpyridine according to a modification of Hafner's azulene synthesis.[43] *t*-Butylation[42] of **13e** with *t*-butyl alcohol in dichloromethane in the presence of H_2SO_4 did not afford a satisfactory result. The *t*-butylation was carried out with *t*-butyl chloride in the presence of $AlCl_3$ in dichloromethane, which afforded 1,6-di-*t*-butylazulene (**13d**) and 1,3,6-tri-*t*-butylazulene (**19**) in 56 and 15% yields, respectively. 1-*t*-Butylazulene (**13f**) was also prepared by the similar *t*-butylation of **13a** in 54% yield together with 1,3-di-*t*-butylazulene (**20**) in 10% yield.

The reaction of **13d** and **14d** (which was obtained in 83% yield by Vilsmeier reaction of **13d**) in acetic acid at room temperature afforded tris(3,6-di-*t*-butyl-1-azulenyl)methane (**9d**) in 71% yield. Hydride abstraction from **9d** with DDQ gave **6d** in quantitative yield. The 6,6′,6″-tri-*t*-butyl (**6e**) and 3,3′,3″-tri-*t*-butyl (**6f**) derivatives were similarly synthesized starting from **13e** and **13f** and their 1-formyl derivatives (**14e** and **14f**), which were obtained by Vilsmeier reaction of **13d** and **14f**,[42] in 93 and 95% yields, respectively (Scheme 1).

Syntheses of Di(1-azulenyl)phenylmethyl Hexafluorophosphates (7a—f). **7a—f** were prepared in 84—100% yields by a reaction of the corresponding methane derivatives (**10a—f**) with DDQ. Di(1-azulenyl)phenylmethane (**10a**) was synthesized by the reaction of benzaldehyde with two molar equivalents of azulene (**13a**) in acetic acid at room temperature, in

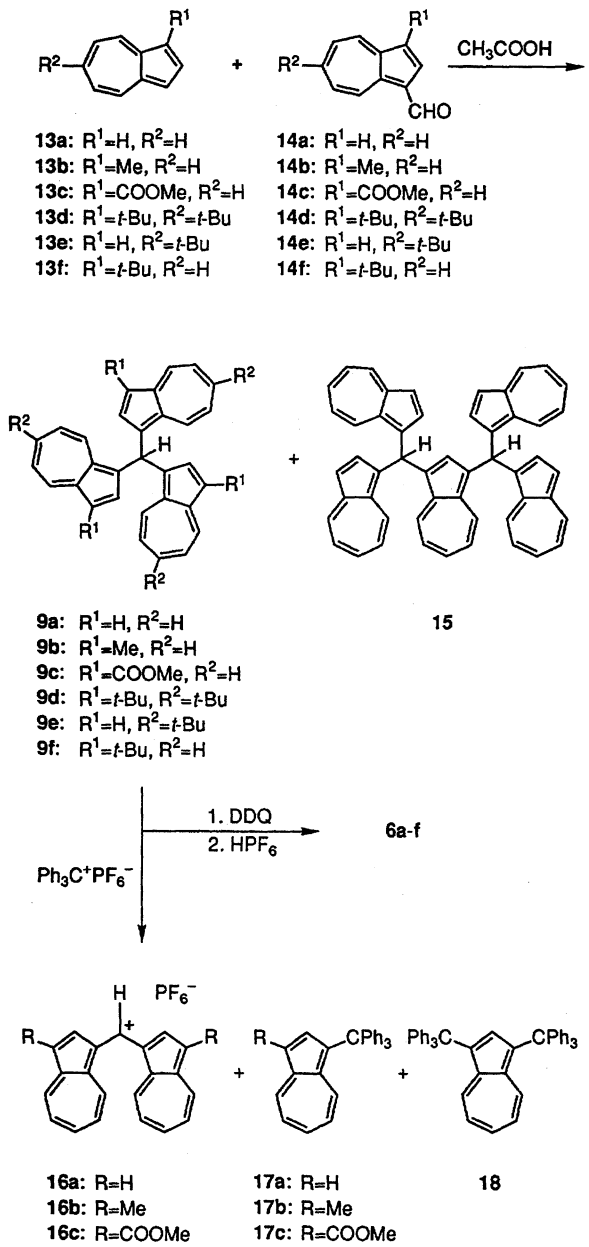

Scheme 1.

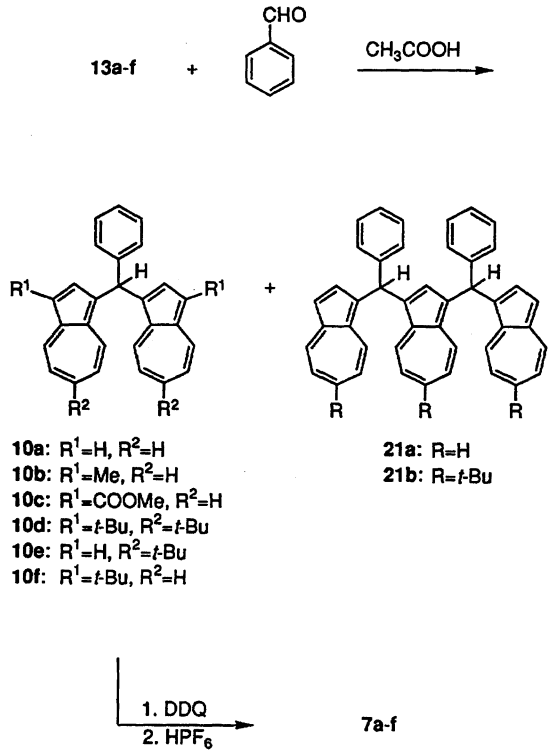

Scheme 2.

51% yield together with 1,3-bis[(1-azulenyl)phenylmethyl]azulene (**21a**) in 19% yield (Scheme 2).[44] Similarly, 3,3′-dimethyl (**10b**), 3,3′-dimethoxycarbonyl (**10c**), 3,3′,6,6′-tetra-*t*-butyl (**10d**), 6,6′-di-*t*-butyl (**10e**), and 3,3′-di-*t*-butyl (**10f**) derivatives were also obtained by the reactions of **13b**—**f** with benzaldehyde in acetic acid in 89, 100, 98, 36, and 56% yields, respectively, together with 1,3-bis[(1-azulenyl)phenylmethyl]-6-*t*-butylazulene (**21b**) in 16% yield, in the case of **13e**.

Syntheses of (1-Azulenyl)diphenylmethyl Hexafluorophosphates (8a—f). (1-Azulenyl)diphenylmethane (**11a**) was synthesized by the reaction of benzhydrol with one molar equivalent of azulene (**13a**) in refluxing acetic acid, in 40% yield together with 1,3-bis(diphenylmethyl)azulene (**22a**) in 37% yield.[42] Similarly, 3-methyl (**11b**), 3-methoxycarbonyl (**11c**), 3,6-di-*t*-butyl (**11d**), 6-*t*-butyl (**11e**), and 3-*t*-butyl (**11f**) derivatives were also obtained by the reactions of **13b**—**f** with benzhydrol in refluxing acetic acid in 46, 89, 28, 31, and 55% yields, respectively, together with 1,3-bis(diphenylmethyl)-6-*t*-butylazulene (**22b**) in 11% yield, in the case of **13e**. **8a**, **8c**, **8d**, and **8f** were also prepared by the reaction of **11a**, **11c**, **11d**, and **11f** with DDQ in quantitative yields (Scheme 3). However, we could not obtain the 3-methyl (**8b**) and 6-*t*-butyl (**8e**) derivatives in pure form by this method, because of the low stabilities of these cations.

The reduction of the cations (**6a**—**b**, **7a**—**b**, and **8a**) with $LiAlH_4$ in THF/dichloromethane solution at room temperature afforded the corresponding (1-azulenyl)methane derivatives (**9a**—**b**, **10a**—**b**, and **11a**) in 15—40% yields. These results lent further support to the cationic structures of these compounds (**6**, **7**, and **8**)

The pK_{R^+} Values. The pK_{R^+} values of most of the cations (**6**, **7**, **8**, and **16**) obtained here were determined spectrophotometrically at 24 °C in a buffer solution prepared in 50% aqueous MeCN,[2,45,46] which are summarized in Table 1. Since the half-neutralization point of **6d** was beyond 14, the pK_{R^+} value of **6d** was determined by extrapolation using the equation $pH=pK_{R^+}+\log [ROH]/[R^+]$. The pK_{R^+} value of **8c** was determined in the H_2SO_4–H_2O system, because of its low stability.

The pK_{R^+} value of **6a** (11.3) (which is 17.7 pK_{R^+} units higher than that of triphenylmethyl cation (**3**) ($pK_{R^+}=-6.4$[9])) is extremely high for a methyl cation substituted with only hydrocarbon groups. As ex-

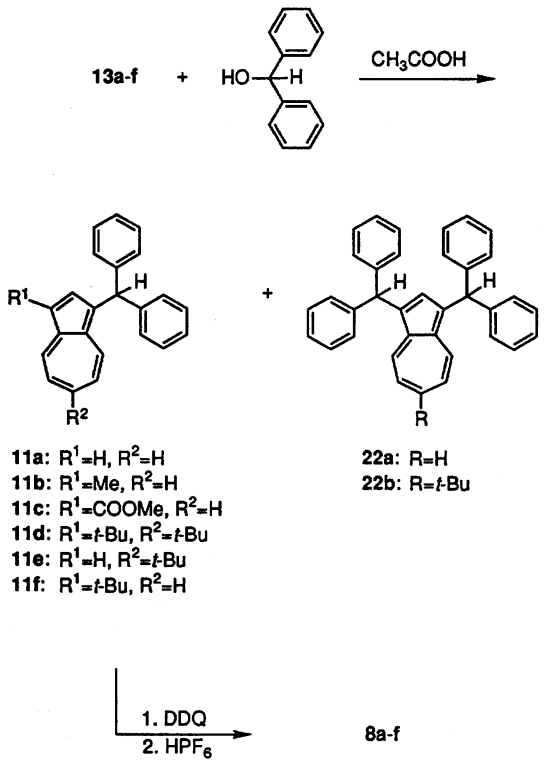

Scheme 3.

Table 1. pK_{R+} Values of **6**, **7**, **8**, and **16** Determined at 24 °C in a Buffered Solution Prepared in 50% Aqueous MeCN

	6	16	7	8
a;	11.3	7.3	10.5	3.0
b;	11.4	8.7	10.8	3.7[a)]
c;	10.3	2.1	3.4	0.08[b)]
d;	14.3		12.4	4.6
e;	13.7		11.7	3.6[a)]
f;	13.3		10.7	3.6

a) Measured for impure samples. b) Measured in H_2SO_4–H_2O system.

pected, the methyl substituents slightly increase the pK_{R+} value (**6b**; 11.4) and the methoxycarbonyl groups decrease the stability (**6c**; 10.3), but there is a small difference in the pK_{R+} values of **6a**—**c**. The pK_{R+} values of **16a**—**c** are smaller by 4.0, 2.7, and 8.2 pK_{R+} units than those of **6a**—**c**, respectively. The methoxycarbonyl groups particularly destabilized **16**. The small difference in the pK_{R+} values of **6a**—**c** can be explained in terms of steric protection by the azulene rings of the cation from attack by bases. Therefore, it is considered that the extreme stability of **6** mainly depends on the contribution of the resonance structure **6′** and to some extent on the steric effect of the three azulene rings.

Introduction of bulky *t*-butyl groups at the 3,3′,3″- and/or 6,6′,6″-positions stabilized the cation effectively. The pK_{R+} values of **6d**—**f** are substantially larger than those of **6a**—**c**. *The pK_{R+} value 14.3 of **6d** is the highest value for a methyl cation substituted with hydrocarbon groups ever reported, and is 3.0 pK_{R+} units higher than that of **6a** and 1.3 pK_{R+} units higher than that of **1**.*[2)] The large difference of the pK_{R+} values between **6f** and **6b** shows that the extreme stability of **6f** is attributable to the steric effects of bulky *t*-butyl groups at 3,3′,3″-positions. The small difference in the pK_{R+} value of **6e** and that of **6f** indicates that the inductive electron-donating effect of the 6,6′,6″-tri-*t*-butyl groups contribute to the stability in addition to the steric effects. Consequently, the high pK_{R+} value of **6d** must be mainly attributable to steric effects of six bulky *t*-butyl groups in addition to the contribution of the dipolar structure of three azulene rings.

The pK_{R+} value of **7a** (10.5) is also extremely high, and is only 0.8 pK_{R+} units less than that of **6a**. As expected, although the methyl substituents slightly increase the pK_{R+} value (**7b**; 10.8), the methoxycarbonyl groups particularly destabilize **7** and likewise **16c**. The pK_{R+} value of **7c** is 7.1 pK_{R+} units lower than that of **7a**. Although the *t*-butyl groups at 3,3′,3″- and/or 6,6′,6″-positions also stabilized **7**, the effect of stabilization of the *t*-butyl groups was lower than that of **6**. The pK_{R+} values of the *t*-butyl derivatives (**7d**—**f**) are higher by only 1.9, 1.2, and 0.2 pK_{R+} units than that of **7a**, respectively. The small pK_{R+} values of **8** showed the relatively low stabilities of the cations. However, the pK_{R+} value of **8a** is 9.4 pK_{R+} units higher than that of **3**.

A plot of the pK_{R+} values vs. the number of azulene rings is shown in Fig. 2. The pK_{R+} values dramatically increase with the number of azulene rings. The pK_{R+} values of **3** are increased 9.4—11.0 pK_{R+} units by the substitution of one azulene ring, except for **8c**. A second substitution of another azulene ring increased the pK_{R+} values by an additional 7.1—8.1 pK_{R+} units, except for **7c**. Saturation of the stabilization was observed between the second and third substitution of the azulene rings. The third substitution stabilized the cation only by 0.6—2.6 pK_{R+} units, except for **6c**.

Redox Properties. Redox potentials (V vs. Ag^+) of **6**, **7**, **8**, and **16** measured by cyclic voltammetry in MeCN are summarized in Table 2. The first reduction potentials (E_1^{red}) of **6**, **7**, **8**, and **16** were observed to be lower than that of **3** (−0.13 V vs. $Ag/AgNO_3$[47)]), which also shows the enhanced stabilities of these cations. In spite of the high pK_{R+} values, the E_1^{red} values of **6**, **7**, **8**, and **16** are relatively positive compared with those of the cyclic cations; e.g., −1.120 for **1**[2)] and −2.20 V vs. Ag^+ for **2**.[6)]

The E_1^{red} values become more negative with the number of azulene rings, and tend to correlate with their stabilities (pK_{R+} values), e.g., −0.78 for **6a**, −0.66 for **7a**, and −0.48 V for **8a**. Reversibilities were found in most of the first reduction waves of **6** and **7**. Therefore, the azulene rings should stabilize not only carbocations, but also radical species (e.g., **23**). The oxidation of **6**

shows two adjacent waves, e.g., +0.98 and +1.07 V for **6a**, which are due to the oxidation of two azulene rings to give a cation radical, such as **25** (Chart 5). The E_1^{ox} values of **7** are slightly more positive than those of **6**, except for that of **7a**, and the oxidation of **7** no longer shows two waves as observed in **6**. Relatively positive E_1^{ox} values were observed at an oxidation of **8**, because there is no azulene ring for oxidation like **6** and **7**.

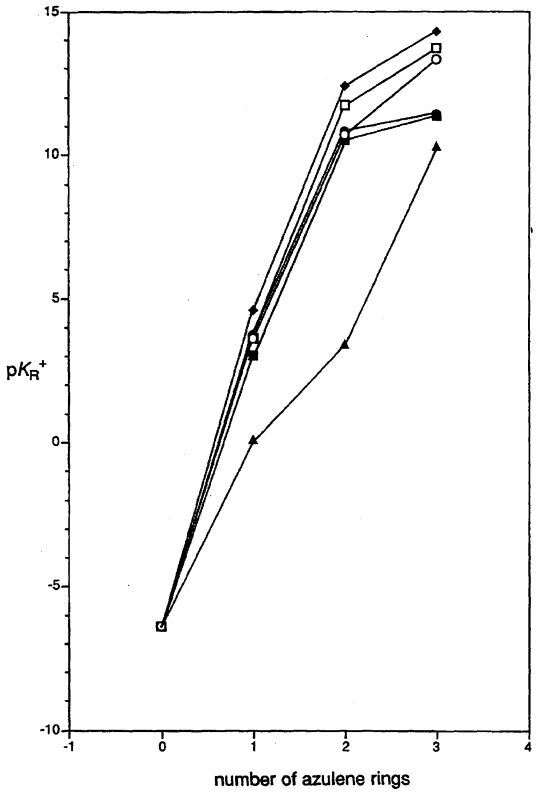

Fig. 2. Plot of the pK_{R+} values vs. the number of azulene rings. (■) R^1=H, R^2=H; (●) R^1=Me, R^2=H; (▲) R^1=COOMe, R^2=H; (◆) R^1=*t*-Bu, R^2=*t*-Bu; (□) R^1=H, R^2=*t*-Bu; (○) R^1=*t*-Bu, R^2=H.

Table 2. Redox Potentials (V vs. Ag^+) of **6**, **7**, **8**, and **16** Determined by Cyclic Voltammetry in MeCN[a)]

	E_1^{red}	E_2^{red}	E_1^{ox}	E_2^{ox}	E_3^{ox}
6a	−0.78	(−1.56)	(+0.98)	(+1.07)	
6b	−0.82	(−1.59)	(+0.85)	(+0.94)	
6c	−0.61	(−1.30)	(+1.26)	(+1.36)	
6d	−0.91	(−1.72)	+0.84	+0.95	(+1.50)
6e	−0.85	(−1.66)	(+0.92)	(+1.03)	
6f	−0.83	(−1.01)	+0.82	+0.99	(+1.51)
16a	(−0.58)		(+0.95)		
16b	(−0.62)		+0.89	(+1.34)	
16c	(−0.38)	(−0.52)	(+1.42)		
7a	−0.66	(−1.52)	(+0.82)		
7b	−0.70	(−1.57)	(+0.90)		
7c	(−0.49)	(−0.57)	(+1.32)		
7d	−0.78	(−1.64)	+0.88	(+1.38)	
7e	−0.74	(−1.59)	(+0.97)		
7f	−0.71	(−1.57)	+0.93	(+1.40)	
8a	(−0.48)		(+1.41)		
8c	(−0.36)		(+1.82)		
8d	−0.59	(−1.54)	(+1.53)		
8f	(−0.54)		(+1.55)		

a) Irreversible processes are shown in parentheses.

Spectroscopic Properties. High-resolution mass spectra of **6**, **7**, **8**, and **16** ionized by FAB showed the correct $M^+ - PF_6$ ion peaks, which were also indicative of the cationic structure of **6**, **7**, **8**, and **16**.

6, **7**, **8**, and **16** showed strong absorption maxima in the visible region. The maxima (nm) and coefficients ($\log \varepsilon$) in the visible region are summarized in Table 3. There is no apparent correlation between the absorption maxima (nm) and the stabilities (pK_{R+} values). The absorption maxima of **6** are 15—31 nm shorter than that of **7**, which nearly equal to those of **16**. 3-Methyl and 3-*t*-butyl substituents apparently showed a bathochromic shift of 31—38 nm, 6-*t*-butyl groups slightly shifted to longer wavelength (1—3 nm), and 3-methoxycarbonyl substituent showed a hypsochromic shift of 13—23 nm. The absorption maxima of **8** are greatly different from those of **6**, **7**, and **16**. Those maxima existed in a narrow range of 483 to 495 nm.

The characteristic bands of hexafluorophosphate were

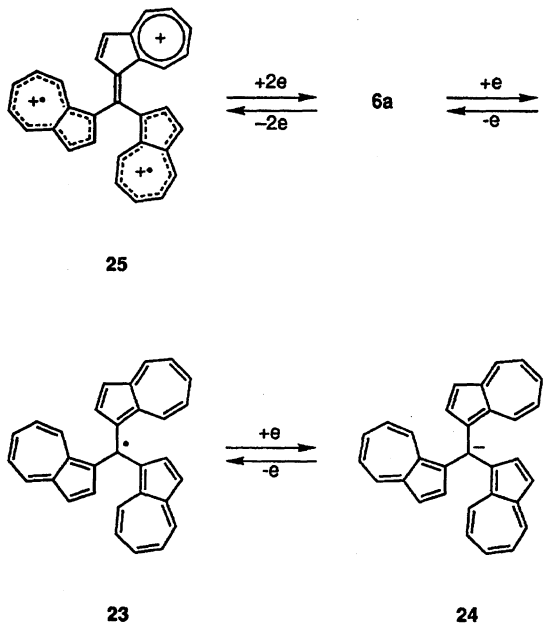

Chart 5.

Table 3. Absorption Maxima (nm) and Their Coefficients ($\log \varepsilon$ in the Parentheses) of **6**, **7**, **8**, and **16** in MeCN in the Visible Region

	6	**16**	**7**	**8**
a;	614 (4.70)	616 (4.81)	639 (4.57)	487 (4.16)
b;	652 (4.57)	647 (4.87)	676 (4.53)	495 (4.21)
c;	601 (4.72)	599 (5.03)	616 (4.60)	493 (4.12)
d;	650 (4.62)		681 (4.61)	489 (4.11)
e;	615 (4.64)		642 (4.60)	483 (4.17)
f;	650 (4.61)		678 (4.53)	495 (4.14)

Table 4. ^{1}H NMR Chemical Shifts (ppm) of Tri(1-azulenyl)methyl Cations (**6**) and the Corresponding Hydro Derivatives (**9**)[a)]

	Solvent	Temp	Assignment							
		°C	CH	2	3 or 3-sub	4	5	6 or 6-sub	7	8
9a	$CDCl_3$	—	7.36	7.40	7.26	8.28	7.17	7.49	6.95	8.28
6a	$CDCl_3$	58		7.87	7.68	8.73	7.82	7.97	7.37	7.83
				(+0.47)	(+0.42)	(+0.45)	(+0.65)	(+0.48)	(+0.42)	(−0.45)
9b	$CDCl_3$	—	7.25	7.25	2.53	8.14	6.93	7.40	6.79	8.12
6b	$CDCl_3$	58		7.69	2.73	8.60	7.76	7.89	7.25	7.68
				(+0.44)	(+0.20)	(+0.46)	(+0.83)	(+0.49)	(+0.46)	(−0.44)
9c	$CDCl_3$	—	7.15	7.78	3.82	9.67	7.52	7.77	7.26	8.35
6c	$CDCl_3$	58		8.13	3.94	10.01	8.05	8.08	7.84	8.13
				(+0.35)	(+0.12)	(+0.34)	(+0.53)	(+0.31)	(+0.58)	(−0.22)
9d	50%CD_2Cl_2/CS_2	—	7.08	7.29	1.45	8.44	7.06	1.37	6.95	8.13
6d	DMSO-d_6	90		7.56	1.50	9.11	8.07	1.40	7.56	7.75
				(+0.27)	(−0.05)	(+0.67)	(+1.01)	(+0.17)	(+0.61)	(−0.38)
6e	DMSO-d_6	80		7.81	7.72	8.84	8.09	1.40	7.63	7.79
9f	$CDCl_3$	—	7.22	7.42	1.47	8.56	6.92	7.40	6.80	8.22
6f	DMSO-d_6	80		7.72	1.57	9.18	7.91	8.04	7.40	7.78
				(+0.30)	(+0.10)	(+0.62)	(+0.99)	(+0.64)	(+0.60)	(−0.44)

a) $\Delta\delta$ values are shown in the parentheses.

Table 5. ^{1}H NMR Chemical Shifts (ppm) of Di(1-azulenyl)phenylmethyl Cations (**7**) and the Corresponding Hydro Derivatives (**10**)[a)]

	Solvent	Temp	Assignment										
		°C	CH	2	3 or 3-sub	4	5	6 or 6-sub	7	8	2′,6′	3′,5′	4′
10a	$CDCl_3$	—	6.74	7.45	7.27	8.26	7.07	7.50	6.97	8.26		7.22—7.11	
7a	$CDCl_3$	58		7.86	7.70	8.78	7.99	8.11	7.59	7.96	7.41	7.59	7.77
				(+0.41)	(+0.43)	(+0.52)	(+0.92)	(+0.61)	(+0.62)	(−0.30)			
10b	$CDCl_3$	—	6.67	7.30	2.55	8.13	6.93	7.40	6.82	8.13		7.25—7.08	
7b	$CDCl_3$	58		7.68	2.66	8.65	7.98	8.05	7.49	7.84	7.38	7.58	7.74
				(+0.38)	(+0.11)	(+0.52)	(+1.05)	(+0.65)	(+0.67)	(−0.29)			
10c	$CDCl_3$	—	6.60	7.84	3.84	9.65	7.49	7.74	7.27	8.34		7.26—7.18	
7c	$CDCl_3$	58		8.31	3.97	10.03	8.23	8.29	7.86	8.30	7.46	7.64	7.84
				(+0.47)	(+0.13)	(+0.30)	(+0.74)	(+0.55)	(+0.59)	(−0.04)			
10d	$CDCl_3$	—	6.63	7.38	1.49	8.53	7.14	1.40	7.04	8.16		7.17—7.15	
7d	$CDCl_3$	50		7.58	1.59	9.08	8.18	1.46	—	7.86		7.73—7.38 (H-7)	
				(+0.20)	(+0.10)	(+0.55)	(+1.04)	(+0.06)	—	(−0.30)			
10e	CD_2Cl_2	—	6.69	7.36	7.18	8.23	7.28	1.40	7.20	8.23		7.20	
7e	$CDCl_3$	50		—	—	8.76	8.17	1.44	—	7.90		7.79—7.35 (H-2,3,7)	
						(+0.53)	(+0.89)	(+0.04)		(−0.33)			
10f	$CDCl_3$	—	6.67	7.45	1.50	8.58	6.96	7.43	6.85	8.19		7.28—7.09	
7f	$CDCl_3$	50		7.71	1.59	9.10	—	—	—	—		8.21—7.35 (H-5,6,7,8)	
				(+0.26)	(+0.09)	(+0.52)							

a) $\Delta\delta$ values are shown in the parentheses.

observed at around 834—840 (strong) and 556—560 (medium) cm^{-1} in the IR spectra of **6**, **7**, **8**, and **16**, which supported the cationic structure of these compounds.

Time-Averaged ^{1}H and ^{13}C NMR Spectra. Rotation of the azulene ring(s) of most of **6**, **7**, and **8** around 50 °C was fast on the NMR time scale. Therefore, static NMR spectra of **6**, **7**, and **8** were determined above the coalescence temperature, except for **8d** and **8f**. ^{1}H and ^{13}C NMR spectra of **6**, **7**, and **8** and those

Table 6. ^{1}H NMR Chemical Shifts (ppm) of (1-Azulenyl)diphenylmethyl Cations (**8**) and the Corresponding Hydro Derivatives (**11**)[a)]

	Solvent	Temp	Assignment										
		°C	CH	2	3 or 3-sub	4	5	6 or 6-sub	7	8	2′,6′	3′,5′	4′
11a	$CDCl_3$	—	6.14	7.49	–	8.28	7.10	7.58	7.08	8.22	7.38—7.16 (H-3)		
8a	$CDCl_3$	58		7.91	7.80	8.97	8.53	8.48	8.11	8.20	7.40	7.61	7.77
				(+0.42)	—	(+0.69)	(+1.43)	(+0.90)	(+1.03)	(−0.02)			
11b	$CDCl_3$	—	6.08	7.31	2.54	8.09	6.91	7.37	6.81	8.09	7.26—7.06		
11c	$CDCl_3$	—	6.06	7.90	3.88	9.64	7.48	7.75	—	8.34	7.42—7.06 (H-6)		
8c	$CDCl_3$	—		8.39	4.00	10.09	—	—	—	8.61	8.48—8.73 (H-5,6,7)		
				(+0.49)	(+0.12)	(+0.45)				(+0.27)			
11d	$CDCl_3$	—	6.07	7.31	1.50	8.55	—	1.40	7.08	8.08	7.29—7.04 (H-5)		
8d	$CDCl_3$	50		—	1.57	9.25	8.78	1.51	8.12	8.12	7.87—7.26 (H-2)		
					(+0.07)	(+0.70)		(+0.11)	(+1.04)	(+0.04)			
11e	$CDCl_3$	—	6.11	7.39	br	8.21	—	1.40	—	8.17	7.32—7.04 (H-5,6)		
11f	$CDCl_3$	—	6.10	7.42	1.51	8.59	6.98	7.45	6.88	8.13	7.30—7.11		
8f	$CDCl_3$	50		—	1.57	9.25	8.36—8.70		8.26—7.92 (H-2)		7.82—7.26		
					(+0.06)	(+0.66)							

a) $\Delta\delta$ values are shown in the parentheses.

of the corresponding methane derivatives (**9**, **10**, and **11**) are summarized in Tables 4, 5, 6, 7, 8, and 9.

The ^{1}H NMR chemical shifts of the methine protons of **9**, **10**, and **11** were observed at lower field compared to triphenylmethane (5.57 ppm); 7.08—7.36 for **9**, 6.60—6.74 for **10**, and 6.07—6.14 ppm for **11**, which disappeared on the ^{1}H NMR spectra of **6**, **7**, and **8**. Large downfield shifts were observed at H-2—7. The largest $\Delta\delta$ value was observed at H-5, i.e., +0.53—+1.01 for **6**, +0.74—+1.05 for **7**, and +1.43 ppm for **8a**. The large downfield shifts of H-5 are predicted by the resonance structure of **6**, **7**, and **8**. The tendency to increase the $\Delta\delta$ value of H-5, i.e., +0.65 for **6a**, +0.92 for **7a**, and +1.43 ppm for **8a**, agreed with the order of stabilities of these cations. However, there are no apparent correlations between the $\Delta\delta$ values and the stabilities of the cations, such as **6a**—**f**. The $\Delta\delta$ values of H-8 for **6** and **7** were negative, i.e., −0.22—−0.45 for **6** and for −0.04—−0.33 for **7**, in contrast to the other positions. The upfield shifts of H-8 for **6** and **7** are regarded as being the effect of the neighboring azulenium structure. However, the reasons for the upfield shifts of H-8 for **6** and **7** are now being investigated.

The chemical shifts (^{13}C NMR) of the central cationic carbon of **6**, **7**, and **8** were observed at 151.82—161.38, 161.11—169.83, and 168.58—177.68 ppm, respectively. The upfield shifts observed in **6**, compared to those of **7** and **8**, are indicative of decreased charge densities on the cationic carbons and their enhanced thermodynamic stabilities. The chemical shift of the central cationic carbon in **6d** (151.82 ppm), which is slightly upfield compared with those of other tri(1-azulenyl)-methyl cations (**6a**—**c** and **6e**—**f**), agreed with its enhanced thermodynamic stability. However, good correlations between the ^{13}C NMR chemical shifts of the central cationic carbon and the stabilities of the cations were not observed in **6**, **7**, and **8**.

Large $\Delta\delta$ values were observed at C-3, 3a, 5, 7, and 8a. The largest $\Delta\delta$ value was observed at C-5, i.e., +8.55—+11.79 for **6**, +10.51—+14.30 for **7**, and +16.45—+24.24 ppm for **8**. The downfield shifts of C-3a, 5, 7, and 8a were predicted based on the resonance structure of the cations, and those of C-3 were attributed to the decreased azulenic character. The cationic structure does not affect the chemical shifts of the C-1 of **6** and **7**, whose $\Delta\delta$ values were only −3.00—+0.02 and −4.84—+1.28 ppm, respectively. Therefore, the NMR spectra of **6**, **7**, and **8** showed most of the positive charge to be delocalized on the azulene rings, which effectively stabilized the carbocation.

Dynamic Stereochemistry of 6b. 3,3′,3″-Trimethyl derivative (**6b**) was utilized for the analysis of the dynamic stereochemistry of **6** in order to avoid the complexities of the temperature-dependent NMR spectra. As expected, the threshold rotation mechanism for **6b** was a one-ring flip, which is the first example for a molecular propeller.

The ^{1}H NMR (600 MHz) spectra of **6b** in $CDCl_3$ at 60 °C and −60 °C are shown in Fig. 3. At −60 °C the NMR (methyl region) consisted of four signals (as indicated a, b, c, and d) in the ratio of intensities of ca. 1 : 1 : 1 : 1.4. These signals indicate that the ground state of **6b** is a propeller (helical) conformation. The possibilities of stereoisomerism and isomerization for **6b** were analyzed by using the flip mechanism.[15—18)] Four propeller conformations (including stereoisomers) are possible for a molecule of this type. These isomers make up

Table 7. ^{13}C NMR Chemical Shifts (ppm) of Tri(1-azulenyl)methyl Cations (**6**) and the Corresponding Hydro Derivatives (**9**)[a)]

	Solvent	Temp	Assignment															
		°C	CH or C^+	1	2	3	3-sub	3-sub	3a	4	5	6	6-sub	6-sub	7	8	8a
9a	$CDCl_3$	—	35.98	134.00	138.15	116.41			140.95	136.41	121.62	136.96			122.17	133.42	134.49
6a	$CDCl_3$	50	157.40	132.67	145.60	124.32			151.27	140.91	132.67	142.40			131.85	138.35	145.72
			(+121.42)	(−1.33)	(+7.45)	(+7.91)			(+10.32)	(+4.50)	(+11.05)	(+5.44)			(+9.68)	(+4.93)	(+11.23)
9b	$CDCl_3$	—	35.26	132.70	139.38	124.47	12.76		136.97	133.38	120.51	136.97			120.84	132.92	134.71
6b	$CDCl_3$	50	154.20	131.67	145.58	132.82	12.84		148.76	137.70	131.46	142.19			131.41	137.95	146.29
			(+118.94)	(−1.03)	(+6.20)	(+8.33)	(+0.08)		(+11.79)	(+4.42)	(+10.95)	(+5.22)			(+10.57)	(+5.03)	(+11.58)
9c	$CDCl_3$	—	50.96	131.67	140.85	115.33	165.54 (s)	75.57 (q)	141.76	137.95	127.70	139.05			126.24	134.87	139.69
6c	MeCN-d_3	50	161.38	131.69	149.46	123.36	164.83 (s)	52.05 (q)	150.31	142.17	136.72	145.28			135.65	140.89	148.76
			(+110.42)	(+0.02)	(+8.61)	(+8.03)	(−0.71)	(−23.52)	(+8.55)	(+4.22)	(+9.02)	(+6.23)			(+9.41)	(+6.02)	(+9.07)
9d	50%CD_2Cl_2/CS_2	—	35.22	132.45	136.77	138.08	33.81 (s)	32.92 (q)	135.13	135.37	119.09	160.88	38.69 (s)	32.51 (q)	119.85	132.78	134.88
6d	DMSO-d_6	90	151.82	129.45	141.63	143.70	32.43 (s)	30.80 (q)	144.82	136.51	128.76	166.14	38.25 (s)	30.63 (q)	128.47	138.11	144.65
			(+116.60)	(−3.00)	(+4.86)	(+5.62)	(−1.38)	(−2.12)	(+9.69)	(+1.14)	(+9.67)	(+5.26)	(−0.44)	(−1.88)	(+8.62)	(+5.33)	(+9.77)
6e	$CDCl_3$	50	156.69	132.36	144.80	123.70			149.83	139.77	130.65	167.60	31.68	39.36	129.40	137.45	144.25
9f	$CDCl_3$	—	35.31	131.72	137.14	137.60	33.20 (s)	32.14 (q)	135.44	134.98	119.98	136.56			120.59	132.94	135.31
6f	$CDCl_3$	50	154.28	130.92	143.61	145.53	33.48 (s)	31.68 (q)	147.14	138.03	131.23	142.11			130.92	139.37	145.53
			(+118.97)	(−0.80)	(+6.47)	(+7.93)	(+0.28)	(−0.46)	(+11.70)	(+3.05)	(+11.25)	(+5.55)			(+10.33)	(+6.43)	(+10.22)

a) $\Delta\delta$ values are shown in the parentheses.

Table 8. ^{13}C NMR Chemical Shifts (ppm) of Di(1-azulenyl)phenylmethyl Cations (**7**) and the Corresponding Hydro Derivatives (**10**)[a)]

	Solvent	Temp	Assignment																		
		°C	CH or C^+	1	2	3	3-sub	3-sub	3a	4	5	6	6-sub	6-sub	7	8	8a	1′	2′,6′	3′,5′	4′
10a	$CDCl_3$	—	42.87	133.12	138.15	116.50			140.92	136.50	121.78	137.08			122.23	133.48	134.92	145.50	128.67	128.09	125.77
7a	$CDCl_3$	50	165.54	128.84	146.64	126.79			154.26	141.58	135.75	143.74			134.87	139.81	148.16	141.67	134.78	129.23	133.71
			(+122.67)	(−4.84)	(+8.49)	(+10.29)			(+13.34)	(+5.08)	(+13.97)	(+6.66)			(+12.64)	(+6.33)	(+13.24)	(−3.83)	(+6.11)	(+1.14)	(+7.94)
10b	$CDCl_3$	—	42.35	131.53	139.25	124.40	12.59		136.90	133.36	120.59	136.99			120.86	132.84	135.04	145.68	128.64	128.03	125.68
7b	$CDCl_3$	50	161.58	132.46	145.57	135.51	12.88		151.97	138.44	134.75	143.32			134.60	139.11	148.77	142.03	134.40	129.02	133.01
			(+119.23)	(+0.93)	(+6.32)	(+11.11)	(+0.29)		(+15.07)	(+5.08)	(+14.16)	(+6.33)			(+13.74)	(+6.27)	(+13.73)	(−3.65)	(+5.76)	(+0.99)	(+7.33)
10c	$CDCl_3$	—	42.67	131.76	140.94	115.23	165.57 (s)	50.99 (q)	141.67	137.89	127.67	139.02			126.21	135.11	139.99	143.93	128.80	128.59	126.49
7c	MeCN-d_3	50	169.83	131.84	149.77	124.46	163.85 (s)	51.53 (q)	151.57	141.84	138.18	145.56			136.96	141.14	149.67	141.14	135.41	129.25	134.70
			(+127.16)	(+0.08)	(+8.83)	(+9.23)	(−1.72)	(+0.54)	(+9.90)	(+3.95)	(+10.51)	(+6.54)			(+10.75)	(+6.03)	(+9.68)	(−2.79)	(+6.61)	(+0.66)	(+8.21)
10d	$CDCl_3$	—	42.01	130.41	136.14	137.45	33.20 (s)	32.20 (q)	134.58	134.25	118.06	160.01	38.08 (s)	31.77 (q)	119.00	131.96	134.06	146.11	128.87	128.64	125.44
7d	$CDCl_3$	50	161.11	131.69	142.66	147.45	33.36 (s)	31.16 (q)	149.19	139.22	132.36	168.97	39.39 (s)	31.53 (q)	131.69	138.30	148.42	141.56	134.16	129.00	132.91
			(+119.10)	(+1.28)	(+6.52)	(+10.00)	(+0.16)	(−1.04)	(+14.61)	(+4.97)	(+14.30)	(+8.96)	(+1.31)	(−0.24)	(+12.69)	(+6.34)	(+14.36)	(−4.55)	(+5.22)	(+0.13)	(+7.47)
10e	CD_2Cl_2	—	42.99	133.18	137.27	116.11			139.92	135.95	120.37	161.47	38.69 (s)	31.95 (q)	120.92	132.81	133.94	146.35	129.00	128.42	126.11
7e	$CDCl_3$	50	164.20	133.28	145.54	126.24			152.77	140.45	133.89	169.45	39.65 (s)	31.60 (q)	133.22	138.68	146.49	141.58	134.50	129.02	132.16
			(+121.21)	(+0.10)	(+8.00)	(+10.13)			(+12.85)	(+4.50)	(+13.52)	(+7.98)	(+0.96)	(−0.35)	(+12.30)	(+5.87)	(+12.55)	(−4.77)	(+5.50)	(+0.60)	(+6.05)
10f	$CDCl_3$	—	42.35	130.62	137.11	137.72	33.23 (s)	33.17 (q)	135.83	135.13	120.25	136.75			120.83	132.97	135.41	145.77	128.61	127.94	125.59
7f	$CDCl_3$	50	162.16	131.88	143.71	147.80	33.40 (s)	31.11 (q)	150.45	140.08	134.41	143.44			134.17	139.29	149.93	141.64	134.17	129.08	133.19
			(+119.81)	(+1.26)	(+6.60)	(+10.39)	(+0.17)	(−2.06)	(+14.62)	(+4.95)	(+14.16)	(+6.69)			(+13.34)	(+6.32)	(+14.52)	(−4.13)	(+5.56)	(+1.14)	(+7.60)

a) $\Delta\delta$ values are shown in the parentheses.

Table 9. ^{13}C NMR Chemical Shifts (ppm) of (1-Azulenyl)diphenylmethyl Cations (**8**) and the Corresponding Hydro Derivatives (**11**)[a)]

	Solvent	Temp	Assignment															
		°C	CH or C$^+$	1	2	3	3-sub	3a	4	5	6	6-sub	6-sub	7	8	8a	1′	2′,6′	3′,5′	4′
11a	$CDCl_3$	—	49.79	132.05	138.09	116.53		140.89	136.56	121.93	137.17			122.48	133.48	135.28	144.67	129.00	128.09	125.95
11b	$CDCl_3$	—	49.58	130.41	139.16	124.46	12.59	139.16	136.93	120.80	137.14			121.04	132.87	135.14	144.77	129.00	128.06	125.89
11c	$CDCl_3$	—	49.70	131.53	140.92	115.04	165.47 (s)	50.89 (q)	141.50	137.72	127.51	138.88		126.08	135.19	140.25	143.88	129.00	128.30	126.26
8c	$CDCl_3$	—	177.68	135.45	151.70	129.53	163.04 (s)	52.39 (q)	157.04	143.59	143.96	148.56		142.22	144.14	154.14	139.90	135.45	129.53	135.45
			(+127.98)	(+3.92)	(+10.78)	(+14.49)	(−2.43)	(+1.50)	(+15.54)	(+5.87)	(+16.45)	(+9.68)		(+16.14)	(+8.95)	(+13.89)	(−3.98)	(+6.45)	(+1.23)	(+9.19)
11d	$CDCl_3$	—	49.67	129.19	135.89	137.48	33.17 (s)	32.20 (q)	135.01	134.49	118.42	160.35	38.11 (s) 31.74 (q)	119.22	132.11	134.00	144.89	129.03	128.00	125.77
8d	$CDCl_3$	50	168.58	136.90	142.45	154.58	33.48 (s)	30.03 (q)	159.07	141.38	142.66	174.07	40.31 (s) 31.37 (q)	141.53	139.19	154.83	140.83	134.64	129.43	133.61
																	139.70	133.55	128.88	133.03
			(+118.91)	(+7.71)	(+6.56)	(+17.10)	(+0.31)	(−2.17)	(+24.06)	(+6.89)	(+24.24)	(+13.72)	(+2.20)	(−0.37)	(+22.31)	(+7.08)	(+20.83)	(−4.63)	(+5.07)	(+1.16)	(+7.55)
11e	$CDCl_3$	—	49.73	131.59	137.17	115.92		139.55	135.65	120.16	160.89	38.39 (s)	31.83 (q)	120.59	132.60	134.09	144.86	129.03	128.06	125.86
11f	$CDCl_3$	—	49.73	129.58	136.93	137.75	33.20 (s)	32.17 (q)	136.23	135.28	120.43	136.93		121.04	133.03	135.28	144.74	129.00	128.03	125.86
8f	$CDCl_3$	50	170.16	136.81	147.17	154.46	33.54 (s)	30.06 (q)	160.01	142.24	143.52	143.83		142.66	141.93	156.63	141.15	134.98	129.52	133.91
																	140.10	133.91	129.00	133.45
			(+120.43)	(+7.23)	(+10.24)	(+16.71)	(+0.34)	(−2.11)	(+23.78)	(+6.96)	(+23.09)	(+6.90)		(+21.62)	(+8.90)	(+21.35)	(−4.12)	(+5.45)	(+1.23)	(+7.82)

a) $\Delta\delta$ values are shown in the parentheses.

two diastereomeric sets of enantiomers, as illustrated in Fig. 4. One set of enantiomers (A and $\overline{A}$, hereafter $A\overline{A}$) has C_3 symmetry (symmetrical propellers) and each enantiomer has three equivalent methyl groups. The other set of enantiomers (B and $\overline{B}$, hereafter $B\overline{B}$) has C_1 symmetry (unsymmetrical propellers) and each enantiomer has three nonequivalent methyl groups. Therefore, the low-temperature ^{1}H NMR spectrum exhibited four signals in the methyl region attributed to a mixture of diastereomers ($A\overline{A}$ and $B\overline{B}$). The lower field three resonances (a, b, and c) correspond to those of $B\overline{B}$, while the more intense peak (d) is assigned to those of $A\overline{A}$. The spectrum of **6b** at −60 °C was consistent with the postulated propeller geometry for the ground-state conformation, and with a ratio of $B\overline{B}$ to $A\overline{A}$ of 3.0 : 1.4. The spectrum of **6b** at 60 °C indicated that the three azulene rings were rapidly rotating at this temperature, and that the spectrum was easily analyzable using simple decoupling techniques.

The propeller geometry of **6b** was also supported by an X-ray crystallographic analysis.[48)] A crystal of **6b** was grown by slow evaporation of a THF/dichloromethane solution with the incorporation of one molecule of THF for each cation. Two crystallographically independent molecules were found in the unit cell, which had both approximate C_3 symmetries (symmetrical propellers such as $A\overline{A}$). However, we could not refine the structure of **6b**. Therefore, the accurate structure of **6b** could not be obtained by the X-ray crystallographic analysis.

^{1}H NMR spectra (600 MHz, methyl region) of **6b** at various temperatures are shown in Fig. 5. When the sample was warmed to ca. −5 °C, noticeable line broadening occurred, and further warming resulted in the coalescence of all four peaks to a singlet, which became sharp at ca. 60 °C. Possible interconversions of the stereoisomers for **6b** were analyzed by the flip mechanism. Their four flip mechanisms are illustrated in Fig. 6. We label the methyl groups of $A\overline{A}$ and $B\overline{B}$ of **6b** by the same letters, a—d, corresponding to the low-temperature NMR spectrum, for convenience. The asterisks show the positions of a methyl group during the course of interconversions. There are a total of nine distinct pathways for all possible interconversions for **6b**.

In the zero-ring flip connecting A and $\overline{A}$ (Fig. 6a), since no methyl group interconverts, the process is not detectable by the temperature-dependent ^{1}H NMR spectra. Similarly, the zero-ring flip connecting B and $\overline{B}$ also cannot be observed for the same reason. Furthermore, the transition state of the zero-ring flip in which all three azulene rings rotate through the reference plane, is unfavorable on steric grounds. Therefore, these mechanisms were excluded from an analysis of the temperature-dependent ^{1}H NMR spectra of **6b**.

The one- and two-ring flips connecting B and $\overline{B}$ comprise hexagonal cyclic interconversions, and each B and

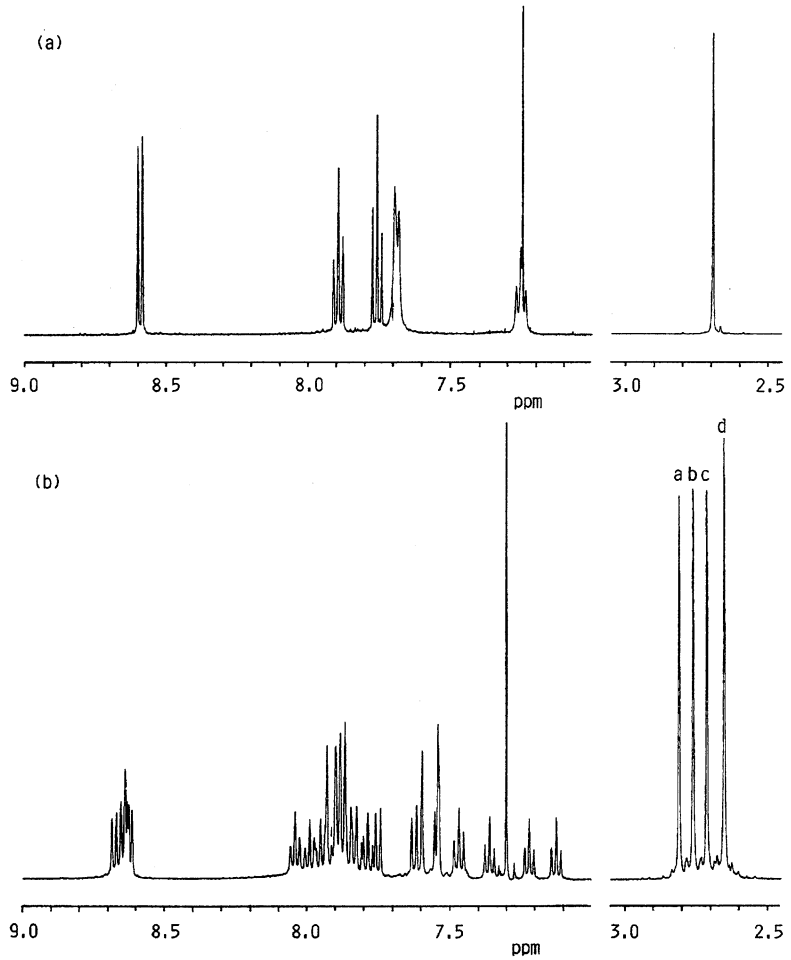

Fig. 3. ^{1}H NMR spectra of **6b** (600 MHz) in $CDCl_3$. (a) at 60 °C; (b) at −60 °C.

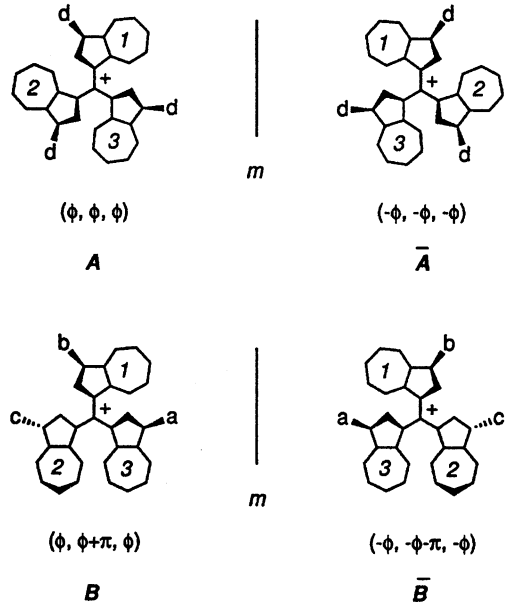

Fig. 4. Stereoisomers of **6b**, which are characterized by the torsion angles of the three azulene rings.

$\overline{B}$ is interconverted to A or $\overline{A}$ by each mechanism. Therefore, each of these mechanisms makes up the cubic type interconversions, as illustrated in Figs. 6b and 6c, respectively.

There are a total of three distinct pathways for the one-ring flips. In the one-ring flip interconverting A and $\overline{B}$ (or $\overline{A}$ and B), the three methyl groups (a, b, and c) of $B\overline{B}$ interconvert to those (d) of $A\overline{A}$; therefore, these processes cause a coalescence of all four methyl resonances (a, b, c, and d) of $A\overline{A}$ and $B\overline{B}$ to a singlet. In the other two, one-ring flips interconverting B and $\overline{B}$, a and b interconvert to c with different rates, which show the coalescence of all four methyl resonances (a, b, c, and d) of $A\overline{A}$ and $B\overline{B}$ to two lines. There are a total of three idealized transition states of the mechanism. The nonflipping two azulene rings at the transition states are oriented in two types of parallel ($B\overline{B}$) and an antiparallel ($A\overline{B}$) relationships, as shown in Fig. 6b. The interconversion of $B\overline{B}$ through one-ring flips must be unfavorable compared to those of A and $\overline{B}$ (or $\overline{A}$ and B) on the steric interaction of the non-flipping two azulene rings at the transition state of the rotation. Therefore, three exchanges (a→d, b→d, and c→d) of the methyl groups by A and $\overline{B}$ (or $\overline{A}$ and B) should be observed as preferred interconversions in the one-ring flip mechanism.

The two-ring flip interconverting A and $\overline{B}$(or $\overline{A}$

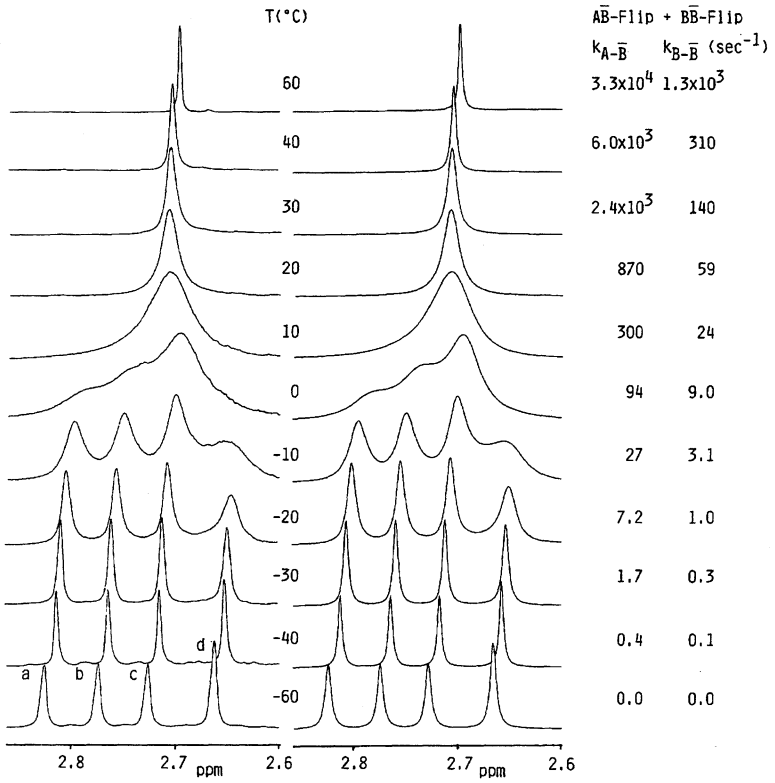

Fig. 5. ^{1}H NMR of **6b** (600 MHz, methyl region) in $CDCl_3$ at various temperatures. The left-hand panel displays the experimental spectra. The right-hand panel shows the calculated spectra for the combination of the $A \rightarrow \overline{B}$ (or $\overline{A} \rightarrow B$) and $B \rightarrow \overline{B}$ flip.

and B) also causes three energetically equal exchanges (a→d, b→d, and c→d) of the methyl groups, which coalesce all four methyl resonances (a, b, c, and d) of $A\overline{A}$ and $B\overline{B}$ to a singlet. The enantiomeric two-ring flips, which interconvert B and $\overline{B}$, causes energetically equal exchanges (a→b, a→c, and b→c) of the methyl groups, and coalesce the three methyl signals (a, b, and c) to a singlet. Interconversions of $B\,\overline{B}$ are favorable compared to those of $A\overline{B}$ (and $\overline{A}B$) on the steric interaction of the flipping two azulene rings at the transition state of the rotation, because the anti-parallel arrangement of the two azulene rings (transition state of $B\overline{B}$) is considered to reduce the steric interaction at the transition state, compared with the parallel arrangement (that of $A\overline{B}$). Therefore, three exchanges of the methyl groups by $B\overline{B}$ should be observed as preferred interconversions in the two-ring flip mechanism.

Since no methyl group interconverts in the three-ring flip connecting A and $\overline{A}$ (Fig. 6d), the process is not also detectable by the temperature-dependent ^{1}H NMR spectra. Therefore, the only process to be considered is the enantiomerization of B and $\overline{B}$, which renders two azulenyl groups enantiotopic. However, the three-ring flip, in which all three rings rotate through planes perpendicular to the reference plane, were also ruled out from an analysis of the temperature-dependent NMR spectra of **6b** on steric grounds.

The analysis indicates that the only mechanisms which can explain the variable temperature ^{1}H NMR spectra of **6b** are those which interconvert A and $\overline{B}$ (and $\overline{A}$ and B), i.e., the appropriate one- or two-ring flip, or a combination of these with other pathways.

On the basis of the analysis mentioned above, a simulation of the variable-temperature ^{1}H NMR spectra of **6b** was accomplished by iteratively employing three energetically equal exchanges (a→d, b→d, and c→d) of the methyl groups of $A\overline{B}$ interconversions and those (a→b, a→c, and b→c) of $B\overline{B}$.[49,50]

The simplest explanation for the observed coalescence is the sole operation of the process $A \rightarrow \overline{B}$ (or $\overline{A} \rightarrow B$). A calculation of ^{1}H NMR line shape expected for the process $A \rightarrow \overline{B}$ (or $\overline{A} \rightarrow B$) was found to be in good agreement with the experimental spectra. Thus, the dynamic stereochemistry of **6b** mainly depends on the process $A \rightarrow \overline{B}$ (or $\overline{A} \rightarrow B$). Furthermore, a better fit with the experimental spectra was obtained by a consideration of the process $B \rightarrow \overline{B}$, which is also shown in Fig. 5.

The spectral data permitted a calculation of the energy relationships among the stereoisomers of **6b** and the magnitudes of the barriers separating these isomers. The relative intensities of the ^{1}H NMR signals at −60 °C show that $B\overline{B}$ is slightly more stable than $A\overline{A}$ at this temperature. As the sample is warmed, the population of $B\overline{B}$ increases relative to that of $A\overline{A}$. Qualitatively, this indicates a positive $\Delta S°$ value for the equilibrium $A\overline{A} \rightarrow B\overline{B}$. A plot of ΔG_T° (derived from the simulation of the temperature-dependent ^{1}H NMR over the range from −60 to 60 °C) yields, for the equi-

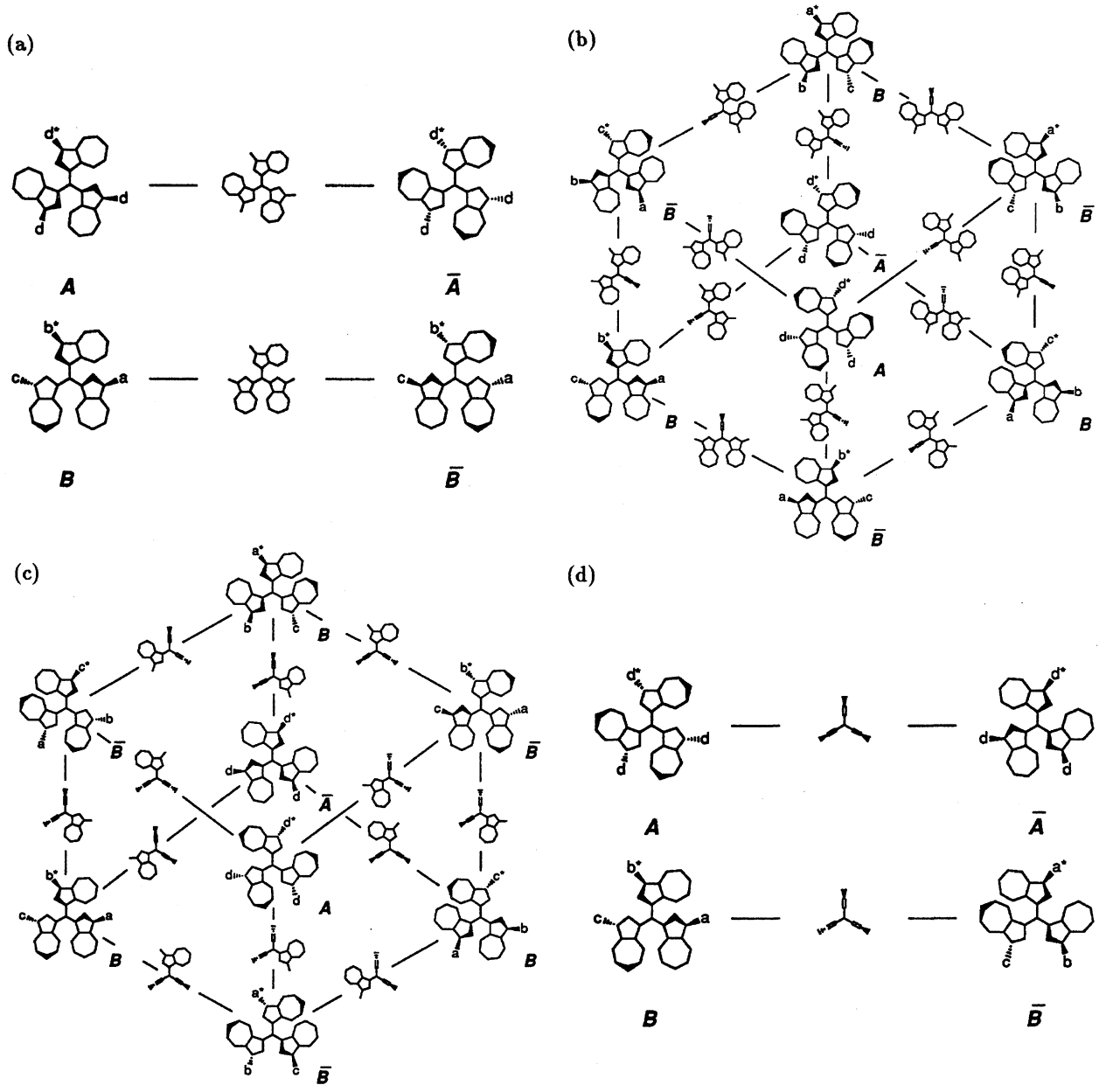

Fig. 6. Possible interconversion of the stereoisomers ($A\overline{A}$ and $B\overline{B}$) and the idealized chemical transition state for **6b**. (a) Zero-ring flip mechanism; (b) One-ring flip mechanism; (c) Two-ring flip mechanism; (d) Three-ring flip mechanism.

librium $A\overline{A} \rightarrow B\overline{B}$, $\Delta H^\circ = 5.4 \pm 0.4$ kJ mol^{-1} and $\Delta S^\circ = 29 \pm 1.3$ J K^{-1} mol^{-1}. The temperature at which ΔG° is equal to zero (crossover temperature) is therefore ca. -89 °C. The major part of the entropy difference is accounted for by the difference in symmetry (C_3 vs. C_1) of the two diastereomers ($A\overline{A}$ and $B\overline{B}$).

The rate data was used to calculate the free energies of activation for the various exchange processes at 20 °C. The results are shown schematically in Fig. 7. For the equilibrium $B\overline{B} \rightarrow A\overline{A}$, ΔG°_{20} is 3.2 ± 0.5 kJ mol^{-1}. For the conversion of $B\overline{B}$ to $A\overline{A}$, the calculations yielded $\Delta G^{\neq}_{20} = 58.7 \pm 5.2$ kJ mol^{-1}, and for the reverse reaction ($A\overline{A} \rightarrow B\overline{B}$) $\Delta G^{\neq}_{20} = 55.5 \pm 5.1$ kJ mol^{-1}. The barrier to enantiomerization of B and $\overline{B}$ is $\Delta G^{\neq}_{20} = 61.8 \pm 5.1$ kJ mol^{-1}. Thus, at 20 °C the interconversion of $B\overline{B} \rightarrow A\overline{A}$ is energetically more favorable by 3.1 kJ mol^{-1} than that of $B\overline{B} \rightarrow B\overline{B}$. Therefore, the lowest energy pathway for the observed isomerizations of **6b** is the one-ring flip. A conjugative interaction between cationic carbon (C^+) and three azulene rings for **6b** largely contributes to the transition state of the ring flipping as well as to the ground state. Consequently, the two-ring flip process for **6b** becomes less stable than that of a one-ring flip.

Dynamic Stereochemistry of 7b. 3,3′-Dimethyl derivative (**7b**) was utilized for the analysis of the

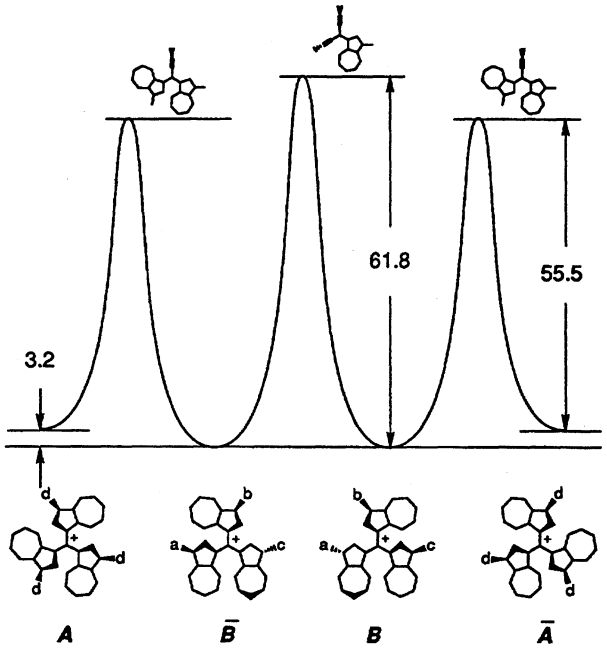

Fig. 7. Schematic representation of the energetics (ΔG/kJ mol^{-1} at 20 °C) for the stereoisomerization of **6b**.

dynamic stereochemistry of **7** to avoid the complexities of the temperature dependent NMR spectra, and was also analyzed by the flip mechanism. The dynamic stereochemistry of **7b** was established by utilizing a flip mechanism of one azulene ring between three conformers as the threshold rotation mechanism.

The ^{1}H NMR (600 MHz, methyl region) spectra of **7b** in 50% CD_2Cl_2/CS_2 at various temperatures are shown in Fig. 8. At −100 °C the NMR consists, in the methyl region, of four signals (as indicated a, b, c, and d) in the ratio of intensities of ca. 1.2 : 1.2 : 3 : 1. Six isomeric propeller conformations (including stereoisomers) are possible for a molecule of this type. The possibilities of stereoisomerism and isomerization may be analyzed by flip mechanism. These isomers consist of the three diastereomeric sets of enantiomer illustrated in Fig. 9. One set of enantiomers (A and $\overline{A}$) have C_1 symmetry and each enantiomer has two nonequivalent methyl groups. The other two sets of enantiomers (B, $\overline{B}$, C, and $\overline{C}$) have C_2 symmetry and each set of enantiomers has two equivalent methyl groups. Therefore, the ^{1}H NMR spectrum at −100 °C exhibits four resonance signals in the methyl region attributable to a mixture of diastereomers. On the basis of the analysis given above, two resonances (a and b) in the higher field correspond to those of A (and $\overline{A}$). However, the other more intense peak (c) and the remaining less intense peak (d) are assigned to those of B (and $\overline{B}$) and C (and $\overline{C}$), respectively, by considering their stabilities based on the analysis of molecular models. Thus, the spectrum of **7b** at −100 °C is consistent with the postulated propeller geometry for the ground state conformation,

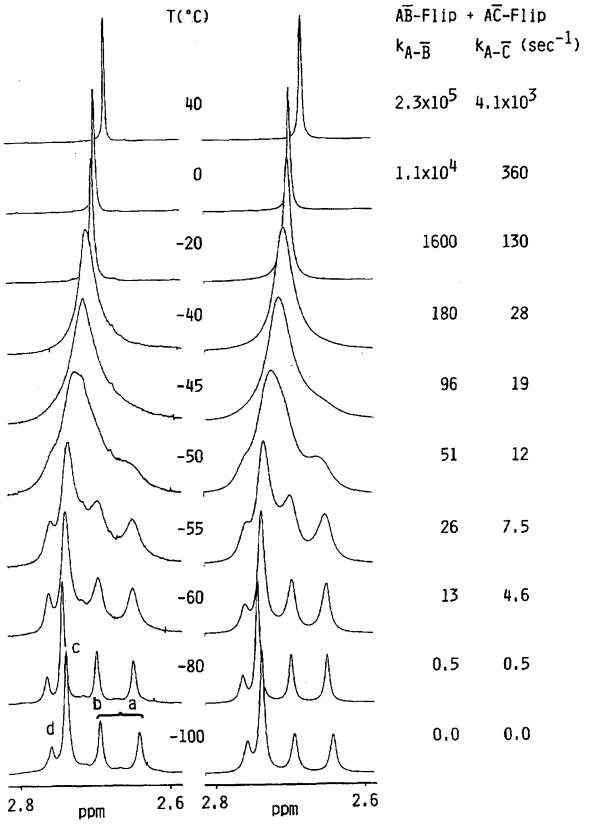

Fig. 8. ^{1}H NMR of **7b** (600 MHz, methyl region) at various temperatures. The left-hand panel displays the experimental spectra. The right-hand panel shows the calculated spectra for the combination of the $A \rightarrow \overline{B}$ (or $\overline{A} \rightarrow B$) and $A \rightarrow \overline{C}$ (or $\overline{A} \rightarrow C$) flips.

and with a ratio of $A\overline{A} : B\overline{B} : C\overline{C}$ of 2.4 : 3 : 1.

When the sample was warmed to ca. −50 °C, noticeable line broadening occurred and further warming resulted in a coalescence of all four peaks to a singlet, which became sharp at 40 °C. Possible interconversions of the stereoisomers of **7b** are described by the flip mechanism. The four flip mechanisms of **7b** are illustrated in Fig. 10.

In the zero-ring flip, although each conformer ($A\overline{A}$, $B\overline{B}$, and $C\overline{C}$) interconverts to its enantiomer, no methyl group interconverts in this mechanism (Fig. 10a). In one- and two-ring flip, since each conformer interconverts to the other three isomers having opposite helicities, the mechanisms consist of cubic-type interconversions, as shown in Figs. 10b and 10c, respectively. In the one-ring flip, the $A\overline{B}$ (or $\overline{A}B$) and $A\overline{C}$ (or $\overline{A}C$) interconversions consist of two sets of exchanges of methyl groups (a→c, b→c and a→d, b→d) (Fig. 10b). Whereas, in the two-ring flip, two energetically different exchanges (a→b, c→d) are represented by $A\overline{A}$ and $B\overline{C}$ (or $\overline{B}C$) interconversions in addition to the two sets of exchanges (a→c, b→c and a→d, b→d), which are identical with the one-ring flip mechanism (Fig. 10c). Enantiomerization of A and $\overline{A}$, and interconversions of $B\overline{C}$ (or $\overline{B}C$) will occur via three-ring flip (Fig. 10d). The

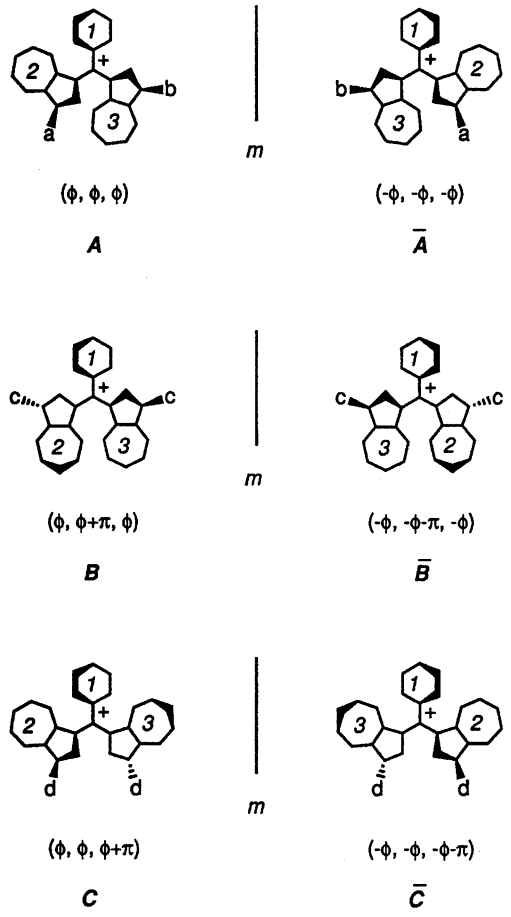

Fig. 9. Stereoismers of **7b**.

three-ring flip process has two exchanges (a→b, c→d) of methyl groups. These analyses also indicate that the flip of the phenyl ring, which has local C_2 symmetry, does not affect the temperature dependence of the methyl groups. The temperature-dependent ^{1}H NMR of **7b** showed complex signals in the olefinic region. Therefore, information concerning the rotation of the phenyl ring could not be obtained.

Simulation[49,50] of the variable temperature ^{1}H NMR spectra of **7b** by consideration of only two sets of exchanges (a→c, b→c and a→d, b→d) of methyl groups by $A\overline{B}$ (or $\overline{A}B$) and $A\overline{C}$ (or $\overline{A}C$) interconversions matches the experimental spectra. The results of the simulation are also shown in Fig. 8. The analysis indicates that the mechanism, which can explain the temperature dependence of methyl groups, is a one-ring flip of azulene or a two-ring flip of azulene and phenyl rings, or a combination of these pathways. Therefore, the flip of one azulene, regardless of the flip of phenyl ring, is a threshold rotation mechanism of **7b**. The two azulene rings do not flip simultaneously.

The spectral data permitted a calculation of the energy relationships among the stereoisomers of **7b** and the magnitudes of the barriers separating these isomers. The relative intensities of the NMR signals at −100 °C show that $B\overline{B}$ is slightly more stable than $A\overline{A}$ or $C\overline{C}$ at this temperature. As the sample is warmed, the population of $A\overline{A}$ increases relative to that of $B\overline{B}$ or $C\overline{C}$. An analysis of the temperature-dependent NMR over the range −100 °C to −60 °C yields, for the equilibrium $A\overline{A}\rightarrow B\overline{B}$, $\Delta H^\circ = -2.0\pm0.3$ kJ mol^{-1} and $\Delta S^\circ = -9.4\pm1.4$ J K^{-1} mol^{-1} and, for $A\overline{A}\rightarrow C\overline{C}$, $\Delta H^\circ = -3.5\pm0.7$ kJ mol^{-1} and $\Delta S^\circ = -27\pm3.5$ J K^{-1} mol^{-1}. The crossover temperatures are therefore, for $A\overline{A}\rightarrow B\overline{B}$, ca. −61 °C and, for $A\overline{A}\rightarrow C\overline{C}$, ca. −145 °C. The major part of the entropy difference is accounted for by the difference in the symmetry (C_2 vs. C_1) of the two diastereomers.

The rate data determined by line-shape analysis were used to calculate the free energies of activation for the various exchange processes at 20 °C. The results are shown schematically in Fig. 11. For the equilibrium $A\overline{A}\rightarrow B\overline{B}$, ΔG°_{20} is 0.8±0.5 kJ mol^{-1} and, for $A\overline{A}\rightarrow C\overline{C}$, ΔG°_{20} is 4.5±1.2 kJ mol^{-1}. For the conversion of $A\overline{A}$ to $B\overline{B}$, the calculations yielded $\Delta G^{\neq}_{20}=45.2\pm4.3$ kJ mol^{-1}, and for the reverse reaction ($B\overline{B}\rightarrow A\overline{A}$) $\Delta G^{\neq}_{20}=44.4\pm4.3$ kJ mol^{-1}. The barrier for the conversion of $A\overline{A}$ to $C\overline{C}$ is $\Delta G^{\neq}_{20}=53.8\pm4.3$ kJ mol^{-1}, and for the reverse reaction ($C\overline{C}\rightarrow A\overline{A}$) $\Delta G^{\neq}_{20}=49.3\pm4.5$ kJ mol^{-1}. Therefore, the flip of one azulene is a threshold rotation mechanism for **7b**.

Dynamic Stereochemistry of 8a. ^{1}H NMR (400 MHz) spectra of **8a** in $CDCl_3$ at various temperatures are shown in Fig. 12. At −60 °C the NMR comprises two sets of *p*- and *o*-phenyl proton signals (as indicated a and b) with equal intensities, single *m*-phenyl proton signals, and a azulenyl proton signals in the aromatic region. The two *p*-phenyl proton signals corresponds to the restricted rotation of the azulene ring, and the only two *o*-phenyl proton signals indicates that the two phenyl rings are rapidly rotating, even at −60 °C, unless the accidental chemical shifts are equivalent. When the sample was warmed to −20 °C, noticeable line broadening of the *o*- and *p*-phenyl proton signals occurred, and further warming resulted in a coalescence of the four signals, which became a set of sharp signals at 60 °C. Therefore, the spectrum change of the phenyl region corresponds to a rotation of the azulene ring.

Simulations of the variable temperature ^{1}H NMR spectra in the phenyl region of **8a** were accomplished in a similar manner to those of others (**6b** and **7b**). The rate data determined by a line-shape analysis were used to calculate the free energies of activation for the process at 20 °C. The calculation yielded the rotational barrier of the azulene ring for **8a** ($\Delta G^{\neq}_{20}=52.9\pm2.5$ kJ mol^{-1}).

In contrast to **8a**, ^{13}C NMR spectra of *t*-butyl derivatives (**8d** and **8f**) in $CDCl_3$ at 50 °C showed eight phenyl carbon signals attributed to two set of *ipso*-, *o*-, *m*-, and *p*-positions. These results indicate the restricted rotation of the azulene ring and the rapid rotation of the phenyl rings at 50 °C, unless the accidental chemical shifts are equivalent. Therefore, the rotational barriers

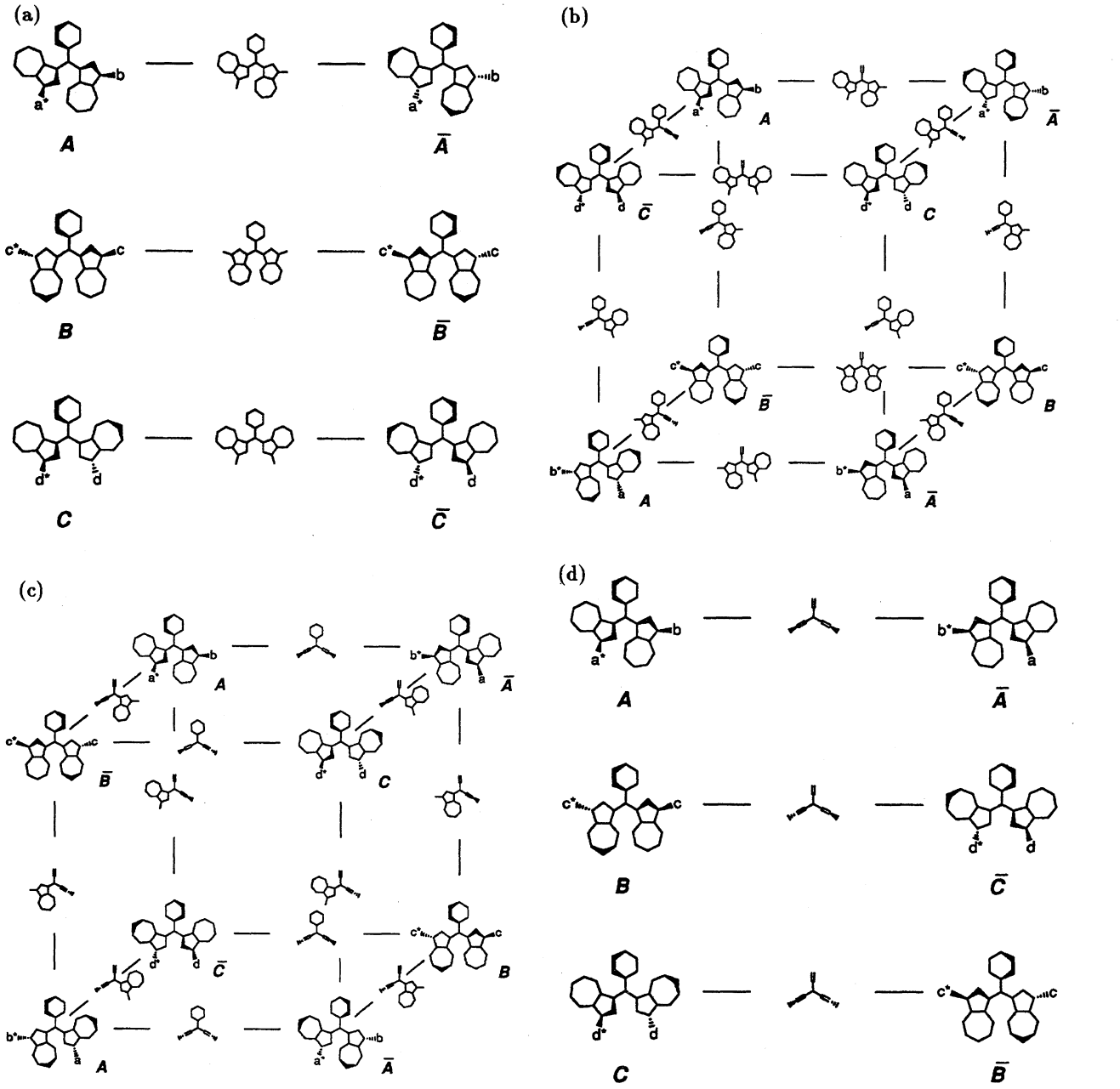

Fig. 10. Four-flip mechanisms of **7b**. (a) Zero-ring flip mechanism; (b) One-ring flip mechanism; (c) Two-ring flip mechanism; (d) Three-ring flip mechanism.

($\Delta G^{\neq}_{50}$) of those for **8d** and **8f** were calculated to be over 68.6 kJ mol^{-1}. These results show that the *t*-butyl groups increase the π-donation of the azulene rings. Consequently, the *t*-butyl groups stabilize the carbocations to a considerable extent.

Conclusions

In conclusion, the stabilities of a series of azulene analogues (**6**, **7**, and **8**) of triphenylmethyl cation (**3**) dramatically increase with the number of azulene rings, and the introduction of bulky *t*-butyl groups to each of the three azulene rings further increase their stabilities.

The lowest energy pathway for the observed isomerizations of **6** is a one-ring flip process, which is the first example for a dynamic stereochemistry of molecular propellers. Therefore, the threshold rotational mechanisms for molecular propellers are not uniformly of the two-ring flip type. The mechanisms switch from a two-ring flip to a one-ring flip due to conjugative interactions of the central atoms and steric effects between the three rings. These results indicate that the conjugative effects largely contribute to the transition state of the ring flipping as well as to the ground state. Consequently, (1-azulenyl)methyl cations (**6**, **7**, and **8**) show unique dynamic stereochemical behaviors.

Experimental

General. The melting points were determined on a

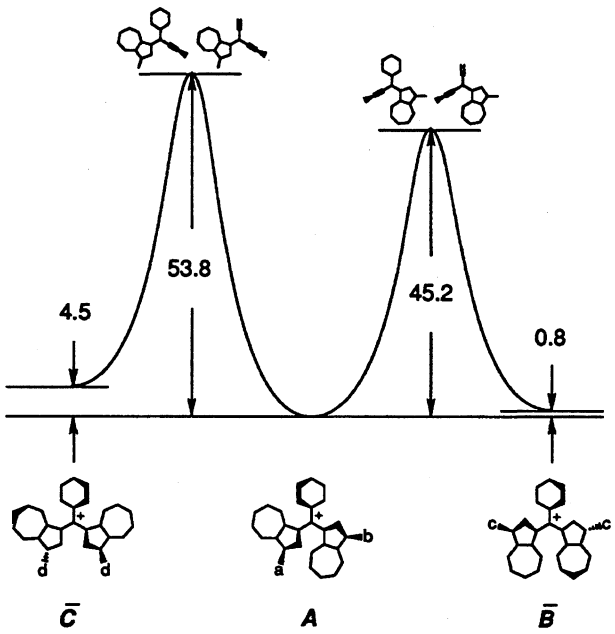

Fig. 11. Schematic representation of the energetics (ΔG/kJ mol^{-1} at 20 °C) of the stereoisomerization of **7b**.

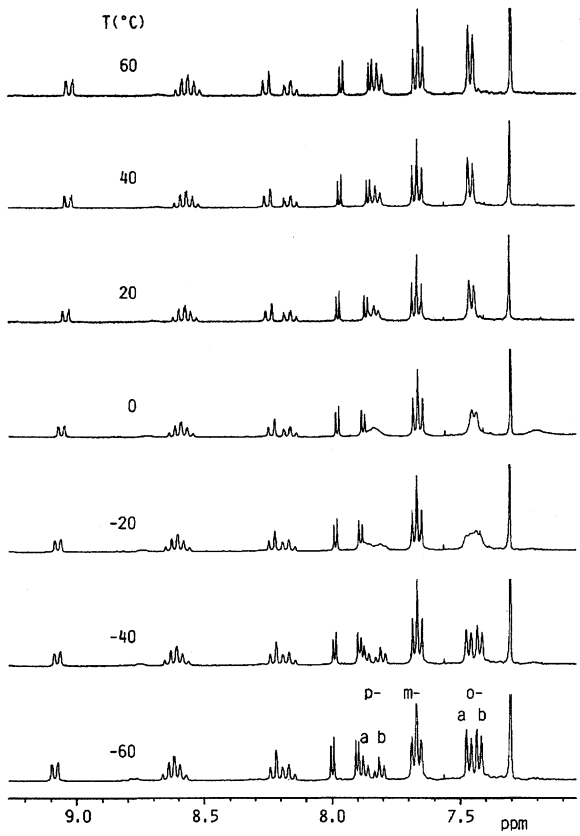

Fig. 12. ^{1}H NMR spectra of **8a** (400 MHz) at various temperatures in $CDCl_3$.

Yanagimoto micro melting-point apparatus (MP-S3) and are uncorrected. Electron-impact mass spectra were obtained on a JEOL HX-110 instrument usually at 70 eV. IR and UV spectra were measured by on a Hitachi 215 or 270-30 and a Hitachi 340 or U-3410 spectrophotometer, respectively. ^{1}H NMR spectra were recorded on a Hitachi R-90H at 90 MHz, a JEOL GSX-270 at 270 MHz, a JEOL GSX-400 at 400 MHz, or a Bruker AM-600 spectrometer at 600 MHz. ^{13}C NMR spectra were recorded on a Hitachi R-90H at 22.5 MHz, a JEOL GSX-400 at 100 MHz, or a Bruker AM-600 spectrometer at 150 MHz. Temperatures were calibrated by the chemical shift separation of the protons of a 4% methanol in CD_3OD sample, and are considered to be accurate to ±2 °C. Medium-pressure chromatographic separations were performed using a Kusano prepacked column Si-50. Gel-permeation chromatographies (GPC) were performed on Showadenko Shodex K2001 and K2002. Voltammetry measurements were carried out with a BAS100B/W electrochemical workstation equipped with Pt working and auxiliary electrodes, and a reference electrode formed from $Ag/AgNO_3$ (0.01 M, 1 M=1 mol dm^{-3}) and tetrabutylammonium perchlorate solution (0.1 M) in MeCN. All measurements were made under argon on a 1 mM sample of the substrate in 10 ml of dry MeCN containing 0.1 M tetraethylammonium perchlorate (TEAP) as a supporting electrolyte, at a scan rate of 100 mV s^{-1}. Elemental analyses were performed at the Instrumental Analysis Center of Chemistry, Faculty of Science, Tohoku University.

6-*t*-Butylazulene (13e). A mixture of 2,4-dinitrochlorobenzene (20.2 g, 99.7 mmol) and 4-*t*-butylpyridine (25.0 g, 185 mmol) was stirred at 80 °C for 4 h, during which time a yellow precipitate was formed. After cooling to 0 °C, dimethylamine (15.0 ml, 226 mmol) and dry pyidine (100 ml) were added dropwise. The resulting reddish-brown reaction mixture was warmed to room temperature and stirred for 12 h. Then, cyclopentadiene (6.10 g, 101 mmol) and 2.5 M sodium methoxide solution (40 ml) were added dropwise to the reaction mixture. After the addition was complete, stirring was continued for another 4 h. The mixture was heated under a N_2 atmosphere, and a mixture of pyridine and methanol was distilled off until the temperature reached 105 °C. Then, dry pyridine (130 ml) was added and the blue mixture was heated for 12 h. After cooling to room temperature, the pyridine was removed under reduced pressure. The blue residue was extracted in a Soxhlet apparatus with hexane and the solvent was removed under reduced pressure. The blue residue was purified by column chromatography on silica gel with hexane to yield the azulene **13e** (18.3 g, 99%). Blue plates; mp 95.0—96.0 °C (hexane); MS (70 eV) *m/z* (rel intensity) 184 (M^+, 100), 169 (75), 154 (26), 153 (28), 152 (27), 141 (36), and 128 (27); IR (KBr disk) 2968, 1586, 1476, 1406, 836, and 748 cm^{-1}; UV (hexane) 237 (log ε 4.14), 278 (4.77), 284 (4.77), 330 (3.54), 344 (3.71), 548 (2.39), 569 (2.48), 592 (2.44), 619 (2.45), 647 (2.14), and 684 nm (2.14); ^{1}H NMR (90 MHz, $CDCl_3$) δ=8.28 (d, J=11.0 Hz, 2H), 7.81 (br, 1H), 7.33 (d, J=11.0 Hz, 2H), and 1.44 (s, 9H); ^{13}C NMR (22.5 MHz, $CDCl_3$) δ=160.62 (s), 138.76 (s), 135.86 (d), 120.59 (d), 117.23 (d), 38.36 (s), and 31.86 (q). Found: C, 91.05; H, 8.74%. Calcd for $C_{14}H_{16}$: C, 91.25; H, 8.75%.

1,6-Di-*t*-butylazulene (13d). $AlCl_3$ (13.9 g, 105 mmol) was added to a solution of 6-*t*-butylazulene (**13e**) (18.5 g, 100 mmol) and *t*-butyl chloride (18.6 g, 201 mmol) in CH_2Cl_2 (1 l). After stirring at room temperature for 30 min, the reaction mixture was poured into water. The organic

layer was washed with water, dried with $MgSO_4$, and concentrated in vacuo. The mixture was separated by column chromatography on silica gel with hexane, and medium-pressure column chromatography on silica gel with hexane to afford 1,6-di-*t*-butylazulene (**13d**), (13.6 g, 56%), 1,3,6-tri-*t*-butylazulene (**19**) (4.45 g, 15%), and the recovered **13e** (2.97 g, 16%).

13d: Blue needles; mp 42.0—44.0 °C (sublimination); MS (70 eV) *m/z* (rel intensity) 240 (M^+, 36) and 225 (100); IR (KBr disk) 2972, 2912, 2876, 1578, 1410, 1394, 836, and 760 cm^{-1}; UV (hexane) 241 ($\log\varepsilon$ 4.00), 282 (4.66), 287 (4.63), 292 (4.59), 339 (3.42), 349 (3.42), 349 (3.58), 365 (3.21), 594 (2.46), 651 (2.38), and 723 nm (1.96); ^{1}H NMR (90 MHz, $CDCl_3$) δ=8.60 (d, J=10.8 Hz, 1H), 8.15 (d, J=10.6 Hz, 1H), 7.73 (br, 1H), 7.22 (dd, J=10.8, 1.5 Hz, 1H), 7.17 (dd, J=10.8, 1.5 Hz, 1H), 1.58 (s, 9H), and 1.41 (s, 9H); ^{13}C NMR (22.5 MHz, $CDCl_3$) δ=160.16 (s), 140.10 (s), 138.79 (s), 135.31 (d), 134.43 (d), 134.34 (d), 133.21 (s), 119.73 (d), 118.48 (d), 115.65 (d), 38.08 (s), 33.26 (s), 32.17 (q), and 31.77 (q). Found: C, 89.79; H, 10.04%. Calcd for $C_{18}H_{24}$: C, 89.94; H, 10.06%.

19: Blue needles; mp 134.0—135.0 °C (MeOH); MS (70 eV) *m/z* (rel intensity) 296 (M^+, 47), 282 (25), and 281 (100); IR (KBr disk) 2972, 2908, 2872, 1580, 1464, 1392, 1364, 1242, 1212, and 830 cm^{-1}; UV (hexane) 244 ($\log\varepsilon$ 4.07), 287 (4.73), 291 (4.73), 296 (4.69), 346 (3.52), 355 (3.71), 373 (3.61), 619 (2.44), 672 (2.34), and 748 (1.89); ^{1}H NMR (90 MHz, $CDCl_3$) δ=8.52 (d, J=11.2 Hz, 2H), 7.65 (s, 2H), 7.11 (d, J=11.2 Hz, 2H), 1.57 (s, 18H), and 1.43 (s, 9H); ^{13}C NMR (22.5 MHz, $CDCl_3$) δ=159.83 (s), 136.32 (s), 134.25 (s), 134.00 (d), 133.70 (d), 117.72 (d), 33.20 (s), 32.23 (s), 31.62 (q), and 31.80 (q). Found: C, 88.76; H, 11.01%. Calcd for $C_{22}H_{32}$: C, 89.12; H, 10.88 %.

1-*t*-Butylazulene (13f). The reaction of azulene (**13a**) (6.41 g, 50.0 mmol) with *t*-butyl chloride (9.28 g, 100 mmol) in CH_2Cl_2 (500 ml) in the presence of $AlCl_3$ (6.71 g, 50.4 mmol) at room temperature for 30 min afforded 1-*t*-butylazulene (**13f**) (5.02 g, 54%), 1,3-di-*t*-butylazulene (**20**) (1.10 g, 10%), and the recovered **13a** (1.66 g, 26%).

13f: Blue oil (Ref. 42; blue oil); ^{1}H NMR (90 MHz, $CDCl_3$) δ=8.65 (d, J=9.9 Hz, 1H), 8.23 (d, J=9.2 Hz, 1H), 7.84 (d, J=3.8 Hz, 1H), 7.51 (dd, J=9.7, 9.7 Hz, 1H), 7.27 (d, J=3.8 Hz, 1H), 7.04 (dd J=9.9, 9.7 Hz, 1H), 7.01 (dd, J=9.7, 9.2 Hz, 1H), and 1.59 (s, 9H).

20: Blue needles; mp 97.0—98.0 °C (Ref. 42; mp 96—98 °C); ^{1}H NMR (90 MHz, $CDCl_3$) δ=8.56 (d, J=9.7 Hz, 2H), 7.77 (s, 1H), 7.44 (t, J=9.5 Hz, 1H), 6.92 (dd, J=9.7, 9.5 Hz, 2H), and 1.58 (s, 18H).

3-Formyl-1-methoxycarbonylazulene (14c). $POCl_3$ (5.60 ml, 60.0 mmol) was slowly added at 0 °C to a solution of 1-methoxycarbonylazulene (**13c**) (2.00 g, 10.7 mmol) in DMF (40 ml). The solution was heated at 90 °C for 30 min. The resulting solution was poured into ice-water, made alkaline with 2 M aqueous NaOH, and then extracted with CH_2Cl_2. The organic layer was washed with water, dried with $MgSO_4$, and concentrated in vacuo. Purification of the residue by column chromatography on alumina with CH_2Cl_2 gave the formylazulene **14c** (2.30 g, 100%). Orange needles; mp 114.0—115.0 °C (MeOH); MS (70 eV) *m/z* (rel intensity) 214 (M^+, 100), 213 (64), 183 (91), and 127 (28); IR (KBr disk) 1696, 1663, 1655, 1460, 1447, 1431, 1408, 1401, 1235, 1219, 1190, 777, and 745 cm^{-1}; UV (hexane) 237 ($\log\varepsilon$ 4.57), 277 (4.54), 290 (4.38), 307 (4.54), 374 (3.95), 384 (3.93), 389 (3.92), 510 (2.73), 548 (2.66), and 601 (2.17); ^{1}H NMR (90 MHz, $CDCl_3$) δ=10.25 (s, 1H), 8.70 (d, J=10.1 Hz, 2H), 8.62 (s, 1H), 8.01 (dd, J=9.4, 9.4 Hz, 1H), 7.75 (dd, J=10.1, 9.4 Hz, 2H), and 3.96 (s, 3H); ^{13}C NMR (22.5 MHz, $CDCl_3$) δ=186.76 (d), 164.69 (s), 145.85 (d), 144.99 (s), 142.58 (s), 141.30 (d), 139.81 (d), 139.26 (d), 132.25 (d), 131.76 (d), 124.41 (s), 117.12 (s), and 51.72 (q). Found: C, 72.84; H, 4.80%. Calcd for $C_{13}H_{10}O_3$: C, 72.89; H, 4.70%.

3,6-Di-*t*-butyl-1-formylazulene (14d). The reaction of 1,6-di-*t*-butylazulene (**13d**) (415 mg, 1.73 mmol) with $POCl_3$ (0.48 ml, 5.2 mmol) in DMF (8 ml) at room temperature for 30 min afforded the formylazulene **14d** (383 mg, 83%). Brown needles; mp 96.0—99.0 °C (hexane); MS (70 eV) *m/z* (rel intensity) 268 (M^+, 40), 254 (23), and 253 (100); IR (KBr disk) 2968, 1648, 1464, 1444, 1364, and 1226 cm^{-1}; UV (hexane) 217 ($\log\varepsilon$ 4.34), 239 (4.22), 271 (4.02), 305 (4.51), 316 (4.62), 387 (3.90), 403 (3.92), and 553 nm (2.63); ^{1}H NMR (90 MHz, $CDCl_3$) δ=10.31 (s, 1H), 9.44 (d, J=10.8 Hz, 1H), 8.80 (d, J=11.2 Hz, 1H), 8.12 (s, 1H), 7.74 (dd, J=10.8, 2.0 Hz, 1H), 7.67 (dd, J=11.2, 2.0 Hz, 1H), 1.59 (s, 9H), and 1.49 (s, 9H); ^{13}C NMR (22.5 MHz, $CDCl_3$) δ=185.44 (d), 163.82 (s), 141.17 (s), 140.25 (s), 140.04 (s), 138.42 (d), 136.90 (d), 135.53 (d), 126.84 (d), 124.89 (d), 123.30 (s), 38.66 (s), 32.99 (s), 31.74 (q), and 31.62 (q). Found: C, 84.68; H, 9.04%. Calcd for $C_{19}H_{24}O$: C, 85.03; H, 9.01%.

6-*t*-Butyl-1-formylazulene (14e). The reaction of 6-*t*-butylazulene (**13e**) (3.20 g, 17.4 mmol) with $POCl_3$ (4.7 ml, 52 mmol) in DMF (70 ml) at 0 °C for 15 min afforded the formylazulene **14e** (3.59 g, 98%). Reddish-purple needles; mp 69.0—70.0 °C (hexane); MS (70 eV) *m/z* (rel intensity) 212 (M^+, 21) and 211 (100); UV (hexane) 216 ($\log\varepsilon$ 4.34), 237 (4.18), 266 (3.84), 300 (4.54), 311 (4.66), 374 (3.87), 388 (3.93), 530 (2.69), 573 (2.60), and 631 nm (2.11); IR (KBr disk) 1644 and 1454 cm^{-1}; ^{1}H NMR (90 MHz, $CDCl_3$) δ=10.33 (s, 1H), 9.50 (d, 1H), 8.44 (d, J=10.8 Hz, 1H), 8.17 (d, J=4.2 Hz, 1H), 7.80 (dd, J=10.8, 1.8 Hz, 1H), 7.71 (dd, J=10.8, 1.8 Hz, 1H), 7.24 (d, J=4.2 Hz, 1H), and 1.48 (s, 9H); ^{13}C NMR (22.5 MHz, $CDCl_3$) δ=185.93 (d), 164.22 (s), 144.67 (s), 140.68 (d), 139.13 (s), 137.78 (d), 136.53 (d), 127.23 (d), 126.53 (d), 125.71 (s), 118.33 (d), 38.84 (s), and 31.77 (q). Found: C, 84.72; H, 7.72%. Calcd for $C_{15}H_{16}O$: C, 84.87; H, 7.59%.

Tri(1-azulenyl)methane (9a). A solution of azulene (**13a**) (1.93 g, 15.0 mmol) and 1-formylazulene (**14a**) (1.19 g, 7.62 mmol) in glacial acetic acid (50 ml) was stirred at room temperature for 3 d. The reaction mixture was poured into water, neutralized with $NaHCO_3$, and then extracted with CH_2Cl_2. The organic layer was washed with water, dried with $MgSO_4$, and concentrated in vacuo. The residue was purified by column chromatography on silica gel with CH_2Cl_2/hexane to give tri(1-azulenyl)methane (**9a**) (271 mg, 14%, net 30%), 1,3-bis[di(1-azulenyl)methyl]azulene (**15**) (110 mg, 6%, net 14%), and the recovered **13a** (1.33 g, 69%) and **14a** (983 mg, 83%).

9a: Blue prisms; mp 193.0—200.0 °C decomp (CH_2Cl_2/hexane); MS (70 eV) *m/z* (rel intensity) 394 (M^+, 100), 393 (35), 266 (37), and 265 (79); IR (KBr disk) 1576, 1394, 774, and 734 cm^{-1}; UV (CH_2Cl_2) 238 ($\log\varepsilon$ 4.68), 284 (5.00), 349 (4.16), 362 (4.09), and 602 nm (2.98); ^{1}H NMR

(270 MHz, $CDCl_3$) δ=8.28 (d, J=9.7 Hz, 6H), 7.49 (dd, J=9.7, 9.7 Hz, 3H), 7.40 (d, J=4.0 Hz, 3H), 7.36 (1H, s), 7.26 (d, J=4.0 Hz, 3H), 7.17 (dd, J=9.7, 9.7 Hz, 3H), and 6.95 (dd, J=9.7, 9.7 Hz, 3H). Found: m/z 394.1709. Calcd for $C_{31}H_{22}$: M, 394.1722. Found: C, 93.49; H, 5.81%. Calcd for $C_{31}H_{22}\cdot 1/4H_2O$: C, 93.31; H, 5.68%.

15: Green crystals; mp 243.0—244.5 °C decomp (toluene/hexane); MS (70 eV) m/z (rel intensity) 660 (M^+, 7), 394 (86), 393 (100), 375 (69), 267 (56), 266 (32), and 265 (76); IR (KBr disk) 1394, 766, and 728 cm^{-1}; UV (CH_2Cl_2) 240 ($\log\varepsilon$ 4.84), 283 (5.17), 350 (4.33), 365 (4.31), and 605 nm (3.15); ^1H NMR (600 MHz, $CDCl_3$) δ=8.241 (d, J=9.7 Hz, 2H), 8.187 (d, J=9.7 Hz, 4H), 8.138 (d, J=9.7 Hz, 4H), 7.435 (dd, J=9.9, 9.9 Hz, 4H), 7.361 (t, J=10.0 Hz, 1H), 7.248 (s, 2H), 7.202 (d, J=3.8 Hz, 4H), 7.112 (d, J=3.8 Hz, 4H), 7.048 (s, 1H), 7.020 (dd, J=9.9, 9.7 Hz, 4H), 6.827 (dd, J=10.0, 9.7 Hz, 2H), and 6.820 (dd, J=9.9, 9.7 Hz, 4H); ^{13}C NMR (150 MHz, $CDCl_3$) δ=141.05 (s), 138.31 (d), 137.06 (d), 136.50 (d), 135.51 (s), 134.61 (s), 133.85 (s), 133.79 (d), 133.57 (d), 132.66 (s), 122.35 (d), 122.22 (d), 121.64 (d), 121.40 (d), 116.33 (d), 36.21 (d). Found: C, 91.75; H, 5.82%. Calcd for $C_{52}H_{36}\cdot H_2O$: C, 92.00; H, 5.64%.

Tris(3-methyl-1-azulenyl)methane (9b). A solution of 1-methylazulene (**13b**) (2.69 g, 19.0 mmol) and 1-formyl-3-methylazulene (**14b**) (850 mg, 4.99 mmol) in glacial acetic acid (30 ml) was stirred at room temperature for 21 d. The violet solution turned into a blue suspension. The crystals were collected by filtration and purified by column chromatography on alumina with CH_2Cl_2 to afford the tri(1-azulenyl)methane **9b** (1.52 g, 70%). Greenish-blue needles; mp 257.0—262.0 °C decomp (toluene); MS (70 eV) m/z (rel intensity) 436 (M^+, 100), 421 (29), and 279 (42); IR (KBr disk) 1576, 1362, 752, and 732 cm^{-1}; UV (CH_2Cl_2) 243 ($\log\varepsilon$ 4.64), 271 (4.92), 287 (4.98), 358 (4.18), 372 (4.17), and 632 nm (2.98); ^1H NMR (90 MHz, $CDCl_3$) δ=8.14 (dd, J=9.5, 1.2 Hz, 3H), 8.12 (dd, J=9.5, 1.2 Hz, 3H), 7.40 (dddd, J=9.5, 9.5, 1.2, 1.2 Hz, 3H), 7.25 (s, 4H), 6.93 (dd, J=9.6, 9.5 Hz, 3H), 6.79 (dd, J=9.6, 9.5 Hz, 3H), and 2.53 (s, 9H). Found: m/z 436.2204. Calcd for $C_{34}H_{28}$: M, 436.2191. Found: C, 93.54; H, 6.57%. Calcd for $C_{34}H_{28}$: C, 93.54; H, 6.46%.

Tris(3-methoxycarbonyl-1-azulenyl)methane (9c). A solution of 1-methoxycarbonylazulene (**13c**) (3.18 g, 17.1 mmol) and 3-formyl-1-methoxycarbonylazulene (**14c**) (2.14 g, 9.98 mmol) in glacial acetic acid (60 ml) was refluxed for 7 d. The purple solution turned into a purple suspension. The crystals were collected by filtration, washed with CH_2Cl_2, and dried in vacuo to give the tri(1-azulenyl)methane **9c** (2.55 g, 52%, net 94%). The filtrate was concentrated in vacuo and the residue was dissolved in CH_2Cl_2. The solution was washed with 5% aqueous $NaHCO_3$ and water, dried with $MgSO_4$, and concentrated in vacuo. The residue was purified by column chromatography on silica gel with CH_2Cl_2 to afford the recovered **13c** (1.41 g, 44%) and **14c** (744 mg, 35%). Purple needles; mp >300 °C (toluene); MS (70 eV) m/z (rel intensity) 568 (M^+, 100), 510 (37), 509 (91), 389 (42), 382 (30), 323 (72), and 263 (34); IR (KBr disk) 1696, 1456, 1444, 1418, and 1206 cm^{-1}; UV (CH_2Cl_2) 238 ($\log\varepsilon$ 4.84), 261 (4.63), 292 (4.97), 306 (4.97), 373 (4.34), and 559 nm (3.10); ^1H NMR (90 MHz, $CDCl_3$) δ=9.67 (dd, J=9.8, 1.2 Hz, 3H), 8.35 (dd J=9.4, 1.0 Hz, 3H), 7.78 (s 3H), 7.77 (dddd, J=9.2, 9.2, 1.2, 1.0 Hz, 3H), 7.52 (ddd, J=9.8, 9.2, 1.2 Hz, 3H), 7.26 (ddd, J=9.4, 9.2, 1.2 Hz, 3H), 7.15 (s, 1H), and 3.82 (s, 9H). Found: C, 79.35; H, 5.30%. Calcd for $C_{37}H_{28}O_6\cdot 1/2$toluene: C, 79.14; H, 5.25%.

Tris(3,6-di-*t*-butyl-1-azulenyl)methane (9d). A solution of 1,6-di-*t*-butylazulene (**13d**) (412 mg, 1.71 mmol) and 3,6-di-*t*-butyl-1-formylazulene (**14d**) (228 mg, 0.850 mmol) in glacial acetic acid (6 ml) was stirred at room temperature for 21 d. The blue-purple solution turned into a blue suspension. The crystals were collected by filtration and purified by column chromatography on silica gel with CH_2Cl_2 to afford the tri(1-azulenyl)methane **9d** (429 mg, 71%). Blue crystals; mp 294.0—297.0 °C decomp (toluene/hexane); MS (70 eV) m/z (rel intensity) 731 (M^+, 35), 674 (60), and 673 (100); IR (KBr disk) 2968, 2908, 2872, 1578, 1364, 1228, and 834 cm^{-1}; UV (CH_2Cl_2) 245 ($\log\varepsilon$ 4.57), 275 (4.98), 294 (4.99), 3.60 (4.17), 375 (4.14), and 619 nm (2.96); ^1H NMR (600 MHz, 50% CD_2Cl_2/CS_2) δ=8.443 (d, J=10.6 Hz, 3H), 8.135 (d, J=10.6 Hz, 3H), 7.287 (s, 3H), 7.077 (dd, J=10.6, 1.9 Hz, 3H), 7.075 (s, 1H), 6.974 (dd, J=10.6, 1.9 Hz, 3H), 1.450 (s, 27H), and 1.384 (s, 27H). Found: m/z 730.5458. Calcd for $C_{55}H_{70}$: M, 730.5478. Found: C, 90.52; H, 9.84%. Calcd for $C_{55}H_{70}$: C, 90.35; H, 9.65%.

Tris(6-*t*-butyl-1-azulenyl)methane (9e). A solution of 6-*t*-butylazulene (**13e**) (1.84 g, 9.99 mmol) and 6-*t*-butyl-1-formylazulene (**14e**) (1.03 g, 4.87 mmol) in glacial acetic acid (30 ml) was stirred at room temperature for 21 d. The blue-purple solution turned into a blue suspension. The crystals were collected by filtration and washed with CH_2Cl_2 to afford the tri(1-azulenyl)methane **9e** (2.36 g, 86%). Blue crystals; mp 286.0—290.0 °C decomp (toluene); MS (70 eV) m/z (rel intensity) 562 (M^+, 100) and 505 (42); IR (KBr disk) 2972, 1582, 1404, and 838 cm^{-1}; UV (CH_2Cl_2) 239 ($\log\varepsilon$ 4.58), 289 (4.98), 299 (4.97), 352 (4.16), and 591 nm (2.96). Found: m/z 562.3598. Calcd for $C_{43}H_{46}$: M, 562.3599. Found: C, 88.77; H, 8.29%. Calcd for $C_{43}H_{46}\cdot H_2O$: C, 88.92; H, 8.33%.

Tris(3-*t*-butyl-1-azulenyl)methane (9f). A solution of 1-*t*-butylazulene (**13f**) (372 mg, 2.02 mmol) and 3-*t*-butyl-1-formylazulene (**14f**) (215 mg, 1.01 mmol) in glacial acetic acid (6 ml) was stirred at room temperature for 21 d. The blue-purple solution turned into a green suspension. The crystals were collected by filtration and purified by column chromatography on silica gel with CH_2Cl_2 to afford the tri(1-azulenyl)methane **9f** (328 mg, 58%). Green crystals; mp 228.0—234.0 °C decomp (toluene/hexane); MS (70 eV) m/z (rel intensity) 562 (M^+, 92), 506 (47), and 505 (100); IR (KBr disk) 2968, 1570, 1366, 1226, and 742 cm^{-1}; UV (CH_2Cl_2) 244 ($\log\varepsilon$ 4.60), 271 (4.90), 288 (4.93), 359 (4.14), 374 (4.15), and 631 nm (2.93); ^1H NMR (90 MHz $CDCl_3$) δ=8.56 (d, J=9.7 Hz, 3H), 8.22 (d, J=9.7 Hz, 3H), 7.42 (s, 3H), 7.40 (dd, J=9.9, 9.9 Hz, 3H), 7.22 (s, 1H), 6.92 (dd, J=9.9, 9.7 Hz, 3H), 6.80 (dd, J=9.9, 9.7 Hz, 3H), and 1.47 (s, 27H). Found: m/z 562.3600. Calcd for $C_{43}H_{46}$: M, 562.3599. Found: C, 91.75; H, 8.08%. Calcd for $C_{43}H_{46}$: C, 91.76; H, 8.24%.

Tri(1-azulenyl)methyl Hexafluorophosphate (6a). DDQ (224 mg, 0.988 mmol) was added at room temperature to a solution of tri(1-azulenyl)methane (**9a**) (198 mg, 0.501 mmol) in CH_2Cl_2 (50 ml). The blue color turned to deep blue. After the solution was stirred at the same temperature for 1h, 60% HPF_6 (5 ml) and water (50 ml) were added

to the mixture. The resulting suspension was filtered with suction. The organic layer was washed with water, dried with $MgSO_4$, and concentrated under reduced pressure. The residue was dissolved in CH_2Cl_2 (5 ml); then, Et_2O (50 ml) was added to the solution. The precipitated crystals were collected by filtration, washed with Et_2O, and dried in vacuo to give the tri(1-azulenyl)methyl cation **6a** (233 mg, 86%). Deep purple powder; mp 195.0—200.5 °C decomp (CH_2Cl_2/ether); MS (FAB) m/z 393 (M^+-PF_6); IR (KBr disk) 1464, 1380, 1280, 840, and 558 cm^{-1}; UV (MeCN) 229 ($\log\varepsilon$ 4.71), 279 (4.55), and 614 nm (4.70); ^1H NMR (400 MHz, $CDCl_3$, 58 °C) δ=8.728 (d, J=9.5 Hz, 3H), 7.965 (dd, J=9.7, 9.7 Hz, 3H), 7.868 (d, J=4.3 Hz, 3H), 7.828 (d, J=9.8 Hz, 3H), 7.817 (dd, J=9.7, 9.5 Hz, 3H), 7.677 (d, J=4.3 Hz, 3H), and 7.369 (dd, J=9.8, 9.7 Hz, 3H); ^1H NMR (400 MHz, $CDCl_3$, −60 °C) δ=8.852 (d, J=9.6 Hz, 1H, B_2), 8.806 (d, J=9.6 Hz, 1H, B_3), 8.800 (d, J=9.6 Hz, 1H, A), 8.777 (d, J=9.6 Hz, 1H, B_1), 8.126 (d, J=4.2 Hz, 1H, B_a), 8.121 (dd, J=9.4, 9.4 Hz, 1H, A), 8.078 (dd, J=9.4, 9.4 Hz, 1H, B_1), 8.045 (d, J=4.2 Hz, 1H, B_b), 8.023 (dd, J=9.4, 9.4 Hz, 1H, B_2), 8.014 (d, J=10.0 Hz, 1H, A), 7.983 (dd, J=9.4, 9.4 Hz, 1H, B_3), 7.958 (dd, J=9.6, 9.4 Hz, 1H, A), 7.907 (dd, J=9.6, 9.4 Hz, 1H, A), 7.873 (d, J=10.0 Hz, 1H, B_2), 7.830 (dd, J=9.6, 9.4 Hz, 1H, B_3), 7.826 (d, J=4.2 Hz, 1H, B_a), 7.808 (d, J=4.2 Hz, 1H, B_c), 7.774 (dd, J=9.6, 9.4 Hz, 1H, B_2), 7.773 (d, J=4.2 Hz, 2H, A and B_c), 7.741 (d, J=4.2 Hz, 1H, B_b), 7.724 (d, J=10.0 Hz, 1H, B_1), 7.696 (d, J=10.0 Hz, 1H, B_3), 7.659 (d, J=4.2 Hz, 1H, A), 7.585 (dd, J=10.0, 9.4 Hz, 1H, A), 7.480 (dd, J=10.0, 9.4 Hz, 1H, B_1), 7.333 (dd, J=10.0, 9.4 Hz, 1H, B_2), and 7.242 (dd, J=10.0, 9.4 Hz, 1H, B_3). Found: m/z 393.1594. Calcd for $C_{31}H_{21}^+$: M, 393.1643. Found: C, 68.90; H, 3.91%. Calcd for $C_{31}H_{21}PF_6$: C, 69.15; H, 3.93%.

Tris(3-methyl-1-azulenyl)methyl Hexafluorophosphate (6b). DDQ (1.71 g, 7.54 mmol) was added at room temperature to a solution of tris(3-methyl-1-azulenyl)methane (**9b**) (2.08 g, 4.65 mmol) in CH_2Cl_2 (300 ml). The blue color turned to deep blue. After the solution was stirred at the same temperature for 1 h, 60% HPF_6 (30 ml) and water (300 ml) were added to the mixture. The resulting suspension was filtered with suction. The organic layer was washed with water, dried with $MgSO_4$, and concentrated under reduced pressure. The residue was dissolved in CH_2Cl_2 (10 ml); then, Et_2O (100 ml) was added to the solution. The precipitated crystals were collected by filtration, washed with Et_2O, and dried in vacuo to give the tri(1-azulenyl)-methyl cation **6b** (2.70 g, 100%). Deep purple powder; mp 266.0—269.0 °C decomp (CH_2Cl_2/ether); MS (FAB) m/z 435 (M^+-PF_6); IR (KBr disk) 1466, 1438, 1412, 1396, 1348, 1318, 1290, 838, and 558 cm^{-1}; UV (MeCN) 242 ($\log\varepsilon$ 469), 291 (4.52), 372 (4.16), and 652 nm (4.57); ^1H NMR (400 MHz, $CDCl_3$, 58 °C) δ=8.596 (d, J=9.8 Hz, 3H), 7.888 (dd, J=9.8, 9.8 Hz, 3H), 7.758 (dd, J=9.8, 9.8 Hz, 3H), 7.693 (s, 3H), 7.679 (d, J=9.8 Hz, 3H), 7.251 (dd, J=9.8, 9.8 Hz, 3H), and 2.734 (s, 9H); ^1H NMR (400 MHz, $CDCl_3$, −60 °C) δ=8.686 (d, J=10.0 Hz, 1H, B_2), 8.662 (d, J=10.0 Hz, 1H, A), 8.641 (d, J=10.0 Hz, 1H, B_3), 8.634 (d, J=10.0 Hz, 1H, B_1), 8.056 (dd, J=9.8, 9.4 Hz, 1H, A), 8.005 (dd, J=9.8, 9.4 Hz, 1H, B_1), 7.961 (dd, J=9.8, 9.4 Hz, 1H, B_2), 7.937 (s, 1H), 7.906 (dd, J=9.8, 9.4 Hz, 1H, B_3), 7.906 (dd, J=10.0, 9.4 Hz, 1H, A), 7.887 (d, J=9.8 Hz, 1H, A), 7.870 (s, 1H), 7.858 (dd, J=10.0, 9.4 Hz, 1H, B_2), 7.835 (dd, J=10.0, 9.4 Hz, 1H, B_1), 7.794 (dd, J=10.0, 9.4 Hz, 1H, B_3), 7.760 (d, J=9.8 Hz, 1H, B_2), 7.620 (d, J=9.8 Hz, 1H, B_1), 7.607 (s, 1H), 7.559 (d, J=9.8 Hz, 1H, B_3), 7.545 (s, 1H), 7.468 (dd, J=9.8, 9.8 Hz, 1H, A), 7.361 (dd, J=9.8, 9.8 Hz, 1H, B_1), 7.224 (dd, J=9.8, 9.8 Hz, 1H, B_2), 7.131 (dd, J=9.8, 9.8 Hz, 1H, B_3), 2.815 (s, 3H, B), 2.766 (s, 3H, B), 2.718 (s, 3H, B), and 2.657 (s, 3H, A). Found: m/z 435.2086. Calcd for $C_{34}H_{27}^+$: M, 435.2113. Found: C, 70.10; H, 4.50%. Calcd for $C_{34}H_{27}PF_6$: C, 70.34; H, 4.69%.

Tris(3-methoxycarbonyl-1-azulenyl)methyl Hexafluorophosphate (6c). DDQ (461 mg, 2.01 mmol) was added at room temperature to a solution of tris(3-methoxycarbonyl-1-azulenyl)methane (**9c**) (569 mg, 1.00 mmol) in CH_2Cl_2 (100 ml). The purple suspension turned into a deep-blue solution. After the solution was stirred at the same temperature for 1 h, 60% HPF_6 (10 ml) and water (100 ml) were added to the mixture. The resulting suspension was filtered with suction. The organic layer was dried with $MgSO_4$, and concentrated under reduced pressure. The residue was dissolved in CH_2Cl_2 (20 ml); then, Et_2O (30 ml) was added to the solution. The precipitated crystals were collected by filtration, washed with Et_2O, and dried in vacuo to give the tri(1-azulenyl)methyl cation **6c** (713 mg, 100%). Purple powder; mp 242.5—249.0 °C decomp (CH_2Cl_2/ether); MS (FAB) m/z 567 (M^+-PF_6); IR (KBr disk) 1706, 1454, 1418, 1366, 1224, 1198, 1162, and 1084 cm^{-1}; UV (MeCN) 229 ($\log\varepsilon$ 4.80), 251 (4.74), 301 (4.73), and 601 nm (472); ^1H NMR (400 MHz, $CDCl_3$, 58 °C) δ=10.005 (d, J=9.6 Hz, 3H), 8.130 (br, 6H), 8.083 (dd, J=9.6, 9.6 Hz, 3H), 8.048 (dd, J=9.6, 9.6 Hz, 3H), 7.843 (br, 3H), and 3.938 (s, 9H). Found: C, 60.58; H, 3.99%. Calcd for $C_{37}H_{27}O_6PF_6\cdot H_2O$: C, 60.83; H, 4.00%.

Tris(3,6-di-*t*-butyl-1-azulenyl)methyl Hexafluorophosphate (6d). DDQ (98 mg, 0.43 mmol) was added at room temperature to a solution of tris(3,6-di-*t*-butyl-1-azulenyl)methane (**9d**) (152 mg, 0.208 mmol) in CH_2Cl_2 (40 ml). The blue color turned to deep blue. After the solution was stirred at the same temperature for 1 h, 60% HPF_6 (2 ml) and water (20 ml) were added to the mixture. The resulting suspension was filtered with suction. The organic layer was washed with water, dried with $MgSO_4$, and concentrated under reduced pressure. The residue was dissolved in CH_2Cl_2 (1 ml); then, Et_2O (10 ml) was added to the solution. The precipitated crystals were collected by filtration, washed with Et_2O, and dried in vacuo to give the tri(1-azulenyl)methyl cation **6d** (182 mg, 100%). Brown powder; mp >300 °C (CH_2Cl_2/ether); MS (FAB) m/z 730 (M^+-PF_6); IR (KBr disk) 2972, 1466, 1420, 1368, 1350, 1238, 840, and 558 cm^{-1}; UV (MeCN) 248 ($\log\varepsilon$ 4.74), 300 (4.61), 650 (4.12), and 670 nm (4.60); ^1H NMR (600 MHz, DMSO-d_6, 90 °C) δ=9.105 (d, J=10.8 Hz, 3H), 8.071 (dd, J=10.8, 2.1 Hz, 3H), 7.745 (d, J=10.8 Hz, 3H), 7.563 (dd, J=10.8, 2.1 Hz, 3H), 7.563 (s, 3H), 1.543 (s, 27H), and 1.396 (s, 27H). Found: m/z 729.5376. Calcd for $C_{55}H_{69}^+$: M, 729.5399. Found: C, 75.19; H, 7.97%. Calcd for $C_{55}H_{69}PF_6$: C, 75.49; H, 7.95%.

Tris(6-*t*-butyl-1-azulenyl)methyl Hexafluorophosphate (6e). DDQ (323 mg, 1.42 mmol) was added at room temperature to a solution of tris(6-*t*-butyl-1-azulenyl)methane (**9e**) (564 mg, 1.00 mmol) in CH_2Cl_2 (200 ml). The blue suspension turned into a deep-blue solution. After the solution was stirred at the same temperature for 1 h, 60% HPF_6

(10 ml) and water (100 ml) were added to the mixture. The resulting suspension was filtered with suction. The organic layer was washed with water, dried with $MgSO_4$, and concentrated under reduced pressure. The residue was dissolved in CH_2Cl_2 (5 ml); then, Et_2O (50 ml) was added to the solution. The precipitated crystals were collected by filtration, washed with Et_2O, and dried in vacuo to give the tri(1-azulenyl)methyl cation **6e** (657 mg, 93%). Brown powder; mp 225.0—230.0 °C (CH_2Cl_2/ether); MS (FAB) m/z 561 (M^+-PF_6); IR (KBr disk) 1458, 1382, 1296, 838, and 556 cm^{-1}; UV (MeCN) 243 ($\log\varepsilon$ 4.66), 294 (4.59), and 615 nm (4.64); ^1H NMR (400 MHz, DMSO-d_6, 80 °C) δ=8.835 (d, J=10.2 Hz, 3H), 8.093 (dd, J=10.2, 2.0 Hz, 3H), 7.808 (d, J=4.4 Hz, 3H), 7.793 (d, J=10.2 Hz, 3H), 7.723 (d, J=4.4 Hz, 3H), 7.634 (dd, J=10.2, 2.0 Hz, 3H), and 1.386 (s, 27H). Found: m/z 561.3500. Calcd for $C_{43}H_{45}^+$: M, 561.3522. Found: C, 73.13; H, 6.20%. Calcd for $C_{43}H_{45}PF_6$: C, 73.07; H, 6.42%.

Tris(3-*t*-butyl-1-azulenyl)methyl Hexafluorophosphate (6f). DDQ (71 mg, 0.31 mmol) was added at room temperature to a solution of tris(3-*t*-butyl-1-azulenyl)methane (**9f**) (114 mg, 0.202 mmol) in CH_2Cl_2 (40 ml). The blue color turned to deep blue. After the solution was stirred at the same temperature for 1 h, 60% HPF_6 (2 ml) and water (20 ml) were added to the mixture. The resulting suspension was filtered with suction. The organic layer was washed with water, dried with $MgSO_4$, and concentrated under reduced pressure. The residue was dissolved in CH_2Cl_2 (1 ml); then, Et_2O (30 ml) was added to the solution. The precipitated crystals were collected by filtration, washed with Et_2O, and dried in vacuo to give the tri(1-azulenyl)methyl cation **6f** (135 mg, 95%). Brown powder; mp 252.0—255.0 °C (CH_2Cl_2/ether); MS (FAB) m/z 561 (M^+-PF_6); IR (KBr disk) 1462, 1442, 1410, 1368, 1344, 840, and 558 cm^{-1}; UV (MeCN) 244 ($\log\varepsilon$ 4.75), 294 (4.55), and 650 nm (4.61); ^1H NMR (400 MHz, DMSO-d_6, 80 °C) δ=9.180 (d, J=10.2 Hz, 3H), 8.038 (dd, J=10.0, 10.0 Hz, 3H), 7.907 (dd, J=10.2, 10.0 Hz, 3H), 7.776 (d, J=10.2 Hz, 3H), 7.715 (s, 3H), 7.395 (dd, J=10.2, 10.0 Hz, 3H), and 1.566 (s, 27H). Found: m/z 561.3505. Calcd for $C_{43}H_{45}^+$: M, 561.3521. Found: C, 72.96; H, 6.11%. Calcd for $C_{43}H_{45}PF_6$: C, 73.07; H, 6.42%.

Reaction of Tri(1-azulenyl)methane (9a) with $Ph_3C^+PF_6^-$. $Ph_3C^+PF_6^-$ (144 mg, 0.372 mmol) was added at room temperature to a solution of tri(1-azulenyl)methane (**9a**) (151 mg, 0.382 mmol) in MeCN (20 ml). After stirring at the same temperature for 30 min, the solvent was removed under reduced pressure. The residue was recrystallized from MeCN/ether to give di(1-azulenyl)methyl hexafluorophosphate (**16a**) (154 mg, 98%). The filtrate was purified by PTLC on alumina with hexane and medium-pressure column chromatography on silica gel with 5% ethyl acetate/hexane to afford 1-triphenylmethylazulene (**17a**) (47 mg, 33%) and 1,3-bis(triphenylmethyl)azulene (**18**) (24 mg, 10%).

16a: Violet powder; mp 194.0—204.0 °C decomp (MeCN/ether); MS (FAB) m/z 267 (M^+-PF_6); IR (KBr disk) 1556, 1532, 1420, 1294, 1264, 1054, 840, and 558 cm^{-1}; UV (MeCN) 280 ($\log\varepsilon$ 4.29), 342 (3.98), and 616 nm (4.81); ^1H NMR (270 MHz, DMSO-d_6) δ=9.35 (d, J=9.8 Hz, 2H), 9.14 (s, 1H), 8.75 (d, J=4.5 Hz, 2H), 8.74 (d, J=9.5 Hz, 2H), 8.26 (dd, J=9.8, 9.8 Hz, 2H), 8.15 (dd, J=9.8, 9.8 Hz, 2H) 8.07 (dd, J=9.8, 9.5 Hz, 2H), and 7.80 (d, J=4.5 Hz, 2H). Found: m/z 267.1177. Calcd for $C_{21}H_{15}^+$: M, 267.1174. Found: C, 61.17; H, 3.55%. Calcd for $C_{21}H_{15}PF_6$: C, 61.17; H, 3.67%.

17a: Blue prisms; mp 170.0—171.0 °C (Ref. 42; mp 178 °C); ^1H NMR (90 MHz, $CDCl_3$) δ=8.27 (d, J=9.7 Hz, 1H), 7.67 (d, J=9.9 Hz, 1H), 7.64 (d, J=4.0 Hz, 1H), 7.41 (dd, J=9.9, 9.5 Hz, 1H), 7.25 (d, J=4.0 Hz, 1H), 7.20 (s, 15H), 7.04 (dd, J=9.7, 9.5 Hz, 1H), and 6.70 (dd, J=9.9, 9.9 Hz, 1H).

18: Blue prisms; mp 289.0—291.0 °C (Ref. 42; mp 293 °C); ^1H NMR (90 MHz, $CDCl_3$) δ=7.63 (d, J=9.9 Hz, 2H), 7.38 (s, 1H), 7.25 (t, J=9.5 Hz, 1H), 7.14 (s, 30H), and 6.60 (dd, J=9.9, 9.5 Hz, 2H).

Reaction of Tris(3-methyl-1-azulenyl)methane (9b) with $Ph_3C^+PF_6^-$. $Ph_3C^+PF_6^-$ (472 mg, 1.22 mmol) was added at room temperature to a solution of the tri(1-azulenyl)methane **9b** (437 mg, 1.00 mmol) in CH_2Cl_2 (100 ml). After stirring at the same temperature for 1 h, the precipitated crystals were collected by filtration, washed with Et_2O, and dried in vacuo to give bis(3-methyl-1-azulenyl)-methyl hexafluorophosphate (**16b**) (432 mg, 98%). The filtrate was purified by column chromatography on silica gel with CH_2Cl_2 and medium-pressure column chromatography with 5% ethyl acetate/hexane to afford 3-methyl-1-(triphenylmethyl)azulene (**17b**) (187 mg, 49%).

16b: Brown powder; mp 280.0—285.0 °C decomp (MeCN/ether); MS (FAB) m/z 295 (M^+-PF_6); IR (KBr disk) 1584, 1556, 1526, 1420, 1400, 1338, 1302, 1270, 1050, 882, 838, and 558 cm^{-1}; UV (MeCN) 223 ($\log\varepsilon$ 4.45), 250 (4.30), 284 (4.26), 309 (4.13), 358 (4.01), and 647 nm (4.87); ^1H NMR (90 MHz, MeCN-d_3) δ=9.17 (d, J=9.8 Hz, 2H), 8.82 (s, 1H), 8.54 (d, J=9.6 Hz, 2H), 8.53 (s, 2H), 8.24—7.84 (m, 6H), and 2.64 (s, 6H). Found: m/z 295.1483. Calcd for $C_{23}H_{19}^+$: M, 295.1487. Found: C, 62.92; H, 4.37%. Calcd for $C_{23}H_{19}PF_6$: C, 62.73; H, 4.35%.

17b: Blue prisms; mp 190.5—192.0 °C (hexane); MS (70 eV) m/z (rel intensity) 384 (M^+, 100), 308 (25), and 307 (95); IR (KBr disk) 1570, 1490, 1444, 752, 736, and 702 cm^{-1}; UV (CH_2Cl_2) 239 ($\log\varepsilon$ 4.35), 294 (4.55), 301 (4.54), 359 (3.62), 378 (3.65), and 630 nm (2.52); ^1H NMR (90 MHz, $CDCl_3$) δ=8.15 (d, J=9.5 Hz, 1H), 7.53 (d, J=9.5 Hz, 1H), 7.46 (s, 1H), 7.34 (dd, J=9.6, 9.6 Hz, 1H), 7.19 (s, 15H), 6.94 (dd, J=9.6, 9.5 Hz, 1H), 6.56 (dd, J=9.6, 9.5 Hz, 1H), and 2.58 (s, 3H); ^{13}C NMR (22.5 MHz, $CDCl_3$) δ=147.11 (s), 141.42 (d), 137.88 (s), 137.60 (d), 136.96 (d), 135.90 (s), 133.58 (d), 133.58 (s), 130.86 (d), 127.14 (d), 125.62 (d), 123.24 (s), 121.11 (d), 120.89 (d), 61.74 (s), and 12.65 (q). Found: m/z 384.1875. Calcd for $C_{30}H_{24}$: M, 384.1878. Found: C, 93.57; H, 6.58%. Calcd for $C_{30}H_{24}$: C, 93.71; H, 6.29%.

Reaction of Tris(3-methoxycarbonyl-1-azulenyl)-methane (9c) with $Ph_3C^+PF_6^-$. $Ph_3C^+PF_6^-$ (205 mg, 0.527 mmol) was added at room temperature to a solution of the tri(1-azulenyl)methane **9c** (284 mg, 0.500 mmol) in CH_2Cl_2 (100 ml). After stirring at the same temperature for 1 h, the precipitated crystals were collected by filtration, washed with CH_2Cl_2, and dried in vacuo to give bis(3-methoxycarbonyl-1-azulenyl)methyl hexafluorophosphate (**16c**) (173 mg, 65%). The filtrate was poured into water and extracted with CH_2Cl_2. The organic layer was washed with water, dried with $MgSO_4$, and concentrated in vacuo. The

residue was purified by column chromatography on silica gel with CH_2Cl_2 and medium-pressure column chromatography with 10% ethyl acetate/hexane to afford 1-methoxycarbonyl-3-(triphenylmethyl)azulene (**17c**) (116 mg, 54%).

16c: Purple powder; mp 249.0—255.0 °C decomp (MeCN/ether); MS (FAB) m/z 383 ($M^+ - PF_6$); IR (KBr disk) 1712, 1564, 1508, 1428, 1358, 1320, 1260, 1208, 1050, 840, and 560 cm^{-1}; UV (MeCN) 224 ($\log\varepsilon$ 4.64), 283 (4.41), 304 (4.39), 357 (3.99), and 599 nm (5.03); ^1H NMR (90 MHz, MeCN-d_3) δ=9.78 (dd, J=9.5, 2.0 Hz, 2H), 9.42 (dd, J=9.5, 2.0 Hz, 2H), 9.23 (s, 1H), 9.03 (s, 2H), 8.51— 8.16 (m, 6H), and 4.06 (s, 6H). Found: m/z 383.1248. Calcd for $C_{25}H_{19}O_4^+$: M, 383.1283. Found: C, 55.56; H, 3.48%. Calcd for $C_{25}H_{19}O_4PF_6 \cdot 1/2H_2O$: C, 55.88; H, 3.75%.

17c: Purple needles; mp 216.0—217.0 °C (ethyl acetate/hexane); MS (70 eV) m/z (rel intensity) 428 (M^+, 100), 369 (30), and 351 (99); IR (KBr disk) 1696, 1456, 1444, 1422, 1206, 746, and 702 cm^{-1}; UV (CH_2Cl_2) 237 ($\log\varepsilon$ 4.60), 309 (4.66), 385 (4.05), and 557 nm (2.62); ^1H NMR (90 MHz, $CDCl_3$) δ=9.69 (d, J=9.9 Hz, 1H), 8.12 (s, 1H), 7.89 (d, J=9.9 Hz, 1H), 7.65 (dd, J=9.9, 9.9 Hz, 1H), 7.46 (dd, J=9.9, 9.9 Hz, 1H), 7.20 (s, 15H), 6.98 (dd, J=9.9, 9.9 Hz, 1H), and 3.88 (s, 3H); ^{13}C NMR (22.5 MHz, $CDCl_3$) δ=165.53 (s), 146.35 (s), 142.69 (d), 142.60 (s), 140.86 (s), 139.70 (d), 138.91 (d), 137.81 (d), 134.73 (s), 130.77 (d), 127.78 (d), 127.39 (d), 125.92 (d), 125.62 (d), 114.03 (s), 61.56 (s), and 50.89 (q). Found: m/z 428.1778. Calcd for $C_{31}H_{24}O_2$: M, 428.1776. Found: C, 86.61; H, 5.49%. Calcd for $C_{31}H_{24}O_2$: C, 86.89; H, 5.64%.

Di(1-azulenyl)phenylmethane (10a). A solution of azulene (**13a**) (1.28 g, 9.99 mmol) and benzaldehyde (266 mg, 2.50 mmol) in glacial acetic acid (30 ml) was stirred at room temperature for 2 d. The reaction mixture was poured into water and extracted with CH_2Cl_2. The organic layer was washed with 5% $NaHCO_3$ and water, dried with $MgSO_4$, and concentrated in vacuo. The residue was purified by column chromatography on silica gel with 20% CH_2Cl_2/hexane to afford di(1-azulenyl) phenylmethane (**10a**) (259 mg, 15%, net 51%), 1,3-bis[(1-azulenyl)phenylmethyl]azulene (**21a**) (139 mg, 7%, net 19%), and the recovered **13a** (777 mg, 61%).

10a: Blue crystals; mp 136.0—138.5 °C (Ref. 44; mp 140—141 °C); IR (KBr disk) 1394, 776, and 740 cm^{-1}; UV (CH_2Cl_2) 238 ($\log\varepsilon$ 4.51), 283 (4.81), 289 (4.79), 295 (4.81), 349 (3.96), 365 (3.87), 600 (2.77), 623 (2.72), 651 (2.69), and 718 nm (2.23); ^1H NMR (90 MHz, $CDCl_3$) δ=8.26 (d, J=9.4 Hz, 4H), 7.50 (dd, J=9.8, 9.5 Hz, 2H), 7.45 (d, J=4.0 Hz, 2H), 7.27 (d, J=4.0 Hz, 2H), 7.22—7.11 (m, 5H), 7.07 (dd, J=9.5, 9.4 Hz, 2H), 6.97 (dd, J=9.8, 9.4 Hz, 2H), and 6.74 (s, 1H).

21a: Green crystals; mp 126.0—129.0 °C (CH_2Cl_2/hexane); MS (70 eV) m/z (rel intensity) 560 (M^+, 100), 344 (43), 343 (55), 295 (27), and 128 (41); IR (KBr disk) 1594, 1396, 774, 738, and 722 cm^{-1}; UV (CH_2Cl_2) 239 ($\log\varepsilon$ 4.72), 282 (5.03), 349 (4.14), 365 (4.12), 603 (2.92), and 765 nm (1.94); ^1H NMR (90 MHz, $CDCl_3$) δ=8.26—8.10 (m, 6H), 7.58—6.78 (m, 24H), and 6.67 (s, 2H); ^{13}C NMR (22.5 MHz, $CDCl_3$) δ=145.25 (s), 140.95 (s), 140.89 (s), 139.73 (d), 139.67 (d), 138.09 (d), 137.14 (d), 136.96 (d), 136.38 (d), 135.77 (s), 134.92 (s), 134.86 (s), 133.61 (d), 133.51 (d), 133.45 (d), 132.87 (s), 131.66 (s), 128.58 (d), 127.94 (d), 125.65 (d), 122.23 (d), 121.62 (d), 121.53 (d), 116.41 (d), and 42.81 (d). Found: m/z 560.2507. Calcd for $C_{44}H_{32}$: M, 560.2504. Found: C, 94.31; H, 6.04%. Calcd for $C_{44}H_{32}$: C, 94.25; H, 5.75%.

Bis(3-methyl-1-azulenyl)phenylmethane (10b). A solution of 1-methylazulene (**13b**) (1.44 g, 10.1 mmol) and benzaldehyde (562 mg, 5.29 mmol) in glacial acetic acid (30 ml) was stirred at room temperature for 24 h. The blue solution turned into a green suspension. The crystals were collected by filtration and purified by column chromatography on silica gel with benzene to afford the di(1-azulenyl)-phenylmethane **10b** (1.68 g, 89%). Greenish-blue prisms; mp 198.0—199.0 °C (ethyl acetate/hexane); MS (70 eV) m/z (rel intensity) 372 (M^+, 100), 357 (31), 279 (25), and 215 (38); IR (KBr disk) 1576, 740, 732, and 708 cm^{-1}; UV (CH_2Cl_2) 241 ($\log\varepsilon$ 4.50), 281 (4.84), 356 (3.99), 373 (3.97), and 631 nm (2.97); ^1H NMR (90 MHz, $CDCl_3$) δ=8.13 (d, J=9.4 Hz, 4H), 7.40 (dd, J=9.8, 9.5 Hz, 2H), 7.30 (s, 2H), 7.25—7.08 (m, 5H), 6.93 (dd, J=9.5, 9.4 Hz, 2H), 6.82 (dd, J=9.8, 9.4 Hz, 2H), 6.67 (s, 1H), and 2.55 (s, 6H). Found: m/z 372.1873. Calcd for $C_{29}H_{24}$: M, 372.1878. Found: C, 93.40; H, 6.63%. Calcd for $C_{29}H_{24}$: C, 93.51; H, 6.49%.

Bis(3- methoxycarbonyl- 1- azulenyl)phenylmethane (10c). A solution of 1-methoxycarbonylazulene (**13c**) (720 mg, 3.87 mmol) and benzaldehyde (427 mg, 4.03 mmol) in glacial acetic acid (12 ml) was refluxed for 10 h. The purple solution turned into a purple suspension. The crystals were collected by filtration and purified by column chromatography on silica gel with CH_2Cl_2 to afford the di-(1-azulenyl)phenylmethane **10c** (890 mg, 100%). Purple prisms; mp 258.5—259.0 °C (toluene); MS (70 eV) m/z (rel intensity) 460 (M^+, 100), 401 (60), 383 (31), 86 (54), 84 (82), and 51 (27); IR (KBr disk) 1690, 1458, 1444, 1418, 1216, 1206, and 1040 cm^{-1}; UV (CH_2Cl_2) 238 ($\log\varepsilon$ 4.68), 295 (4.80), 307 (4.84), 3.71 (4.15), 385 (4.18), and 559 nm (2.91); ^1H NMR (90 MHz, $CDCl_3$) δ=9.65 (dd, J=9.2, 1.2 Hz, 2H), 8.34 (dd, J=9.6, 1.0 Hz, 2H), 7.84 (s, 2H), 7.74 (dddd, J=9.4, 9.4, 1.2, 1.0 Hz, 2H), 7.49 (ddd, J=9.4, 9.2, 1.2 Hz, 2H), 7.27 (ddd, J=9.6, 9.4, 1.2 Hz, 2H), 7.26—7.18 (m, 5H), 6.60 (s, 1H), and 384 (s, 6H). Found: m/z 460.1675. Calcd for $C_{31}H_{24}O_4$: M, 460.1674. Found: C, 79.80; H, 5.39%. Calcd for $C_{31}H_{24}O_4 \cdot 1/3H_2O$: C, 79.81; H, 5.33%.

Bis(3,6-di-*t*-butyl-1-azulenyl)phenylmethane (10d). A solution of 1,6-di-t-butylazulene (**13d**) (490 mg, 2.04 mmol) and benzaldehyde (223 mg, 2.10 mmol) in glacial acetic acid (12 ml) was stirred at room temperature for 12 h. The blue solution turned into a greenish-blue suspension. The crystals were collected by filtration and purified by column chromatography on silica gel with CH_2Cl_2 to afford the di(1-azulenyl)phenylmethane **10d** (567 mg, 98%). Blue crystals; mp 233.5—235.0 °C (hexane/EtOH); MS (70 eV) m/z (rel intensity) 568 (M^+, 100) and 512 (36); IR (KBr disk) 2968, 1578, 1366, 1230, and 832 cm^{-1}; UV (CH_2Cl_2) 243 ($\log\varepsilon$ 4.45), 287 (4.91), 304 (4.88), 358 (4.01), 375 (3.93), and 615 nm (2.79); ^1H NMR (90 MHz, $CDCl_3$) δ=8.53 (d, J=10.8 Hz, 2H), 8.16 (d, J=10.8 Hz, 2H), 7.38 (s, 2H), 7.17—7.15 (m, 5H), 7.14 (dd, J=10.8, 2.0 Hz, 2H), 7.04 (dd, J=10.8, 2.0 Hz, 2H), 6.63 (s, 1H), 1.49 (s, 9H), and 1.40 (s, 9H). Found: m/z 568.4077. Calcd for $C_{43}H_{52}$: M, 568.4069. Found: C, 90.61; H, 9.34%. Calcd for $C_{43}H_{52}$: C, 90.79; H, 9.21%.

Bis(6-*t*-butyl-1-azulenyl)phenylmethane (10e). A

solution of 6-*t*-butylazulene (**13e**) (1.84 g, 10.0 mmol) and benzaldehyde (269 mg, 2.54 mmol) in glacial acetic acid (60 ml) was stirred at room temperature for 5 h. The solvent was removed in vacuo, and the residue was dissolved in CH_2Cl_2. The solution was washed with 5% $NaHCO_3$ and water, dried with $MgSO_4$, and concentrated in vacuo. The residue was purified by column chromatography on silica gel with CH_2Cl_2 and GPC with $CHCl_3$ to afford the di(1-azulenyl)phenylmethane **10e** (295 mg, 13%, net 36%), 1,3-bis[(6-*t*-butyl-1-azulenyl)phenylmethyl]azulene (**21b**) (147 mg, 6%, net 16%), and the recovered **13e** (1.15 g, 62%).

10e: Blue plates; mp 259.0—263.5 °C decomp (toluene/hexane); MS (70 eV) *m/z* (rel intensity) 456 (M^+, 100); IR (KBr disk) 2968, 1584, 1406, and 840 cm^{-1}; UV (CH_2Cl_2) 238 ($\log\varepsilon$ 4.48), 283 (4.89), 300 (4.90), 352 (4.03), 367 (3.78), 588 (2.80), and 708 nm (2.24); ^1H NMR (90 MHz, CD_2Cl_2) δ=8.23 (d, J=10.3 Hz, 4H), 7.36 (d, J=4.0 Hz, 2H), 7.28 (dd, J=10.3, 1.8 Hz, 2H), 7.21 (s, 5H), 7.20 (dd, J=10.3, 1.8 Hz, 2H), 7.18 (d, J=4.0 Hz, 2H), 6.69 (s, 1H), and 1.40 (s, 18H). Found: *m/z* 456.2822. Calcd for $C_{35}H_{36}$: M, 456.2817. Found: C, 91.94; H, 8.29%. Calcd for $C_{35}H_{36}$: C, 92.05; H, 7.95%.

21b: Greenish-blue crystals; mp 172.0—179.0 °C decomp (hexane/EtOH); MS (70 eV) *m/z* (rel intensity) 728 (M^+, 0.6), 456 (61), 275 (27), 274 (100), 217 (41), and 184 (46); IR (KBr disk) 1582, 1406, and 836 cm^{-1}; UV (CH_2Cl_2) 239 ($\log\varepsilon$ 4.68), 287 (5.11), 297 (5.06), 351 (4.22), 367 (4.08), and 592 nm (3.00); ^1H NMR (90 MHz, CD_2Cl_2) δ=8.19 (d, J=10.3 Hz, 6H), 7.34—6.98 (m, 21H), 6.64 (s, 2H), 1.40 (s, 18H), and 1.33 (s, 9H). Found: *m/z* 728.4377. Calcd for $C_{56}H_{56}$: M, 728.4382. Found: C, 91.52; H, 7.88%. Calcd for $C_{56}H_{56}\cdot 1/2H_2O$: C, 91.13; H, 7.78%.

Bis(3-*t*-butyl-1-azulenyl)phenylmethane (10f). A solution of 1-*t*-butylazulene (**13f**) (365 mg, 1.98 mmol) and benzaldehyde (214 mg, 2.01 mmol) in glacial acetic acid (12 ml) was stirred at room temperature for 12 h. The blue solution turned into a blue suspension. The crystals were collected by filtration and purified by column chromatography on silica gel with CH_2Cl_2 to afford the di(1-azulenyl)-phenylmethane **10f** (252 mg, 56%). Greenish-blue crystals; mp 98.0—100.5 °C (MeOH); MS (70 eV) *m/z* (rel intensity) 456 (M^+, 100), 441 (27), and 399 (39); IR (KBr disk) 2964, 1570, 1392, 1364, 1228, and 736 cm^{-1}; UV (CH_2Cl_2) 242 ($\log\varepsilon$ 4.49), 282 (4.83), 357 (3.98), 374 (3.99), and 627 nm (2.77); ^1H NMR (90 MHz, $CDCl_3$) δ=8.58 (d, J=9.7 Hz, 2H), 8.19 (d, J=9.5 Hz, 2H), 7.45 (s, 2H), 7.43 (dd, J=10.1, 9.9 Hz, 2H), 7.28—7.09 (m, 5H), 6.96 (dd, J=10.1, 9.7 Hz, 2H), 6.85 (dd, J=9.9, 9.5 Hz, 2H), 6.67 (s, 1H), and 1.50 (s, 18H). Found: *m/z* 456.2818. Calcd for $C_{35}H_{36}$: M, 456.2817. Found: C, 92.00; H, 8.10%. Calcd for $C_{35}H_{36}$: C, 92.05; H, 7.95%.

Di(1-azulenyl)phenylmethyl Hexafluorophosphate (7a). DDQ (196 mg, 0.858 mmol) was added at room temperature to a solution of di(1-azulenyl)phenylmethane (**10a**) (173 mg, 0.501 mmol) in CH_2Cl_2 (50 ml). The blue color turned to deep blue. After the solution was stirred at the same temperature for 1 h, 60% HPF_6 (2.5 ml) and water (25 ml) were added to the mixture. The resulting suspension was filtered with suction. The organic layer was washed with water, dried with $MgSO_4$, and concentrated under reduced pressure. Et_2O was added to the residue. The precipitated crystals were collected by filtration, washed with Et_2O, and dried in vacuo to give the di(1-azulenyl)-phenylmethyl cation **7a** (245 mg, 100%). Brown powder; mp 187.0—191.0 °C (CH_2Cl_2/ether); MS (FAB) *m/z* 343 (M^+-PF_6); IR (KBr disk) 1470, 1378, 1276, 836, and 558 cm^{-1}; UV (MeCN) 229 ($\log\varepsilon$ 4.57), 280 (4.39), 305 (4.23), 355 (4.19), 455 (3.81), and 639 nm (4.57); ^1H NMR (400 MHz, $CDCl_3$, 58 °C) δ=8.777 (dd, J=9.6, 0.9 Hz, 2H), 8.105 (ddd, J=9.8, 9.6, 0.9 Hz, 2H), 7.994 (ddd, J=9.6, 9.6, 0.9 Hz, 2H), 7.959 (d, J=10.0 Hz, 2H), 7.862 (d, J=4.6 Hz, 2H), 7.774 (tt, J=7.6, 1.4 Hz, 1H), 7.702 (d, J=4.6 Hz, 2H), 7.592 (dd, J=8.2, 7.6 Hz, 2H), 7.587 (ddd, J=10.0, 9.8, 0.9 Hz, 2H), and 7.408 (dd, J=8.2, 1.4 Hz, 2H). Found: *m/z* 343.1464. Calcd for $C_{27}H_{19}^+$: M, 343.1487. Found: C, 66.23; H, 3.80%. Calcd for $C_{27}H_{19}PF_6$: C, 66.40; H, 3.92%.

Bis(3-methyl-1-azulenyl)phenylmethyl Hexafluorophosphate (7d). DDQ (303 mg, 1.32 mmol) was added at room temperature to a solution of bis(3-methyl-1-azulenyl)phenylmethane (**10b**) (373 mg, 1.00 mmol) in CH_2Cl_2 (100 ml). The blue color turned to deep blue. After the solution was stirred at the same temperature for 1 h, 60% HPF_6 (5 ml) and water (25 ml) were added to the mixture. The resulting suspension was filtered with suction. The organic layer was washed with water, dried with $MgSO_4$, and concentrated under reduced pressure. Et_2O was added to the residue. The precipitated crystals were collected by filtration, washed with Et_2O, and dried in vacuo to give the di(1-azulenyl)phenylmethyl cation **7b** (517 mg, 100%). Brown powder; mp 209.5—212.5 °C (CH_2Cl_2/ether); MS (FAB) *m/z* 371 (M^+-PF_6); IR (KBr disk) 1482, 1440, 1412, 1398, 1346, 1312, 1288, 836, and 558 cm^{-1}; UV (MeCN) 235 ($\log\varepsilon$ 4.58), 286 (4.39), 362 (4.22), 461 (3.75), 483 (3.75), and 676 nm (4.53); ^1H NMR (400 MHz, $CDCl_3$, 58 °C) δ=8.651 (d, J=9.2 Hz, 2H), 8.045 (dd, J=9.6, 9.6 Hz, 2H), 7.975 (dd, J=9.6, 9.2 Hz, 2H), 7.836 (d, J=9.4 Hz, 2H), 7.742 (t, J=7.6 Hz, 1H), 7.684 (s, 2H), 7.582 (dd, J=7.6, 7.4 Hz, 2H), 7.491 (dd, J=9.6, 9.4 Hz, 2H), 7.380 (d, J=7.4 Hz, 2H), and 2.664 (s, 6H). Found: *m/z* 371.1820. Calcd for $C_{29}H_{23}^+$: M, 371.1800. Found: C, 67.48; H, 4.30%. Calcd for $C_{29}H_{23}PF_6$: C, 67.44; H, 4.49%.

Bis(3-methoxycarbonyl-1-azulenyl)phenylmethyl Hexafluorophosphate (7c). DDQ (353 mg, 1.54 mmol) was added at room temperature to a solution of bis(3-methoxycarbonyl-1-azulenyl)phenylmethane (**10c**) (461 mg, 1.00 mmol) in CH_2Cl_2 (100 ml). The purple color turned to deep blue. After the solution was stirred at the same temperature for 1 h, 60% HPF_6 (5 ml) and water (25 ml) were added to the mixture. The resulting suspension was filtered with suction. The organic layer was dried with $MgSO_4$ and concentrated under reduced pressure. Et_2O was added to the residue. The precipitated crystals were collected by filtration, washed with Et_2O, and dried in vacuo to give the di(1-azulenyl)phenylmethyl cation **7c** (596 mg, 99%). Brown powder; mp 181.0—183.0 °C (CH_2Cl_2/ether); MS (FAB) *m/z* 459 (M^+-PF_6); IR (KBr disk) 1714, 1482, 1448, 1366, 1224, 1160, 838, and 558 cm^{-1}; UV (MeCN) 228 ($\log\varepsilon$ 4.57), 263 (4.50), 283 (4.45), 371 (4.11), 444 (3.86), and 616 nm (4.60); ^1H NMR (400 MHz, $CDCl_3$, 58 °C) δ=10.025 (dd, J=9.8, 1.6 Hz, 2H), 8.305 (s, 2H), 8.300 (dd, J=10.0, 1.4 Hz, 2H), 8.291 (dddd, J=9.8, 9.8, 1.6, 1.4 Hz, 2H), 8.225 (ddd, J=9.8, 9.8, 1.6 Hz, 2H), 7.861 (ddd, J=10.0, 9.8, 1.6 Hz, 2H), 7.844 (tt, J=7.8, 1.0 Hz, 1H), 7.636 (dd, J=8.0, 7.8 Hz, 2H), 7.460 (dd, J=8.0, 1.0 Hz,

2H), and 3.973 (s, 6H). Found: m/z 459.1612. Calcd for $C_{31}H_{23}O_4^+$: M, 459.1596. Found: C, 60.83; H, 3.68%. Calcd for $C_{31}H_{23}O_4PF_6 \cdot 1/2H_2O$: C, 60.69; H, 3.94%.

Bis(3,6-di-*t*-butyl-1-azulenyl)phenylmethyl Hexafluorophosphate (7d). DDQ (64 mg, 0.28 mmol) was added at room temperature to a solution of bis(3,6-di-*t*-butyl-1-azulenyl)phenylmethane (**10d**) (114 mg, 0.200 mmol) in CH_2Cl_2 (40 ml). The blue color turned to deep blue. After the solution was stirred at the same temperature for 1 h, 60% HPF_6 (2 ml) and water (20 ml) were added to the mixture. The resulting suspension was filtered with suction. The organic layer was washed with water, dried with $MgSO_4$, and concentrated under reduced pressure. Hexane was added to the residual oil. The precipitated crystals were collected by filtration, washed with hexane, and dried in vacuo to give the di(1-azulenyl)phenylmethyl cation **7d** (142 mg, 100%). Deep blue powder; mp 203.0—209.0 °C (CH_2Cl_2/hexane); MS (FAB) m/z 557 ($M^+ - PF_6$); IR (KBr disk) 1480, 1420, 1370, 1336, 1314, 1244, 838, and 558 cm^{-1}; UV (MeCN) 243 ($\log\varepsilon$ 4.60), 289 (4.43), 313 (4.37), 359 (4.25), and 681 nm (4.61); ^1H NMR (90 MHz, $CDCl_3$, 50 °C) δ=9.08 (d, J=10.8 Hz, 2H), 8.18 (d, J=10.8 Hz, 2H), 7.86 (d, J=10.8 Hz, 2H), 7.73—7.38 (m, 6H), 7.58 (s, 2H), 1.59 (s, 18H), and 1.46 (s, 18H). Found: m/z 567.3990. Calcd for $C_{43}H_{51}^+$: M, 567.3991. Found: C, 70.93; H, 6.74%. Calcd for $C_{43}H_{51}PF_6 \cdot 1/4CH_2Cl_2$: C, 70.77; H, 7.07%.

Bis(6-*t*-butyl-1-azulenyl)phenylmethyl Hexafluorophosphate (7e). DDQ (71 mg, 0.31 mmol) was added at room temperature to a solution of bis(6-*t*-butyl-1-azulenyl)phenylmethane (**10e**) (94 mg, 0.21 mmol) in CH_2Cl_2 (40 ml). The blue color turned to deep blue. After the solution was stirred at the same temperature for 1 h, 60% HPF_6 (2 ml) and water (20 ml) were added to the mixture. The resulting suspension was filtered with suction. The organic layer was washed with water, dried with $MgSO_4$, and concentrated under reduced pressure. Hexane was added to the residual oil. The precipitated crystals were collected by filtration, washed with hexane, and dried in vacuo to give the di(1-azulenyl)phenylmethyl cation **7e** (104 mg, 84%). Deep blue powder; mp 159.0—167.5 °C (CH_2Cl_2/hexane); MS (FAB) m/z 455 ($M^+ - PF_6$); IR (KBr disk) 1474, 1400, 1378, 1304, 840, and 558 cm^{-1}; UV (MeCN) 232 ($\log\varepsilon$ 4.53), 284 (4.45), 313 (4.34), 351 (4.24), 399 (3.93), and 642 nm (4.60); ^1H NMR (90 MHz, $CDCl_3$ 50 °C) δ=8.76 (d, J=10.6 Hz, 2H), 8.17 (d, J=10.6 Hz, 2H), 7.90 (d, J=10.8 Hz, 2H), 7.79—7.35 (m, 11H), and 1.44 (s, 18H). Found: m/z 455.2741. Calcd for $C_{35}H_{35}^+$: M, 455.2739. Found: C, 70.22; H, 5.62%. Calcd for $C_{35}H_{35}PF_6$: C, 69.99; H, 5.87%.

Bis(3-*t*-butyl-1-azulenyl)phenylmethyl Hexafluorophosphate (7f). DDQ (68 mg, 0.30 mmol) was added at room temperature to a solution of bis(3-*t*-butyl-1-azulenyl)phenylmethane (**10f**) (91 mg, 0.20 mmol) in CH_2Cl_2 (40 ml). The blue color turned to deep blue. After the solution was stirred at the same temperature for 1 h, 60% HPF_6 (2 ml) and water (20 ml) were added to the mixture. The resulting suspension was filtered with suction. The organic layer was washed with water, dried with $MgSO_4$, and concentrated under reduced pressure. Hexane was added to the residual oil. The precipitated crystals were collected by filtration, washed with hexane, and dried in vacuo to give the di(1-azulenyl)phenylmethyl cation **7f** (120 mg, 100%). Deep blue powder; mp 165.0—171.0 °C (CH_2Cl_2/hexane); MS (FAB) m/z 455 ($M^+ - PF_6$); IR (KBr disk) 1474, 1412, 1338, 1296, 1176, 840, and 558 cm^{-1}; UV (MeCN) 235 ($\log\varepsilon$ 4.60), 285 (4.34), 362 (4.17), 455 (3.75), and 678 nm (4.53); ^1H NMR (90 MHz, $CDCl_3$, 50 °C) δ=9.10 (d, J=11.7 Hz, 2H), 8.21—7.35 (m, 13H), 7.71 (s, 2H), and 1.59 (s, 18H). Found: m/z 455.2707. Calcd for $C_{35}H_{35}^+$: M, 455.2739. Found: C, 68.12; H, 6.43%. Calcd for $C_{35}H_{35}PF_6 \cdot H_2O$: C, 67.95; H, 6.03%.

(1-Azulenyl)diphenylmethane (11a). A solution of azulene (**13a**) (1.28 g, 10.0 mmol) and benzhydrol (3.69 g, 20.0 mmol) in glacial acetic acid (60 ml) was refluxed for 10 h. The solvent was removed in vacuo, and the residue was dissolved in benzene. The solution was washed with 5% $NaHCO_3$ and water, dried with $MgSO_4$, and concentrated in vacuo. The residue was purified by medium-pressure column chromatography on silica gel with 3% ethyl acetate/hexane to afford (1-azulenyl)diphenylmethane (**11a**) (1.18 g, 40%), and 1,3-bis(diphenylmethyl)azulene (**22a**) (1.70 g, 37%).

11a: Blue needles; mp 120.0—122.0 °C (Ref. 42; mp 123 °C); IR (KBr disk) 1578, 1496, 1456, 1398, 786, 742, 720, and 698 cm^{-1}; UV (CH_2Cl_2) 237 ($\log\varepsilon$ 4.27), 284 (4.67), 288 (4.68), 294 (4.68), 348 (3.71), 364 (3.55), 598 (2.49), and 646 nm (2.42); ^1H NMR (90 MHz, $CDCl_3$) δ=8.28 (d, J=9.1 Hz, 1H), 8.22 (d, J=9.3 Hz, 1H), 7.58 (dd, J=9.6, 9.6 Hz, 1H), 7.49 (d, J=4.0 Hz, 1H), 7.38—7.16 (m, 11H), 7.08 (dd, J=9.6, 9.1 Hz, 1H), 7.10 (dd, J=9.6, 9.3 Hz, 1H), and 6.14 (s, 1H).

22a: Blue needles; mp 143.0—144.0 °C (Ref. 42; mp 146 °C); IR (KBr disk) 1574, 1496, 1454, 730, and 698 cm^{-1}; UV (CH_2Cl_2) 240 ($\log\varepsilon$ 4.55), 292 (4.87), 302 (4.89), 357 (3.94), 374 (3.94), 617 (2.71), and 672 nm (2.63); ^1H NMR (90 MHz, $CDCl_3$) δ=8.17 (d, J=9.4 Hz, 2H), 7.45 (t, J=9.5 Hz, 1H), 7.30—6.98 (m, 21H), 6.93 (dd, J=9.5, 9.4 Hz, 2H), and 6.08 (s, 2H); ^{13}C NMR (22.5 MHz, $CDCl_3$) δ=144.55 (s), 139.52 (d), 137.39 (d), 136.17 (s), 133.55 (d), 130.67 (s), 128.91 (d), 128.03 (d), 125.89 (d), and 49.67 (d)

(3-Methyl-1-azulenyl)diphenylmethane (11b). A solution of 1-methylazulene (**13b**) (1.42 g, 10.0 mmol) and benzhydrol (3.69 g, 20.0 mmol) in glacial acetic acid (50 ml) was refluxed for 24 h. The solvent was removed in vacuo, and the residue was dissolved in benzene. The solution was washed with 5% $NaHCO_3$ and water, dried with $MgSO_4$, and concentrated in vacuo. The residue was purified by medium-pressure column chromatography on silica gel with 3% ethyl acetate/hexane to afford the (1-azulenyl)diphenylmethane **11b** (1.41 g, 46%). Blue plates; mp 124.0—125.0 °C (hexane); MS (70 eV) m/z (rel intensity) 308 (M^+, 100), 293 (39), and 231 (52); IR (KBr disk) 1576, 1496, 1454, 746, 740, 728, 722, and 698 cm^{-1}; UV (CH_2Cl_2) 240 ($\log\varepsilon$ 4.23), 291 (4.67), 355 (3.70), 373 (3.66), and 627 nm (2.51); ^1H NMR (90 MHz, $CDCl_3$) δ=8.09 (d, J=9.7 Hz, 2H), 7.37 (dd, J=9.9, 9.9 Hz, 1H), 7.31 (s, 1H), 7.26—7.06 (m, 10H), 6.91 (dd, J=9.9, 9.7 Hz, 1H), 6.81 (dd, J=9.9, 9.7 Hz, 1H), 6.08 (s, 1H), and 2.54 (s, 3H). Found: m/z 308.1566. Calcd for $C_{24}H_{20}$: M, 308.1565. Found: C, 93.18; H, 6.59%. Calcd for $C_{24}H_{20}$: C, 93.46; H, 6.54%.

(3-Methoxycarbonyl-1-azulenyl)diphenylmethane (11c). A solution of 1-methoxycarbonylazulene (**13c**) (546 mg, 2.93 mmol) and benzhydrol (1.08 g, 5.89 mmol) in glacial acetic acid (18 ml) was refluxed for 6 h. The solvent was removed in vacuo, and the residue was dissolved in benzene. The solution was washed with 5% $NaHCO_3$ and

water, dried with $MgSO_4$, and concentrated in vacuo. The residue was purified by column chromatography on silica gel with CH_2Cl_2 to afford the (1-azulenyl)diphenylmethane **11c** (922 mg, 89%). Purple needles; mp 156.0—158.0 °C (ethyl acetate/hexane); MS (70 eV) m/z (rel intensity) 352 (M^+, 100), 293 (48), 275 (44), and 215 (26); IR (KBr disk) 1700, 1464, 1452, 1438, 1420, 1396, 1200, 1174, 1038, 868, 778, 742, 732, and 696 cm^{-1}; UV (CH_2Cl_2) 238 ($\log\varepsilon$ 4.43), 296 (4.55), 308 (4.64), 384 (3.93), and 558 nm (2.62); ^1H NMR (90 MHz, $CDCl_3$) δ=9.64 (d, J=9.7 Hz, 1H), 8.34 (d, J=9.5 Hz, 1H), 7.90 (s, 1H), 7.75 (dd, J=9.7, 9.7 Hz, 1H), 7.48 (dd, J=9.5, 9.4 Hz, 1H), 7.42—7.06 (m, 11H), 6.06 (s, 1H), and 3.88 (s, 3H). Found: m/z 352.1464. Calcd for $C_{25}H_{20}O_2$: M, 352.1463. Found: C, 85.14; H, 5.88%. Calcd for $C_{25}H_{20}O_2$: C, 85.20; H, 5.72%.

(3,6-Di-*t*-butyl-1-azulenyl)diphenylmethane (11d). A solution of 1,6-di-*t*-butylazulene (**13d**) (496 mg, 2.06 mmol) and benzhydrol (746 mg, 4.05 mmol) in glacial acetic acid (12 ml) was refluxed for 6 h. The solvent was removed in vacuo, and the residue was dissolved in benzene. The solution was washed with 5% $NaHCO_3$ and water, dried with $MgSO_4$, and concentrated in vacuo. The residue was purified by column chromatography on silica gel with hexane to afford the (1-azulenyl)diphenylmethane **11d** (239 mg, 28%). Blue needles; mp 163.0—164.0 °C (EtOH); MS (70 eV) m/z (rel intensity) 406 (M^+, 44), 392 (43), 391 (100), 349 (14), 85 (81), and 83 (96); IR (KBr disk) 2960, 1578, and 698 cm^{-1}; UV (CH_2Cl_2) 241 ($\log\varepsilon$ 4.20), 292 (4.73), 303 (4.80), 357 (3.74), 375 (3.58), and 609 nm (2.49); ^1H NMR (90 MHz, $CDCl_3$) δ=8.55 (d, J=11.0 Hz, 1H), 8.08 (d, J=10.8 Hz, 1H), 7.31 (s, 1H), 7.29—7.04 (m, 11H), 7.08 (dd, J=10.8, 1.8 Hz, 1H), 6.07 (s, 1H), 1.50 (s, 9H), and 1.40 (s, 9H). Found: m/z 406.2660. Calcd for $C_{31}H_{34}$: M, 406.2661. Found: C, 90.84; H, 8.51%. Calcd for $C_{31}H_{34}\cdot 1/4H_2O$: C, 90.57; H, 8.46%.

(6-*t*-Butyl-1-azulenyl)diphenylmethane (11e). A solution of 6-*t*-butylazulene (**13e**) (1.85 g, 10.0 mmol) and benzhydrol (3.68 g, 20.0 mmol) in glacial acetic acid (60 ml) was refluxed for 6 h. The solvent was removed in vacuo, and the residue was dissolved in benzene. The solution was washed with 5% $NaHCO_3$ and water, dried with $MgSO_4$, and concentrated in vacuo. The residue was purified by column chromatography on silica gel with hexane to afford the (1-azulenyl)diphenylmethane **11e** (1.09 g, 31%) and 6-*t*-butyl-1,3-bis(diphenylmethyl)azulene (**22b**) (594 mg, 11%).

11e: Blue prisms; mp 157.0—159.5 °C (hexane); MS (70 eV) m/z (rel intensity) 352 (M^+, 100) and 273 (44); IR (KBr disk) 1586, 1496, 1452, 1410, 836, 728, and 698 cm^{-1}; UV (CH_2Cl_2) 236 ($\log\varepsilon$ 4.24), 287 (4.75), 292 (4.73), 298 (4.82), 351 (3.78), 367 (3.35), and 585 nm (2.52); ^1H NMR (90 MHz, $CDCl_3$) δ=8.21 (d, J=10.6 Hz, 1H), 8.17 (d, J=10.8 Hz, 1H), 7.39 (br, 1H), 7.32—7.04 (m, 12H), 6.11 (s, 1H), and 1.40 (s, 9H). Found: m/z 350.2034. Calcd for $C_{27}H_{26}$: M, 350.2035. Found: C, 92.59; H, 7.72%. Calcd for $C_{27}H_{26}$: C, 92.52; H, 7.48%.

22b: Blue needles; mp 184.5—185.0 °C (CH_2Cl_2/MeOH); MS (70 eV) m/z (rel intensity) 516 (M^+, 100); IR (KBr disk) 1584, 1496, and 700 cm^{-1}; UV (CH_2Cl_2) 239 ($\log\varepsilon$ 4.32), 295 (4.73), 358 (3.80), 376 (3.67), and 604 nm (2.54); ^1H NMR (90 MHz, $CDCl_3$) δ=8.12 (d, J=11.0 Hz, 2H), 7.28—6.99 (m, 23H), 6.06 (s, 2H), and 1.35 (s, 9H); ^{13}C NMR (22.5 MHz, $CDCl_3$) δ=160.89 (s), 144.70 (s), 138.52 (d), 134.86 (s), 132.60 (d), 130.25 (s), 128.91 (d), 127.97 (d), 125.80 (d), 119.98 (d), 49.61 (d), 38.26 (s), and 31.74 (q). Found: m/z 516.2820. Calcd for $C_{40}H_{36}$: M, 516.2817. Found: C, 92.93; H, 7.15%. Calcd for $C_{40}H_{36}$: C, 92.28; H, 7.02%.

(3-*t*-Butyl-1-azulenyl)diphenylmethane (11f). A solution of 1-*t*-butylazulene (**13f**) (190 mg, 1.03 mmol) and benzhydrol (369 mg, 2.00 mmol) in glacial acetic acid (6 ml) was refluxed for 8 h. The solvent was removed in vacuo, and the residue was dissolved in benzene. The solution was washed with 5% $NaHCO_3$ and water, dried with $MgSO_4$, and concentrated in vacuo. The residue was purified by column chromatography on silica gel with 5% ethyl acetate/hexane to afford the (1-azulenyl)diphenylmethane **11f** (198 mg, 55%). Blue needles; mp 143.0—145.0 °C (hexane); MS (70 eV) m/z (rel intensity) 350 (M^+, 92), 336 (34), and 335 (100); IR (KBr disk) 2972, 1568, 1496, 1456, 1364, 1228, 740, 722, and 700 cm^{-1}; UV (CH_2Cl_2) 241 ($\log\varepsilon$ 4.24), 292 (4.66), 355 (3.69), 373 (3.69), and 625 nm (2.47); ^1H NMR (90 MHz, $CDCl_3$) δ=8.59 (d, J=9.5 Hz, 1H), 8.13 (d, J=9.5 Hz, 1H), 7.45 (dd, J=9.9, 9.9 Hz, 1H), 7.42 (s, 1H), 7.30—7.11 (m, 10H), 6.98 (dd, J=9.9, 9.5 Hz, 1H), 6.88 (dd, J=9.9, 9.5 Hz, 1H), 6.10 (s, 1H), and 1.52 (s, 9H). Found: m/z 350.2036. Calcd for $C_{27}H_{26}$: M, 350.2035. Found: C, 92.56; H, 7.77%. Calcd for $C_{27}H_{26}$: C, 92.52; H, 7.48%.

(1-Azulenyl)diphenylmethyl Hexafluorophosphate (8a). DDQ (305 mg, 1.35 mmol) was added at room temperature to a solution of (1-azulenyl)diphenylmethane (**11a**) (295 mg, 1.00 mmol) in CH_2Cl_2 (50 ml). The blue color turned to red. After the solution was stirred at the same temperature for 1 h, 60% HPF_6 (2.5 ml) and water (10 ml) were added to the mixture. The resulting suspension was filtered with suction. The organic layer was dried with $MgSO_4$, and concentrated under reduced pressure. The residue was dissolved in CH_2Cl_2 (1 ml); then, Et_2O (30 ml) was added to the solution. The precipitated crystals were collected by filtration, washed with Et_2O, and dried in vacuo to give the (1-azulenyl)diphenylmethyl cation **8a** (439 mg, 100%). Red powder; mp 142.0—146.0 °C (CH_2Cl_2/ether); MS (FAB) m/z 293 (M^+-PF_6); IR (KBr disk) 1520, 1426, 1374, 1342, 846, 754, 704, and 558 cm^{-1}; UV (MeCN) 223 ($\log\varepsilon$ 4.37), 260 (4.31), 324 (3.96), 396 (4.05), and 487 nm (4.16); ^1H NMR (400 MHz, $CDCl_3$, 58 °C) δ=8.972 (dd, J=9.8, 1.6 Hz, 1H), 8.532 (ddd, J=10.0, 9.8, 1.8 Hz, 1H), 8.481 (dddd, J=10.0, 9.8, 1.8, 1.6 Hz, 1H), 8.200 (dd, J=9.4, 1.8 Hz, 1H), 8.106 (ddd, J=9.8, 9.4, 1.8 Hz, 1H), 7.909 (d, J=5.0 Hz, 1H), 7.796 (d, J=5.0 Hz, 1H), 7.768 (t, J=7.6 Hz, 2H), 7.609 (dd, J=7.6 Hz, 4H), and 7.404 (d, J=7.8 Hz, 4H); ^1H NMR (400 MHz, $CDCl_3$, −60 °C) δ=9.084 (dd, J=9.8, 1.6 Hz, 1H), 8.640 (ddd, J=10.0, 9.8, 1.8 Hz, 1H), 8.595 (dddd, J=10.0, 9.8, 1.8, 1.6 Hz, 1H), 8.230 (dd, J=9.4, 1.8 Hz, 1H), 8.171 (ddd, J=9.8, 9.4, 1.8 Hz, 1H), 8.000 (d, J=5.0 Hz, 1H), 7.904 (d, J=5.0 Hz, 1H), 7.880 (t, J=7.6 Hz, 1H), 7.816 (t, J=7.6 Hz, 1H), 7.673 (dd, J=7.8, 7.6 Hz, 4H), 7.470 (d, J=7.8 Hz, 2H), and 7.427 (d, J=7.8 Hz, 2H). Found: m/z 293.1314. Cacld for $C_{23}H_{17}^+$: M, 293.1330. Found: C, 62.44; H, 3.77%. Calcd for $C_{23}H_{17}PF_6\cdot 1/3H_2O$: C, 62.17; H, 4.01%.

(3- Methoxycarbonyl- 1- azulenyl)diphenylmethyl Hexafluorophosphate (8c). DDQ (164 mg, 0.723 mmol) was added at room temperature to a solution of (3-methoxy-

carbonyl-1-azulenyl)diphenylmethane (**11c**) (178 mg, 0.506 mmol) in CH_2Cl_2 (50 ml). The purple color turned to red, and a brown precipitate was formed. After the solution was stirred at the same temperature for 1 h, 60% HPF_6 (2.5 ml) and water (10 ml) were added to the mixture. The resulting suspension was filtered with suction. The organic layer was dried with $MgSO_4$, and concentrated under reduced pressure. The residue was dissolved in CH_2Cl_2 (1 ml); then, Et_2O (30 ml) was added to the solution. The precipitated crystals were collected by filtration, washed with Et_2O, and dried in vacuo to give the (1-azulenyl)diphenylmethyl cation **8c** (223 mg, 89%). Orange powder; mp 191.0—193.0 °C (CH_2Cl_2/ether); MS (FAB) m/z 351 (M^+-PF_6); IR (KBr disk) 1718, 1540, 1524, 1426, 1376, 1358, 1266, 834, and 558 cm^{-1}; UV (MeCN) 234 ($\log\varepsilon$ 4.39), 264 (4.22), 293 (4.25), 304 (4.30), 375 (4.01), and 493 nm (4.12); ^1H NMR (90 MHz, $CDCl_3$) δ=10.21—9.97 (m, 1H), 8.68—8.53 (m, 1H), 8.48—8.73 (m, 13H), 8.39 (s, 1H), and 4.00 (s, 3H). Found: m/z 351.1370. Calcd for $C_{25}H_{19}O_2^+$: M, 351.1385. Found: C, 60.58; H, 4.03%. Calcd for $C_{25}H_{19}O_2PF_6$: C, 60.49; H, 3.86%.

(3,6-Di-*t*-butyl-1-azulenyl)diphenylmethyl Hexafluorophosphate (8d). DDQ (62 mg, 0.27 mmol) was added at room temperature to a solution of (3,6-di-*t*-butyl-1-azulenyl)diphenylmethane (**11d**) (81 mg, 0.20 mmol) in CH_2Cl_2 (40 ml). The blue color turned to red. After the solution was stirred at the same temperature for 1 h, 60% HPF_6 (2 ml) and water (20 ml) were added to the mixture. The resulting suspension was filtered with suction. The organic layer was dried with $MgSO_4$, and concentrated under reduced pressure. Hexane was added to the residual oil. The precipitated crystals were collected by filtration, washed with hexane, and dried in vacuo to give the (1-azulenyl)diphenylmethyl cation **8d** (110 mg, 100%). Red powder; mp 137.0—146.0 °C (CH_2Cl_2/hexane); MS (FAB) m/z 550 (M^+-PF_6); IR (KBr disk) 840 and 558 cm^{-1}; UV (MeCN) 264 ($\log\varepsilon$ 4.24), 333 (4.02), 399 (4.01), and 489 nm (4.11); ^1H NMR (90 MHz, $CDCl_3$, 50 °C) δ=9.25 (d, J=11.2 Hz, 1H), 8.78 (d, J=11.2 Hz, 1H), 8.12 (s, 2H), 7.87—7.26 (m, 11H), 1.57 (s, 9H), 1.51 (s, 9H). Found: m/z 405.2558. Calcd for $C_{31}H_{33}^+$: M, 405.2582. Found: C, 67.38; H, 6.29%. Calcd for $C_{31}H_{33}PF_6$: C, 67.36; H, 6.04%.

(3-*t*-Butyl-1-azulenyl)diphenylmethyl Hexafluorophosphate (8f). DDQ (62 mg, 0.28 mmol) was added at room temperature to a solution of (3-*t*-butyl-1-azulenyl)-diphenylmethane (**11f**) (72 mg, 0.21 mmol) in CH_2Cl_2 (40 ml). The blue color turned to red. After the solution was stirred at the same temperature for 1 h, 60% HPF_6 (2 ml) and water (20 ml) were added to the mixture. The resulting suspension was filtered with suction. The organic layer was dried with $MgSO_4$, and concentrated under reduced pressure. Hexane was added to the residual oil. The precipitated crystals were collected by filtration, washed with hexane, and dried in vacuo to give the (1-azulenyl)diphenylmethyl cation **8f** (102 mg, 100%). Red powder; mp 95.0—98.0 °C (CH_2Cl_2/hexane); MS (FAB) m/z 349 (M^+-PF_6); IR (KBr disk) 838 and 558 cm^{-1}; UV (MeCN) 262 ($\log\varepsilon$ 4.26), 328 (3.96), 351 (3.91), 398 (4.02), and 495 nm (4.14); ^1H NMR (90 MHz, $CDCl_3$, 50 °C) δ=9.25 (d, J=11.2 Hz, 1H), 8.70—8.36 (m, 2H), 8.26—7.92 (m, 3H), 7.82—7.26 (m, 10H), and 1.57 (s, 9H). Found: m/z 349.1918. Calcd for $C_{27}H_{25}^+$: M, 349.1956. Found: C, 62.81; H, 4.70%. Calcd for $C_{27}H_{25}PF_6\cdot 1/3CH_2Cl_2$: C, 62.80; H, 4.95%.

Reduction of Tri(1-azulenyl)methyl Hexafluorophosphate (6a). $LiAlH_4$ (16 mg, 0.43 mmol) was added at room temperature to a solution of the tri(1-azulenyl)-methyl cation **6a** (54 mg, 0.10 mmol) in THF (1 ml) and CH_2Cl_2 (15 ml). The deep blue color turned to greenish-brown. After the solution was stirred at same temperature for 1 h, water (10 ml) was added to the mixture. The resulting suspension was filtered with suction and extracted with CH_2Cl_2. The organic layer was washed with water, dried with $MgSO_4$, and concentrated under reduced pressure. The residue was purified by column chromatography on silica gel with CH_2Cl_2 and GPC with $CHCl_3$ to afford tri(1-azulenyl)methane (**9a**) (7.9 mg, 20%).

Reduction of Tris(3-methyl-1-azulenyl)methyl Hexafluorophosphate (6b). The reaction of the tri-(azulenyl)methyl cation **6b** (58 mg, 0.10 mmol) with $LiAlH_4$ (14 mg, 0.37 mmol) in THF (1 ml) and CH_2Cl_2 (15 ml) took place at room temperature for 1 h; purification by column chromatography on silica gel with 30% ethyl acetate/hexane afforded tris(3-methyl-1-azulenyl)methane (**9b**) (8.3 mg, 19%).

Reduction of Di(1-azulenyl)phenylmethyl Hexafluorophosphate (7a). The reaction of the di(1-azulenyl)phenylmethyl cation **7a** (49 mg, 0.10 mmol) with $LiAlH_4$ (33 mg, 0.88 mmol) in THF (2 ml) and CH_2Cl_2 (15 ml) took place at room temperature for 10 min; purification by column chromatography on silica gel with 15% ethyl acetate/hexane and medium-pressure column chromatography with 5% ethyl acetate/hexane afforded di(1-azulenyl)-phenylmethane (**10a**) (5.8 mg, 17%).

Reduction of Bis(3-methyl-1-azulenyl)phenylmethyl Hexafluorophosphate (7b). The reaction of the di(1-azulenyl)phenylmethyl cation **7b** (52 mg, 0.10 mmol) with $LiAlH_4$ (48 mg, 1.3 mmol) in THF (3 ml) and CH_2Cl_2 (15 ml) took place at room temperature for 10 min; purification by column chromatography on silica gel with 10% ethyl acetate/hexane and medium-pressure column chromatography with 3% ethyl acetate/hexane afforded bis-(3-methyl-1-azulenyl)methane (**10b**) (15 mg, 40%).

Reduction of (1-azulenyl)diphenylmethyl Hexafluorophosphate (8a). The reaction of the (1-azulenyl)diphenylmethyl cation **11a** (44 mg, 0.10 mmol) with $LiAlH_4$ (30 mg, 0.80 mmol) in THF (3 ml) and CH_2Cl_2 (15 ml) took place at room temperature for 10 min; purification by column chromatography on silica gel with CH_2Cl_2 and medium-pressure column chromatography with 3% ethyl acetate/hexane afforded (1-azulenyl)diphenylmethane (**11a**) (4.7 mg, 16%).

Determination of pK_{R^+} Values. For the preparation of a sample solution of the cations, except for **6d—f**, **7d—f**, and **8c**, buffer solutions of slightly different acidities were prepared by mixing CH_3COONa (1 M) and HCl (1 M) for pH 0.65—2.0, CH_3COONa (0.1 M) and CH_3COOH (0.1 M) for pH 3.5—5.0, KH_2PO_4 (0.1 M) and $Na_2B_4O_7$ (0.05 M) for pH 6.0—9.0, $Na_2B_4O_7$ (0.05 M) and Na_2CO_3 (0.05 M) for pH 10.0, and $Na_2B_4O_7$ (0.05 M) and NaOH (0.1 M) for pH 11.0—11.6, in various portions. Each 1 ml portion of the stock solution, prepared by dissolving 3—5 mg of the cation in MeCN (20 ml), was pipetted out and made up to 10 ml by adding the appropriated buffer solution (5 ml) and MeCN. Sample solutions of the cations

6d—**f** and **7d**—**f** were prepared by dissolving in a glycine (0.1 M)–NaOH (0.1 M) buffer solution (50 ml) and made up to 100 ml by adding MeCN. A sample solution with lower acidity was made by further alkalification with 20% aqueous NaOH. The sample solution of **8c** was prepared by dissolving in 50% H_2SO_4 and by adding the appropriated amount of 50% H_2SO_4 and H_2O. The concentration of the cation was determined by spectrophotometrically at 24 °C. The pH of each sample was measured on a Horiba pH meter F-13 calibrated with standard buffers before use, and the H_R values calculated from the concentration of H_2SO_4.[9] The observed absorbance at the specific absorption maxima of each cation was plotted against the pH or H_R, giving a classical titration curve whose midpoint was taken as the pK_{R+} value.

Complete spectral data of MS, IR, UV, ^{1}H NMR, and ^{13}C NMR for the reported compounds (**6a**—**f**, **7a**—**f**, **8a**, **8c**—**d**, **8f**, **9a**—**f**, **10a**—**f**, **11a**—**f**, **13d**—**f**, **14c**—**e**, **15**, **16a**—**c**, **17a**—**c**, **18**—**20**, **21a**—**b**, **22a**—**b**) are deposited as Document No. 68021 at the Office of the Editor of Bull. Chem. Soc. Jpn.

This work was supported by a Grant-in-Aid for Scientific Research No. 03854053 to S. I. and that on Priority Areas No. 02230103 to T. A. from the Ministry of Education, Science and Culture, and the Research Aid of Inoue Foundation for Science.

References

1) A part of this work has been published in preliminary form: S. Ito, N. Morita, and T. Asao, *Tetrahedron Lett.*, **32**, 773 (1991); **33**, 6669 (1992); **35**, 751 (1994); *Chem. Lett.*, **1994**, 477.

2) K. Komatsu, H. Akamatsu, Y. Jinbu, and K. Okamoto, *J. Am. Chem. Soc.*, **110**, 633 (1988).

3) K. Komatsu, H. Akamatsu, S. Aonuma, Y. Jinbu, N. Maekawa, and K. Takeuchi, *Tetrahedron*, **47**, 6951 (1991).

4) K. Komatsu, I. Tomioka, and K. Okamoto, *Tetrahedron Lett.*, **21**, 947 (1980).

5) R. A. Moss and R. C. Munjal, *Tetrahedron Lett.*, **21**, 1221 (1980).

6) K. Okamoto, K. Takeuchi, K. Komatsu, Y. Kubota, R. Ohara, M. Arima, K. Takahashi, Y. Waki, and S. Shirai, *Tetrahedron*, **39**, 4011 (1983).

7) R. A. Moss, S. Shen, K. Krogh-Jespersen, J. A. Potenza, H. J. Schugar, and R. C. Munjal, *J. Am. Chem. Soc.*, **108**, 134 (1986).

8) I. Agranat and E. Aharon-Shalom, *J. Org. Chem.*, **41**, 2379 (1976).

9) E. M. Arnett and R. D. Buhick, *J. Am. Chem. Soc.*, **86**, 1564 (1964).

10) R. C. Kerber and C. -M. Hsu, *J. Am. Chem. Soc.*, **95**, 3239 (1973).

11) J. O. Morly, *J. Am. Chem. Soc.*, **110**, 7660 (1988).

12) A. J. Anderson, Jr., and B. M. Steckler, *J. Am. Chem. Soc.*, **81**, 4941 (1959).

13) K. Mislow, *Acc. Chem. Res.*, **9**, 26 (1976).

14) M. Oki, "Application of Dynamic NMR Spectroscopy to Organic Chemistry," VCH Publishers, Florida (1985), pp. 227—233.

15) A. K. Colter, I. I. Schuster, and R. J. Kurkland, *J. Am. Chem. Soc.*, **87**, 2278 (1965).

16) R. J. Kurkland, I. I. Schuster, and A. K. Colter, *J. Am. Chem. Soc.*, **87**, 2279 (1965).

17) I. I. Schuster, A. K. Colter, and R. J. Kurkland, *J. Am. Chem. Soc.*, **90**, 4679 (1968).

18) D. Gust and K. Mislow, *J. Am. Chem. Soc.*, **95**, 1535 (1973).

19) J. W. Rakshys, Jr., S. V. McKindley, and H. H. Freedman, *J. Am. Chem. Soc.*, **92**, 3518 (1970).

20) J. W. Rakshys, Jr., S. V. McKindley, and H. H. Freedman, *J. Am. Chem. Soc.*, **93**, 6522 (1971).

21) F. Strohbusch, *Tetrahedron*, **28**, 1915 (1972).

22) J. F. Blount, P. Fincchiaro, D. Gust, and K. Mislow, *J. Am. Chem. Soc.*, **95**, 7019 (1973).

23) J. P. Hummel, D. Gust, and K. Mislow, *J. Am. Chem. Soc.*, **96**, 3679 (1974).

24) M. J. Sabacky, S. M. Johnson, J. C. Martin, and I. C. Paul, *J. Am. Chem. Soc.*, **91**, 7542 (1969).

25) P. Finocchiaro, D. Gust, and K. Mislow, *J. Am. Chem. Soc.*, **96**, 2165 (1974).

26) J. D. Andose and K. Mislow, *J. Am. Chem. Soc.*, **96**, 2168 (1974).

27) P. Finocchiaro, D. Gust, and K. Mislow, *J. Am. Chem. Soc.*, **96**, 2176 (1974).

28) P. Finocchiaro, D. Gust, and K. Mislow, *J. Am. Chem. Soc.*, **96**, 3198 (1974).

29) P. Finocchiaro, D. Gust, and K. Mislow, *J. Am. Chem. Soc.*, **96**, 3205 (1974).

30) E. W. Turnblom, R. J. Boettcher, and K. Mislow, *J. Am. Chem. Soc.*, **97**, 1766 (1975).

31) M. R. Kates, J. D. Andose, P. Finocchiaro, D. Gust, and K. Mislow, *J. Am. Chem. Soc.*, **97**, 1772 (1975).

32) R. J. Boettcher, D. Gust, and K. Mislow, *J. Am. Chem. Soc.*, **95**, 7157 (1973).

33) D. Hellwinkel, M. Melan, and C. R. Degel, *Tetrahedron*, **29**, 1895 (1973).

34) R. Glaster, J. F. Blount, and K. Mislow, *J. Am. Chem. Soc.*, **102**, 2777 (1980).

35) S. E. Biali and Z. Rappoport, *J. Am. Chem. Soc.*, **106**, 477 (1984).

36) S. E. Biali and Z. Rappoport, *J. Org. Chem.*, **51**, 2245 (1986).

37) K. Hafner, H. Pelster, and J. Schneider, *Justus Liebigs Ann. Chem.*, **650**, 62 (1961).

38) S. Takekuma, Y. Matsubara, H. Yamamoto, and T. Nozoe, *Nippon Kagaku Kaishi*, **1988**, 157.

39) S. Takekuma, Y. Matsubara, H. Yamamoto, and T. Nozoe, *Bull. Chem. Soc. Jpn.*, **60**, 3721 (1987).

40) **14c** was synthesized by Vilsmeier reaction of **13c** with $POCl_3$ in DMF in 98% yields.

41) K. Hafner, A. Stephan, and C. Bernhard, *Justus Liebigs Ann. Chem.*, **650**, 42 (1961).

42) H. Franke and M. Mühlstädt, *J. Prakt. Chem.*, **35**, 249 (1967).

43) K. Hafner and K. -P. Meinhardt, *Org. Synth.*, **62**, 134 (1984).

44) H. Franke and M. Mühlsädt, *J. Prakt. Chem.*, **35**, 262 (1967).

45) M. Feldman and W. C. Flythe, *J. Am. Chem. Soc.*, **91**, 4577 (1969).

46) K. Komatsu, K. Masumoto, Y. Waki, and K.

Okamoto, *Bull. Chem. Soc. Jpn.*, **55**, 2470 (1982).
47) E. D. Arnett and S. Venimadhavan, *J. Am. Chem. Soc.*, **113**, 6967 (1991).
48) Crystal data for **6b** are as follows: $C_{34}H_{27}PF_6 \cdot C_4H_8O$; space group *Cc*; $a=11.899$, $b=13.413$, $c=40.555$ Å, $\beta=96.85°$; $Z=8$; total of 2041 reflections within $I>3\sigma(I)$.
49) Simulation of the temperature dependent ^{1}H NMR spectra was performed using the program DNMR5 (*QCPE*, **10**, 365 (1978)) by D. S. Stephenson and G. Binsch.
50) E. E. Wille, D. S. Stephenson, P. Capriel, and G. Binsch, *J. Am. Chem. Soc.*, **104**, 405 (1982).